

https://dspace.org/

Assessment of the speciation and bioavailability of arsenic in acid mine drainage

Ramaqele, Mathabo

2019
https://hdl.handle.net/10539/27057

Downloaded from a DSpace repository. https://dspace.org/

ASSESSMENT OF THE SPECIATION AND BIOAVAILABILITY OF ARSENIC IN ACID MINE DRAINAGE



UNIVERSITY OF THE
WITWATERSRAND,
JOHANNESBURG

Mathabo Ramaqele

A dissertation submitted to the Faculty of Science, University of the Witwatersrand, Johannesburg, in fulfilment of the requirements of the Master of Science degree

University of the Witwatersrand

Johannesburg

2019

Declaration

I declare that this dissertation is my own work. It is being submitted for the Degree of Master of Science at the University of Witwatersrand, Johannesburg. It has not been submitted before for any degree or Examination at any University.



Mathabo Ramaqele

Date: 07th February 2019

Abstract

The mining industry is a major economic development factor for many countries however, industrialization is one of the major causes of environmental pollution worldwide. The Witwatersrand basin in South Africa is the largest gold basin in the whole world. The main ore occurs in association with many other minerals of which some such as arsenic are highly toxic even at trace levels. The mining processes in the region have brought to the surface the minor minerals in the form of mine dumps and mine tailing dams which contribute to acid mine drainage (AMD). Though the problem has manifested itself mostly along these gold fields, it has been seen in other mining provinces too.

This study presents data pertaining to speciation of arsenic present in the Witwatersrand mining area and also discuss the conditions that impact on arsenic bioavailability and toxicity. Electrochemical methods such as differential pulse anodic stripping voltammetry (DPASV) and other techniques such as inductively coupled plasma-optical emission spectroscopy (ICP-OES), inductively coupled plasma-mass spectrometry (ICP-MS) and ion chromatography (IC) were applied in this work. Geochemical modelling using a PHREEQC program was also applied to study the distribution of arsenic species. The DPASV method was optimized using 100 μg L^{-1} As(III) standard solution for parameters including deposition potential (DP), deposition time (DT), rotation speed (RS) and modulation amplitude (MA). The optimum conditions were obtained at -0.4 V, 180 s, 500 rpm and 0.04V for DP, DT, RS and MA, respectively. Acid mine drainage and Fleurhof dam water were used to assess the method viability. The results show that DPASV was more sensitive in dam water with recovery percentage of 81.6% and 123% for As(III) and As(V), respectively. While in AMD, the interference of various trace metals and anions was observed. Thus making this method more effective for determination of arsenic species in natural water.

The total arsenic concentrations were determined to be 0.2786 mg L^{-1} and 0.0120 mg L^{-1} by spectrometric techniques in AMD and Fleurhof dam samples, respectively. PHREEQC modelling was applied to simulate the environment and determine the species distribution in AMD. The method was also utilized to study

how parameters such as pH and temperature may influence the species distribution. Acidic conditions which are characteristic of AMD and neutral conditions representing natural waters were simulated. It was discovered that acidic conditions favour dissolution of both As(III) and As(V) species but As(III) was the more dominant species. At neutral pH, it was discovered that As(V) was the dominant species but the overall dissolved metals were shown to be limited by precipitation. Only slight contribution of temperature was observed as both simulations for cold and warm temperatures did not show much difference in terms of species distribution.

Dedication

This work is dedicated to my son, Mohau Motsoahae.

Acknowledgements

First I would like to thank God almighty for giving me the strength to endure all the hardships I met throughout this program.

I would like to express deep gratitude to my supervisor's Dr Heidi Richards, Prof Ewa Cukrowska and Dr Caren Billing. The support they showed me through completion of this work was tremendous. Their patience, constant encouragement and constructive comments made me a better person I am today, thank you.

Great thanks goes to Prof. Hlanganani Tutu and Prof. Luke Chimuka, your comments and suggestions towards my work during group meetings made a great contribution.

I would also like to thank all members of the Environmental analytical Chemistry group (EACH) at University of the Witwatersrand, it was a pleasure working with you all. To Xolisiwe Maputsoe and Nthabiseng Mots'oane you made Wits feel like home for me. To Dr Somandla Ncube, Yannick Nuapia and Khathutshelo Netshiongolwe, thank you for the motivation and advices, you were true inspirations.

I am forever grateful to my husband, Rethabile Motsoahae who sacrificed so much to ensure that I enrol into this program and endured the parenting responsibilities on his own while I pursued this degree. My deep gratitude also goes to both the Motsoahae and Ramaqele families, who helped take care of my son without complaining for me to pursue this dream, you provided both financial and emotional support and for that, I am deeply thankful.

Last but not least, I would like to thank the National Research Foundation (NRF) for partly funding this project.

Table of contents

Declaration i

Abstract ii

Dedication iv

Acknowledgements v

Table of contents vi

List of figures ix

List of tables xii

List of abbreviations xii

CHAPTER 1 1

INTRODUCTION 1

1.1 Background 2

CHAPTER 2 5

LITERATURE REVIEW 5

2.1 Distribution of arsenic 6

2.1.1 Rock materials 6

2.1.2 Mineral deposits 6

2.1.3 Natural water 8

2.2 Anthropogenic sources of arsenic 10

2.2.1 Mining and smelting of metal ores 10

2.2.2 Agriculture and wood preservation 12

2.2.3 Burning of fossil fuels 12

2.3 Chemistry and speciation of arsenic 13

2.4 Arsenic toxicity and bioavailability 15

2.5 Arsenic remediation 16

2.5.1 Chemical remediation 17
2.5.2 Physical remediation 18
2.5.3 Bio-remediation 18
2.6 An overview of sampling and analytical methods for arsenic determination 19
2.6.1 Sampling, pre-treatment and storage 21
2.6.2 Common analytical techniques for arsenic determination 23
2.6.3 Electrochemical methods, electrodes and interferences 25
2.6.4 Geochemical modelling 29
2.7 Method validation 31
2.7.1 Accuracy 31
2.7.2 Precision 31
2.7.3 Linearity and range 31
2.7.4 Limits of detection and quantification 32
CHAPTER 3 33
AIM AND OBJECTIVES 33
3.1 Aim 34
3.2 Objectives 34
3.3 Hypothesis 34
CHAPTER 4 35
METHODOLOGY 35
4.1 Chemicals and reagents 36
4.2 Instrumentation 36
4.3 Sampling and sample preparation 36
4.4 Electrochemical analysis 38
4.5 Determination of metal concentrations 42

4.6 Determination of anion concentrations 42
4.7 Geochemical modelling 43
Chapter 5 44
Results and discussion 44
5.1 Preliminary studies 45
5.1.1 Electrochemical characterization of the gold electrode 45
5.2 Method optimization 54
5.2.1 Deposition potential 54
5.2.2 Deposition time and rotation speed 56
5.2.3 Modulation Amplitude 58
5.3 Calibration 60
5.4 Optimization of the reduction of As(V) 61
5.5 Analysis of environmental samples 68
5.5.1 Field analysis 68
5.5.2 Metal/metalloid and anion concentrations in environmental samples 69
5.5.3 Electrochemical analysis of samples 70
5.5.4 Simulation of the species distribution in environmental samples using PHREEQC interactive code 75
Chapter 6 81
General conclusions and recommendations 81
6.1 Conclusions 82
6.2 Recommendations 83
References 84
Appendix 96

List of figures

Figure 2.1 Geological image of the Witwatersrand basin (Nkosi et al., 2017).... 11
Figure 2.2 The cycle of arsenic in the environment (Wang and Mulligan, 2006) 13
Figure 2.3 Eh-pH diagram of arsenic species in aqueous medium at 25°C and 1 bar total pressure (Smedley and Kinniburgh, 2002) 15
Figure 2.4 Processes and conditions affecting stability of arsenic speciation throughout stages of chemical analysis (Kumar and Riyazuddin, 2010)..... 20
Figure 2.5 Schematic representation of a three electrode system 26
Figure 4.1 Photograph of the sampling site showing tailings, AMD run off and small AMD ponds 37
Figure 4.2 Schematic representation for the electrochemical system used for determination of arsenic..... 40
Figure 4.3 Flow chart of the reduction of As(V) for electrochemical analysis.... 41
Figure 5.1 CV response of 3 M HCl on a gold disk electrode at 0.2 V s^{-1} scan rate. 45
Figure 5.2 DPASV response of 3 M HCl on a gold disk electrode (DP = -0.15 V and DT = 120 s) 46
Figure 5.3 DPASV response of 0.5 ml of 1 mg L^{-1} As(III) standard additions (DP = -0.15 V and DT = 120 s)..... 47
Figure 5.4 DPASV response on addition of 0.1 ml of 50 mg L^{-1} As(III) standard with electrode conditioning at 0.28 V for 60 s (DP = -0.15 V and DT = 120 s)... 48
Figure 5.5 Replicate DPASV scans of 0.5 mg L^{-1} As(III) standard in 3 M HCl with electrode conditioning at 0.28 V for 60 s (DP = -0.15 V and DT = 120 s)..... 49
Figure 5.6 Electrochemical response of $K_3Fe(CN)_6$ on a gold disk electrode at various scan rates 51
Figure 5.7 The plot of the square root of the scan rate against the forward peak height of a ferricyanide standard solution..... 52
Figure 5.8 Overlay of CV responses for 0.5 M HCl and 0.1 mg L^{-1} As(III) recorded at the scan rate of 0.2 V s^{-1}..... 53
Figure 5.9 DPASV response of As(III) standard addition in 0.5 M HCl on a solid gold electrode (DP= -0.15 V and DT= 120 s)..... 53

Figure 5.10 The effect of varying deposition potential on the peak current of 100 µg L^{-1} As (III) in 0.5 M HCl supporting electrolyte, (n = 3, SD) 55
Figure 5.11 Variation of deposition time at 500 rpm for 100 µg L^{-1} As (III) standard solution in 0.5 M HCl supporting electrolyte (DP = -0.4 V) 56
Figure 5.12 Variation of deposition time at 1000 rpm for 100 µg L^{-1} As (III) standard solution in 0.5 M HCl supporting electrolyte (DP = -0.4 V), (n = 3, SD) 57
Figure 5.13 The effect of increasing modulation amplitude on 100 µg L^{-1} As(III) peak height, (n = 3, SD) 58
Figure 5.14 Effect of varying modulation amplitude on the voltammograms of a 100 µg L^{-1} As(III) standard solution (DP= -0.4 V, DT= 180 s and RS= 500 rpm)60
Figure 5.15 Calibration curve for DPASV determination of As(III) in 0.5 M HCl using -0.4V DP, 180 s DT, 500 rpm RS and 0.04 V MA (n = 3, SD) 61
Figure 5.16 DPASV response of 50 µg L^{-1} As(V) after reduction to As(III) with sodium thiosulphate (15-90 mg) using DP = -0.4 V, DT = 180 s and RS = 500 rpm. 62
Figure 5.17 DPASV response of 25 µg L^{-1} As(V) after reduction to As(III) with sodium thiosulphate (1-15 mg) using DP= -0.4 V, DT= 180 s and RS= 500 rpm.63
Figure 5.18 Standard addition curves for 25 µg L^{-1} As(III) in a 50 µg L^{-1} arsenic standard (25 µg L^{-1} As(III) + 25 µg L^{-1} As(V)) before and after analysis of total arsenic 65
Figure 5.19 Standard addition curves for As(III) and total arsenic in a 50 µg L^{-1} arsenic standard (25 µg L^{-1} As(III) + 25 µg L^{-1} As(V))..... 67
Figure 5.20 As(III) standard addition curve for Fleurhof dam water..... 71
Figure 5.21 DPASV voltammograms of As(III) standard addition on AMD sample (10 times dilution) using -0.4 V DP, 180 s DT, 500 rpm RS and 0.04 V MA..... 72
Figure 5.22 DPASV response of 25 µg L^{-1} Pb, As and Cu in 0.5 M HCl on a gold disc electrode using -0.4 V DP, 180 s DT, 500 rpm RS and 0.04 V MA 73
Figure 5.23 DPASV response of AMD sample (10 times dilution) after As(V) reduction to As(III) using -0.4 V DP, 180 s DT, 500 rpm RS and 0.04 V MA 75

List of tables

Table 2.1 Major and secondary arsenic minerals (Smedley and Kinniburgh, 2002) 7

Table 2.2 Important organic and inorganic arsenic compounds in the environment 14

Table 2. 3 Processes/conditions influencing the stability of arsenic species 20

Table 5.1 The effect of increasing scan rate on the anodic and cathodic peak properties of a ferricyanide standard solution51

Table 5.2 Effect of modulation amplitude on peak properties of 100 µg L^{-1} As(III) standard solution 59

Table 5.3 Recoveries after the reduction of 25 µg L^{-1} As(V) to As(III) using various masses of $Na_2S_2O_3$ (n = 3) 64

Table 5.4 Recovery of As(III) and total As in 50 µg L^{-1} (25 µg L^{-1} (III) + 25 µg L^{-1} As(V)) As standard (n = 7) 66

Table 5.5 Consecutive determinations for As(III) and total arsenic recovery in 50 µg L^{-1} (25 µg L^{-1} (III) + 25 µg L^{-1} As(V)) arsenic standard (n = 4) 68

Table 5.6 Field measurements for AMD and Fleurhof dam samples..... 68

Table 5.7 Concentrations of elements in environmental samples 70

Table 5.8 Recovery of As(III) and As(V) in spiked dam water (25 µg L^{-1} (III) + 25 µg L^{-1} As(V)) (n = 3) 712

Table 5.9 Distribution of species in the AMD sample at room temperature (25°C) 76

Table 5.10 PHREEQC distribution of species in the AMD sample at pH 7 (25°C) 78

Table 5.11 PHREEQC distribution of species in AMD sample at 17°C (pH 2.76) 80

List of abbreviations

AAS: Atomic absorption spectroscopy

AFS: Atomic fluorescence spectroscopy

AMD: Acid mine drainage

As: Arsenic

ASV: Anodic stripping voltammetry

CE: Capillary electrophoresis

CSV: Cathodic stripping voltammetry

CV: Cyclic voltammetry

DP: Deposition potential

DT: Deposition time

DCP: Direct coupled plasma

DMA: Dymethylarsonic acid

DPASV: Differential pulse anodic stripping voltammetry

EMR: Electromagnetic radiation

EDTA: Ethylenediaminetetraacetic acid

Eh: Redox potential

FFF: Field flow fractionation

HMDE: Hanging mercury drop electrode

HPLC: High performance liquid chromatography

ICP-MS: Inductively coupled plasma-mass spectroscopy

ICP-OES: Inductively coupled plasma-optical emission spectroscopy.

IC: Ion chromatography

LOD: Limit of detection

LOQ: Limit of quantitation

LC: Liquid chromatography

MA: Modulation amplitude

MMA: Monomethyl arsenic acid

MIP: Microwave induced plasma

NPASV: normal pulse anodic stripping voltammetry

NMR: Nuclear magnetic resonance

pe: Electron potential

R^2: Coefficient of determination

RSD: Relative standard deviation

RDE: Rotating disk electrode

RS: Rotation speed

SA: South Africa

SD: Standard deviation

SWASV: Square wave anodic stripping voltammetry

$\nu^{½}$: Square root of the scan rate

WHO: World health organization

CHAPTER 1

INTRODUCTION

This chapter gives a general introduction on arsenic, mining in the Witwatersrand basin and its potential contribution to environmental pollution.

1.1 Background

Arsenic pollution is one of the major health issues in many countries (Berg *et al*., 2007; Garelick *et al*., 2008). It is a persistent, non-biodegradable and highly toxic naturally occurring chemical element classified under a group of metalloids (with characteristics of both metals and non-metals). It has the atomic number of 33 and in its pure form, it is crystalline and insoluble in water. Arsenic salts however, have different solubility capabilities depending on the pH and the ionic environment (Garelick *et al*., 2008).

In the environment, arsenic normally occurs in combination with other elements especially sulphur, in sulphur-bearing minerals. It is also produced commercially for use in wood preservation and metal alloying. Arsenic is the 20th most abundant element in the Earth's crust (Mays and Hussam, 2009) and it is highly distributed in soil, various water systems and air due to both anthropogenic and natural activities. As a result of these activities, most of the arsenic released from the natural sources eventually turn up in significant amounts in all environmental components.

Arsenic, even at low concentrations is of concern to human life and the entire environment. The World Health Organization (WHO) has set the guideline value of 10 µg L^{-1} in drinking water indicating that at concentrations lower than this limit, health effects are unlikely (WHO, 2010). The release of different arsenic species into the environment results from various mechanisms including oxidation and leaching of mineral ores, desorption from metal oxides and hydroxides and the action of microorganisms. In addition to these natural mechanisms, a significant increase in arsenic emissions hence pollution is also caused by human related activities such as mining and smelting of metals.

Arsenic in the environment is found in different oxidation states. Combined with other elements, the various forms can be classified into either organic or inorganic depending on the elements bonded to arsenic. The inorganic form of arsenic is the most toxic and is associated with a range of health issues and development of cancer (Hughes, 2002).

Human exposure to arsenic may be through different routes since this element is ubiquitous (present in food, air, water and other environmental samples). Drinking of contaminated water and its uptake by plants and subsequent introduction into the food chain leading to consumption of contaminated food (dietary sources such as sea food and poultry) are the common sources of exposure to arsenic. However the greatest threat is posed by contaminated ground water where the inorganic forms of this element are the most dominant.

Arsenic contamination in different environmental components has received significant attention from researchers all over the world. Analytical procedures for arsenic determination have been described for decades but with recent research studies, the greatest interest is on arsenic speciation. The total arsenic concentration does not present adequate information about the behaviour (mobility, bioavailability and elemental impact on ecological and biological systems) of the element (Michalke, 2003; Rosen and Hieftje, 2004). Determining the distribution of the individual elemental species (forms) in a system, which is defined as speciation analysis, can therefore provide much more relevant and useful information as different chemical forms of an element can have essential, harmless or toxic effects (Caruso and Montes-Bayon, 2003).

There are a number of reports on arsenic pollution from many mining countries and countries with arsenic-rich bedrocks around the world. For example, in India, several researchers have reported elevated arsenic concentration in some parts of the country (Chowdhurry *et al*., 2000; Bera *et al*., 2010). However there is only a limited number of publications reported on arsenic pollution and contamination in South Africa (SA) even though the country has abundance of mineral reserves which pose an increased risk of pollution. South Africa is rich in minerals and it is also home for the Witwatersrand basin which is a major source of South African produced gold and a one of the significant gold mining sites in the world (Tutu *et al*., 2005). Mining in this basin placed South Africa among the top gold producers but countries like China, Russia, United States and Australia have topped it in the recent decades with China currently being the leading gold producer (Neingo and Tholana, 2016).

In the Witwatersrand basin, gold mining was at its peak between the early 1970s and 1886 (Tutu *et al*., 2005) and since then the depths of the gold mines in this area have gone beyond 3900 m making them some the deepest in the world. As the mining goes deeper, the working conditions have become harsh, thus costly measures are required to regulate them to a tolerable state. This high cost has led to closure of some of the mines in this basin. Though mining has reduced significantly since the early 21st century, this sector still contributes a valuable percentage towards the economy of South Africa.

Gold in this basin is found in association with other mineral ores. Lower abundances of other minerals including sulphur and arsenic bearing minerals such as cobaltite (CoAsS) and arsenopyrite (FeAsS) have also been identified in the matrix of the main ore (Naicker *et al*., 2003).

During the mining processes, the gold ore was mined underground and the resulting tailings dumped on the surface forming what are known as mine dumps. This exposes the associated minerals to the atmosphere leading to the problem of acid mine drainage (AMD), which is the flow of acidic polluted water from mining areas resulting from oxidation of the sulphide minerals by air and water. It can contain different elements, including toxic metals and metalloids depending on the geology of the rock hosting the mineral. As sulphide ores are oxidised, the bound metals are also oxidised resulting in the release of metal ions, high sulphate contents and increased acidity in the surrounding environment (Duruibe and Egwurugwu, 2007)

This research is motivated by the knowledge that the Witwatersrand gold resource bears arsenic bound to the major minerals. Due to the acute toxicity and other health effects associated with arsenic species, their presence in AMD presents a great danger to the surrounding environment as they may leach into surface and ground water or even end up in agricultural soil increasing bioavailability to humans and animals. There is therefore a need for assessment of arsenic contamination in areas around the gold mining sites, including identifying and quantifying the species present by applying simple and sensitive analytical techniques.

CHAPTER 2

LITERATURE REVIEW

This chapter presents a detailed review of the sources, the chemistry and remediation of arsenic in the environment. It also covers analytical methods for arsenic determination.

2.1 Distribution of arsenic

There are abundant sources of arsenic in the environment, with more than 200 minerals having arsenic as a major constituent (Smedley and Kinniburgh, 2002). Arsenic has a strong affinity to bond with other elements. In nature, it generally exists in sulphide and oxide forms (Wang and Wai, 2004). It is also found as different species in fossil fuels, mineral deposits and rock materials such as sedimentary and volcanic rocks. In these enriched sources, arsenic can be released through several natural processes (emissions from volcanic eruptions, weathering of arsenic bearing minerals and biological processes) and a range of human related activities promoting its transport and subsequent risk of exposure.

2.1.1 Rock materials

Arsenic concentrations in the Earth's crust are around 5 mg kg^{-1} and most metamorphic rocks also contain arsenic around the same concentration (Garelick *et al*., 2008). Wang and Mulligan (2006) indicates that, volcanic rocks and their secondary products resulting from weathering are the most common sources of arsenic in the environment, and higher concentrations are found in sedimentary rocks compared to igneous rocks. Tanaka (1988) specifies that the sedimentation process is the one responsible for the concentration of arsenic in this rock type.

2.1.2 Mineral deposits

Arsenic is linked with many types of mineral deposits, being more common in ores of gold, silver, copper and lead among many others (Tanaka, 1988). Besides these ores, significant arsenic concentrations are said to occur in coal deposits. It is also highly associated with sulphide minerals with arsenopyrite (FeAsS), orpiment (As_2S_3) and realger (As_4S_4) known as the common arsenic sulphides in hydrothermal and magmatic ore deposits (O'Day, 2006). Among the many known arsenic sulphides, pyrite is said to be the most abundant arsenic ore mineral in the Earth's crust (Pal *et al*., 2009; Bowell *et al*., 2014). Table 2.1 shows arsenic

minerals common in the environment. These mineral ores are the main starting points introducing arsenic into the environment.

Other rich sources of arsenic are the oxide minerals (O'Day, 2006) including many anhydrous metal oxides (Bowell *et al*., 2014; Smedley and Kinniburgh, 2002). Arsenic exists in these minerals either as part of the compound structure or by sorption interactions. This element is known to adsorb onto various oxides including those of iron (Smedley and Kinniburgh, 2002) and aluminium as well as calcite and clay minerals (Goldberg, 2002). In the presence of iron, arsenic precipitates and strongly binds to the iron compounds because of the high affinity that the two elements have for each other (Smedley and Kinniburgh, 2002). This interaction benefits the mining industry as they are able to use iron compounds to capture arsenic in their waste waters therefore reducing the concentrations released into the environment.

Table 2.1 Major and secondary arsenic minerals (Smedley and Kinniburgh, 2002)

Mineral	**Composition**	**Occurrence**
Native arsenic	As	Hydrothermal veins
Niccolite	NiAs	Vein deposits and Norites
Realger	AsS	Vein deposits, often associated with orpiment, clays and limestones, also deposits from hot springs
Orpiment	As_2S_3	Hydrothermal veins, hot springs, volcanic sublimation product
Cobaltite	CoAsS	High-temperature deposits, metamorphic rocks
Arsenopyrite	FeAsS	The most abundant As mineral, dominantly mineral veins
Tennantite	$(Cu,Fe)_{12}As_4S_{13}$	Hydrothermal veins

Enargite	Cu_3AsS_4	Hydrothermal veins
Arsenolite	As_2O_3	Secondary mineral formed by oxidation of arsenopyrite, native arsenic and other arsenic minerals
Claudetite	As_2O_3	Secondary mineral formed by oxidation of realgar, arsenopyrite and other As minerals
Scordite	$FeAsO_4.2H_2O$	Secondary mineral
Annabergite	$(Ni,Co)_3(AsO_4)_2.8H_2O$	Secondary mineral
Hoernesite	$Mg_3(AsO_4)_2.8H_2O$	Secondary mineral, smelter wastes
Haematolite	$(Mn,Mg)_4Al(AsO_4)(OH)_8$	
Conichalcite	$CaCu(AsO_4)(OH)$	Secondary mineral
Pharmacosiderite	$Fe_3(AsO_4)_2(OH)_3.5H_2O$	Oxidation product of arsenopyrite and other As minerals

2.1.3 Natural water

Jian and Ali (2000) state that elevated arsenic concentrations in natural waters has become a problem worldwide hence bringing a challenge to world scientists. This includes water from rivers, dams, reservoirs, aquifers as well as rain water which are the common sources of drinking water in most areas. Water is one of the most studied matrices in which arsenic contamination has been investigated (Paul *et al*., 2007; Zheng *et al*., 2003). This can also be attributed to the increasing evidence that arsenic in water does not only pose danger through drinking, but also through

contaminated irrigation water due to uptake of arsenic species by food crops (WHO, 2010). In their review, Gillispie *et al*. (2015) indicate that rice is one of the common food crops affected by arsenic contamination, which mostly results from continual irrigation with arsenic contaminated ground water. This also agrees with a study by Mukherjee *et* al. (2017) who studied the level of arsenic contamination in rice crops exposed to different levels of arsenic through irrigation water and contaminated agricultural soil and concluded that the level of arsenic in rice grains was influenced by the arsenic content in both the irrigation water and the soil. The common forms of arsenic in water are of danger to human life even at relatively low concentrations.

Wang and Mulligan (2006) state that in natural water, arsenic occurrence is determined by the regional geology, hydrogeology and the geochemical properties of the aquifer. They further state that climate changes and anthropogenic activities are also contributing factors. The elevated quantities of arsenic in water can therefore result from the arsenic-rich geological make-up of the bedrock from which arsenic is released by geochemical processes such as oxidation and dissolution. The latter is highly affected by the pH and redox conditions of the water.

The common arsenic bearing sulphide, pyrite, is also known to form in sediments of water bodies such as rivers, lakes and oceans. This authigenic production of pyrite occurs under reducing conditions and it has the ability to concentrate arsenic as it occurs. However, since pyrite is unstable in aerobic conditions, it will eventually release the associated trace elements as it oxidises hence leading to elevated arsenic levels in natural waters (Smedley and Kinniburgh, 2002).

Contaminated water sources have been reported in several countries around the world. Bangladesh and West Bengal, (in India), where most of the water sources are wells and aquifers, are said to be the worst affected by arsenic contamination worldwide (Bera *et al*., 2010). Arsenic contamination and poisoning from the ground water in these areas has been widely recorded in the past and most of them show arsenic concentrations way higher than the maximal limit of 10 $\mu g\ L^{-1}$ set by WHO in most of their villages (Bera *et al*., 2010; Chakraborti *et al*., 2003).

2.2 Anthropogenic sources of arsenic

A variety of human activities trigger the release of significant amounts of arsenic in the environment. The primary anthropogenic sources are mining and smelting of metal ores. Other anthropogenic sources include, use of arsenic based pesticides in agriculture, burning of arsenic rich fossil fuels, use in metal-alloying industries and application of arsenic containing compounds in wood preservation. These activities release arsenic into the environment and through different means of transport, it ends up in biota (general life on earth) creating health risk.

2.2.1 Mining and smelting of metal ores

Arsenic pollution contributed by mining activities has been reported in Germany (Mkandawire and Dudel, 2005), Ghana (Smedley *et al*., 1996), Mexico (Razo *et al*., 2004) and Canada (Moriarty *et al*., 2014) among many other mining countries around the world. In South Africa, Naiker *et al*. (2003) reported several trace metals (including total arsenic) to be in elevated concentrations in the Witwatersrand area and further showed that the high concentrations continue into areas downstream from the pollution source. Figure 2.1 shows the geographical image of the Witwatersrand basin.

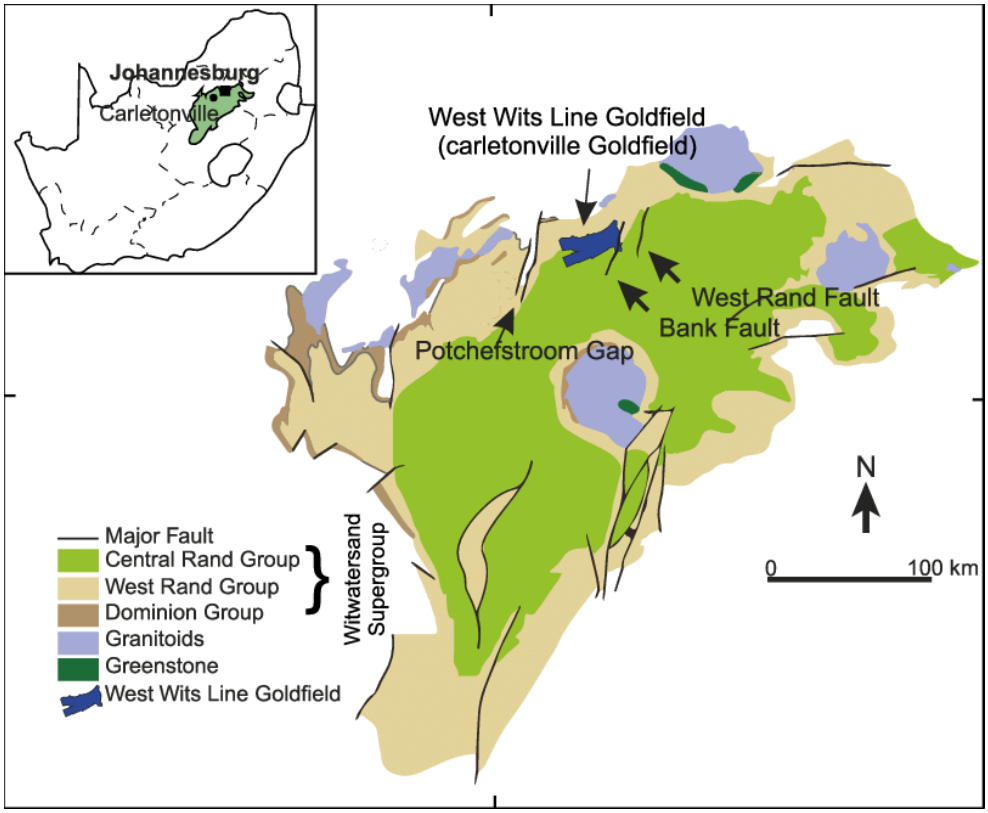

Figure 2. 1 Geological image of the Witwatersrand basin (Nkosi *et al*., 2017)

Most of the arsenic pollution from mining activities does not come from the actual mining of arsenic mineral ores instead it results from mining of other metal ores such as those of gold (Smedley and Kinniburgh, 2002). In the mining operations, to reach the ore deposits of these metals, the Earth's crust is destructed and the waste rock rich in trace elements such as arsenic is brought to the surface. These mine dumps are thus exposed to environmental conditions which results in oxidation hence release and mobilization of arsenic compounds. As a measure of environmental protection, the South African legislation now enforces all mining companies to treat their own waste and to be responsible for environmental remediation and rehabilitation of the mining sites (Feris and Kotze, 2014).

Following mining of metals from the crust, further processing to release them from their ores in their pure forms or as simpler compounds is necessary. This processing can also contribute to the release of arsenic and other associated trace metals in the form of slag (Lin *et al*., 2017), which is the smelting process waste containing a mixture of mineral impurities. This processing uses chemicals and heat to release

the metals from the mineral ores, thereby also releasing toxic gases such as sulphur dioxide, and hydrogen sulphide which contributes to air pollution.

2.2.2 Agriculture and wood preservation

Arsenic compounds have also been used as additives to agricultural chemicals such as pesticides (He *et al*., 2016). Although the use of inorganic species of this element in pesticides has been ceased in some parts of the world because of the high risk of toxicity and exposure, these practices have left elevated arsenic levels in agricultural sites. Arsenic based pesticides are also used in wood preservation to prevent rotting and decay. These compounds are slowly washed off from the wood materials into the soil by rainwater. Since most arsenic compounds have good solubility in water, arsenic in soil has a potential of leaching into lakes and rivers and can therefore end up in drinking water.

2.2.3 Burning of fossil fuels

Fossil fuels are combustible geological deposits of organic nature, buried underground. They result when dead organic matter (plants and animals) are converted over a period of millions of years by heat and high pressures in the Earth's crust forming coal, crude oil, natural gas or heavy oils. Use of fossil fuels is associated with the release of large amounts of arsenic (Owens *et al*., 2005). Human activities including extraction, processing and burning of these fuels in households and power plants, especially coal, to give out heat energy are the sources of arsenic emissions. In the atmosphere, the emitted arsenic can attach to small particles which can either be washed out of air by rain or can be swept by wind and travel long distances. Disposal of coal ashes and fly ash may also lead to further arsenic pollution as it may leach into ground waters.

Following the discharge from the anthropogenic sources in the environment, arsenic can be transported through various means and undergo transformations due to a number of factors, including physical, biological and chemical processes as summarised in Figure 2.2.

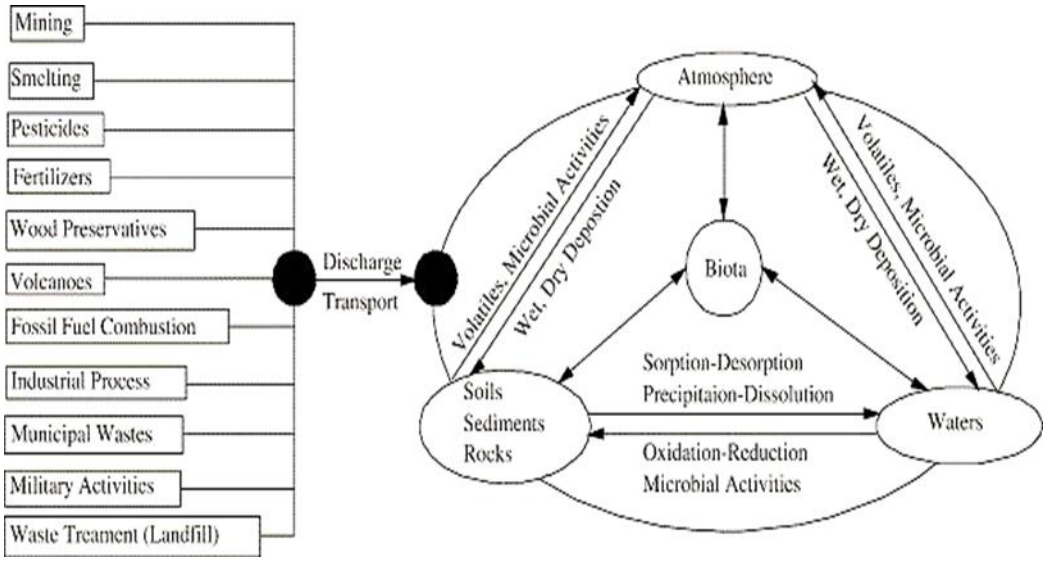

Figure 2.2 The cycle of arsenic in the environment (Wang and Mulligan, 2006)

2.3 Chemistry and speciation of arsenic

Arsenic together with phosphorus, nitrogen, antimony and bismuth is in group V of the periodic table. In the environment arsenic can be present in four oxidation states: As^{5+}, As^{3+}, As^{0} and As^{3-} which can occur in the organic or inorganic form.

In different environmental and food samples, the most studied arsenic species are the inorganic forms of arsenic (arsenate and arsenite) because of their high toxicity but the organic species, dimethylarsonic acid (DMA) and monomethylarsonic acid (MMA) are also included in most food and rice investigations (Llorente-Mirandes *et al.*, 2014; Nookabkaew *et al.*, 2013). Table 2.2 shows some of the important arsenic compounds in the environment. The classification into organic or inorganic arsenic forms depends on the species to which arsenic is bonded to. In combination with oxygen, the cationic arsenic oxidation states (As^{3+} and As^{5+}) are more stabilized because of the strong electronegativity of oxygen in oxidative conditions (O'Day, 2006). This case prevails in water bodies. Smedley and Kinniburgh, (2002) shows that the organic forms of arsenic on the other hand are highly impacted by biological activity and pollutants from industrial activities but their quantities are rarely important in water.

Table 2.2 Important organic and inorganic arsenic compounds in the environment

Name	**Formula**	**References**
Arsenite	$As(OH)_3$	
Arsenate	H_3AsO_4	
Methylarsonic acid or MA^V	$AsO(OH)_2(CH_3)$	
Dimethylarsinic acid or DMA^V	$AsO(OH)(CH_3)_2$	Mishra *et al.* (2017)
Trimethylarsine oxide	$AsO(CH_3)_3$	
Arsenocholine	$(CH_3)_3As + CH_2CH_2 O$	
Arsenobetaine	$(CH_3)_3As + CH_2COOH$	
Arsenosugars (AsS)		
Arsenolipids		Singh *et al.* (2015)

The speciation of arsenic is highly impacted by the pH and the redox potential (Eh). Therefore Eh-pH diagram (Figure 2.3) better explains the species distribution of arsenic under different conditions. The electron potential (pe), which is calculated from the Eh is also indicated in Figure 2.3.

$$pe = \frac{Eh}{0.05916} \text{ at } 25°C \qquad (2.1)$$

The Eh-pH diagram of arsenic shows the presence of the oxyanions in the arsenite (+3) and arsenate (+5) forms over wide redox conditions and pH range including the neutral pH where most toxic trace elements are known to exist in precipitated non-bioavailable forms (Smedley and Kinniburgh, 2002). In reducing conditions at acidic pH levels, the protonated arsenite oxyanion H_3AsO_3 prevails but at higher pH's the existence of $H_2AsO_3^-$ becomes dominant. Under oxidising conditions, the arsenate forms are more dominant. In the presence of a variety of other cations and anions, arsenic complexes may also result in water.

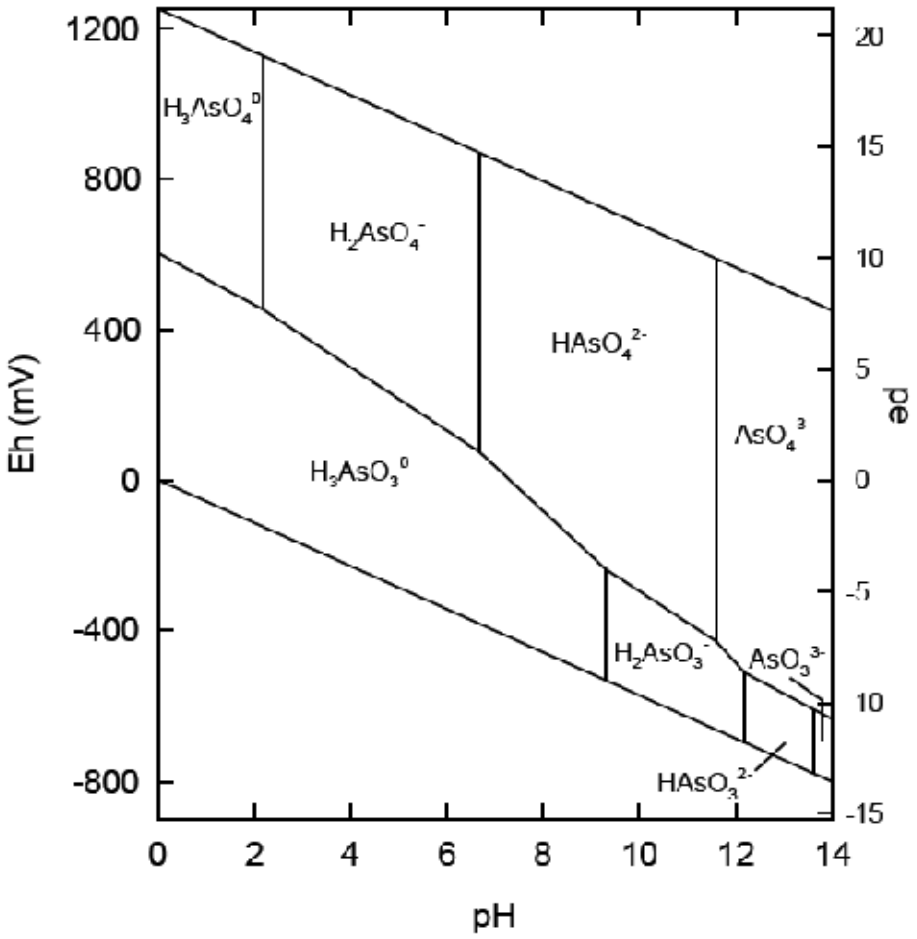

Figure 2.3 Eh-pH diagram of arsenic species in aqueous medium at 25°C and 1 bar total pressure (Smedley and Kinniburgh, 2002)

2.4 Arsenic toxicity and bioavailability

Arsenic is toxic to almost all forms of life. Though plants and microorganisms are known to concentrate arsenic in their tissues, they are also said to have a certain level of tolerance (Mahimairaja *et al*., 2005). The toxicity and high distribution of arsenic, has led to a pressing need for its monitoring and measurement in the environment. Long term exposure to this element is associated with several diseases, thus its regulation is an important public health issue. WHO (2010) shows that conditions that may develop overtime from long term exposure to arsenic include skin lesions, peripheral neuropathy, gastrointestinal symptoms, diabetes, renal system effects, cardiovascular diseases and different types of cancer. The

International Agency of Research on Cancer, classifies arsenic among the group 1 human carcinogens (Martinez *et al*., 2011) meaning that arsenic exposures have been proven to be carcinogenic to humans. In drinking water, WHO (2010) has set the permissible limit of 10 µg L^{-1} and they state in their report that the safe arsenic level in air has not been established yet.

According to Caussy (2003) bioavailability represents the portion of the external dose that reaches the systemic circulation. The bioavailability of arsenic is highly associated with its speciation (Owens *et al*., 2005). This is because not all species may be bioavailable hence the portion that will have an effect on the biological system is not that of the total arsenic in the sample. Owens *et al*. (2005) further indicate that different species may have differences in solubility and mobility, thus since As(III) is more soluble and mobile than As(V) knowledge about the presence and quantity of each species can give relevant bioavailability information as more labile and soluble species are said to be more bioavailable.

Valency is also known to play a significant role in the behaviour and toxicity of arsenic, therefore knowledge about the behaviour of different arsenic species in a sample is critical as their toxicity levels vary greatly. Compounds of As(V) and As(III) are the most prevalent in the environment and the latter oxidation state in the inorganic form is known to be the most toxic to animals and plants because of its potential to complex with the co-enzymes (Ferreira and Barros, 2002).

Arsenic in the body system can be very toxic. Ratnaike (2003) shows that once arsenic is absorbed into the blood stream, it inactivates enzymes and can substitute phosphate in compounds such as ATP, thus, leading to various diseases associated with arsenic exposure. This is because phosphate and arsenate have nearly similar chemical properties including ionization energy and electronegativity. (Estaban *et al.,* 2003; Molin *et al*., 2015; Mishra *et al.,* 2017).

2.5 Arsenic remediation

Remediation is the process of removing harmful pollutants to recover a safe environment and reduce the attenuation of pollution on the environment. It is a

measure of risk management that usually goes together with reduction of pollutant from the source and setting legislation for environmental protection. Soil and water are the common environmental components that most remediation processes target. The high toxicity of arsenic necessitates the need for remediation in contaminated areas for protection of public health.

Numerous physical, chemical and biological arsenic remediation techniques have been developed and studied for arsenic detoxification in various media. Some of these techniques are unfortunately costly and in removing the toxic arsenic, they also alter the natural environment.

2.5.1 Chemical remediation

Chemical remediation uses chemicals to react with pollutants and convert them to less harmful forms. It includes, but it is not limited to, processes such as precipitation and complex formation of pollutants. A typical example of chemical remediation of arsenic pollution is the addition of different iron sources to form insoluble iron oxides. This is because of the affinity of arsenic for iron and its tendency to adsorb to iron compounds thus being immobilized. In their study, Xie and Huang (1998) reported that addition of iron (Fe) and manganese (Mn) significantly reduced the level of water-soluble arsenic species (As(III) and As(V)) in soil which also led to higher rice yields. Mahimairaja *et al*. (2005) also indicates that for arsenic contaminated water, ion exchange resins, iron coated sand and activated alumina are some of the compounds used for remediation.

2.5.2 Physical remediation

This method targets the physical properties of the polluted medium to destruct and reduce the contamination. Some of the common physical remediation techniques used for water are adsorption and membrane filtration while in the case of treating polluted soil, soil mixing is a relevant technique. Physical and chemical remediation techniques often overlap resulting in the use of chemicals in some physical remediation technologies. This is referred to as physico-chemical remediation. For example, in contaminated soil, water and other aqueous solvents such as dilute mineral acids may be used to wash off the contaminant from the soil. The process is usually restricted to small areas as chemicals used may be costly to apply to large areas. Pal and Manna (2010) indicated that some of the disadvantages of physico-chemical processes include cost, necessity of numerous chemical treatments and a need for pre-treatment or post-treatment of the water used in cleaning the soil. This showed that there is a need for more convenient remediation procedures.

2.5.3 Bio-remediation

Bio-remediation shows much greater potential than the previous two technologies discussed as it uses more environmentally friendly processes. This remediation technology makes use of microorganisms and plants to absorb and reduce the effect of toxic pollutants naturally. Some microorganisms act as catalysts for oxidation of Fe(II) to Fe(III) promoting the removal of arsenic in the process by adsorption or co-precipitation. Microorganisms such as *Gallionella ferruginea*, *Leptothrix ochracea* (Katsoyiannis and Zouboulis, 2004) and *Acidithiobacillus ferrooxidans* (Fukushi *et al*., 2003) have been applied and proved to be effective for removal of arsenic.

The use of plants for remediation is referred to as phytoremediation. It involves growing plants that have a genetic ability to concentrate and immobilize the contaminant in a polluted area. As plants absorb water from the contaminated area, they also absorb the pollutants reducing pollutant concentration in soil hence the mobility of the contaminant. In the plant system, the contaminant is metabolized

and eventually volatilized through transpiration. This remediation method is responsive to a variety of pollutants and its advantages include low cost and applicability to large areas while conserving the natural environment.

The similarities between arsenic and phosphorus are believed to be responsible for the plant uptake of the arsenates by phosphate uptake mechanisms. For an uncontrolled study, Ma *et al.* (2001) discovered that among the plants growing in an arsenic contaminated site in Central Florida, only *Pteris vittata* was found to hyperaccumulate arsenic while in a 30 days controlled study, Zhao *et al.* (2002) concluded that *Pteris cretica, Pteris longifolia and Pteris umbrosa* hyperaccumulate arsenic to a similar degree. Estaban *et al.* (2003) on the other hand did a study for up to 4 weeks using *Lupinus albus* to study the uptake of arsenate and phosphate and concluded that arsenate uptake was reduced in the presence of phosphate.

2.6 An overview of sampling and analytical methods for arsenic determination

Accurate determination of metals and metalloids at trace levels is very critical as some of them are known to be toxic even at very low levels. Determination of arsenic speciation in particular is critical and it requires several steps from sampling throughout to the instrumental analysis stage. The illustration below (Figure 2.4) shows steps involved for the whole process of chemical analysis to prevent any loss of analyte or inter-conversion of species.

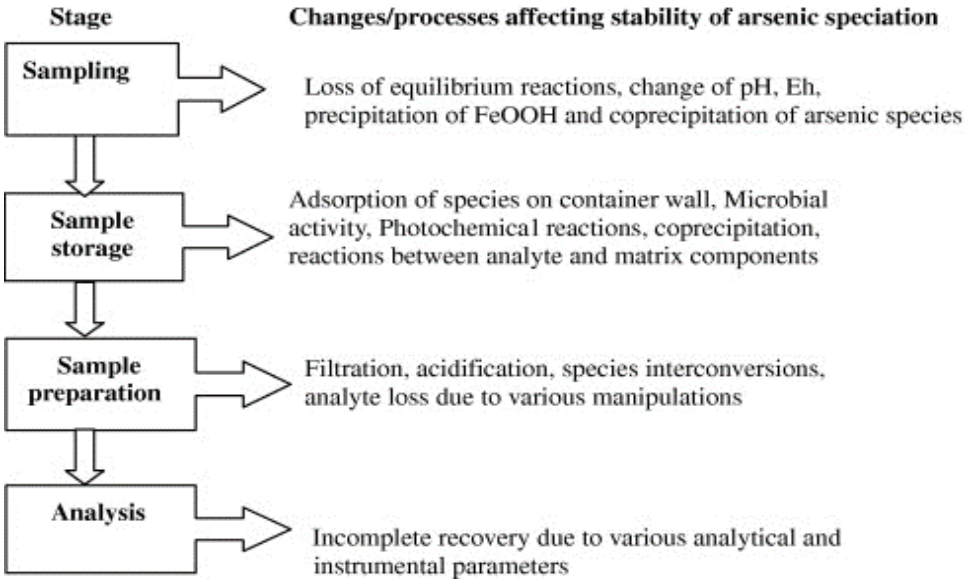

Figure 2.4 Processes and conditions affecting stability of arsenic speciation throughout stages of chemical analysis (Kumar and Riyazuddin, 2010)

Tablle 2.3 is also included showing more recent references on processes affecting arsenic stability.

Table 2. 3 Processes/conditions influencing the stability of arsenic species

Process/Condition	**References**
Change in pH and Eh	Pillay and Kindness, (2016); Radke *et al*. (2012); Rukh *et al*. (2015)
Temperature and salinity	Radke *et al*. (2012)
Chemical extraction	Pillay and Kindness, (2016)
Microbial growth/death in samples, adsorption to containers	Maher *et al*. (2015)

A detailed review of the various stages involved in analysis and methods suitable for application in arsenic speciation are discussed in the subsequent sections.

2.6.1 Sampling, pre-treatment and storage

The sampling step is critical for any analysis as most errors can be introduced during this stage. It requires proper understanding of both the analyte and the matrix. For arsenic speciation analysis, the choice of sampling container is very crucial as it must preserve the species distribution. The sampling container must not promote adsorption or leaching of analytes and it should be made of a material free from the analyte to prevent enhancement of the concentration. Generally for all analytes, clean containers of a suitable material are used for sample collection followed by field measurements such as pH, conductivity and temperature where possible. These field measurements are also predetermined by the condition of sample in the environment as other samples may change during transportation. If instrumental analysis is not done immediately and the sample is to be stored for some time, sample pre-treatment and preservation may also be necessary.

For arsenic speciation studies, sampling containers are normally polyethylene-based with an opaque colour. The dark colour is necessary to prevent photochemical reactions. The sampling container must be rinsed first with the site water before collecting the sample and as part of the sample pre-treatment, water samples are usually filtered to remove particulate matter as it may dissolve over the storage period and thus give inaccurate test results.

Depending on the analysis method to be used, different chemicals may be used for preservation of arsenic speciation. Some of the chemicals that have been studied have proven to be effective to a certain point while others have been found to alter the speciation. Bednar *et al*. (2002) evaluated the use of mineral acids and ethylenediaminetetraacetic acid (EDTA) for preservation of arsenic species distribution in ground water and AMD and they determined 1.25 mM EDTA to be the best preservative. Other studies like that by Paul *et al*. (2007) used concentrated hydrochloric acid (HCl) (1 ml per 100ml sample) for preservation of tube well water, while Salaün *et al*. (2007) on the other hand did not report addition of any preservatives for their arsenic speciation study of seawater and fresh water.

Storage conditions that do not affect the distribution of arsenic species in water samples have also been discussed before. For examples, Komorowicz and Barałkiewicz (2016) froze their water samples immediately after sampling without adding any preservatives and only thawed and filtered the samples on the day of analysis.

Solid samples undergo different sample treatment procedures depending on the type of sample. Soil, sediments, plants and food samples are also some of the common solid matrices studied for arsenic contamination. For soil and sediment sampling, an auger is normally used to collect the sample and transfer it into a storage container. The soil chemistry may change overtime so immediate analysis following sampling is recommended, however this is not always possible hence storage at temperatures below 4°C in a dark may be used. The plant samples on the other hand are often picked by hand at sampling points obtaining the above ground tissue together with the roots depending on the scope of analysis. After sampling, drying and homogenizing of the sample are also necessary. Sanz *et al*. (2007) used 55°C for soil drying and Garcia-Manyes *et al*. (2002) investigated loss of total arsenic at temperatures between 20°C and 100°C and concluded that there was no loss of analyte as the results showed no significant difference in the temperature range used for drying.

For solid samples, prior to analysis by most instrumental techniques, the sample must be converted to an aqueous form. This step is often associated with introduction of several errors and alteration of the original nature of the sample. Various sample treatment procedures have been used in arsenic determination studies including microwave assisted extraction (B'Hymer and Caruso, 2004). This extraction method results in a homogeneous liquid sample free from organic matter suitable for spectroscopic and electrochemical analysis methods. Microwave assisted extraction is also affected by the nature of the matrix and solvent used for extraction as the solvent must be both microwave absorbing and analyte selective. Tatke and Jaiswal, (2011) indicate that since some solvents are transparent to microwaves hence do not heat up upon microwave treatment, a mixture of transparent and microwave active solvents to achieve ideal results may be used.

They further state that matrices with finer particle sizes may be ideal for effectiveness of this process even though separation after extraction may be difficult. Which they in turn suggest that an extra step of filtration or centrifugation can overcome. In an analysis for arsenic species in contaminated soil samples, Garcia-Manyes *et al*. (2002) employed microwave assisted extraction using a solution of phosphoric acid (1.0 mM L^{-1}) and ascorbic acid (0.1 mM L^{-1}) as an extracting solution, while Sanz *et al*. (2007) used ultrasound probe sonication to assist arsenic extraction from soil samples with only phosphoric acid as an extracting agent and reported the method to be an effective sample treatment tool.

2.6.2 Common analytical techniques for arsenic determination

There are a number of instrumental techniques that are applicable for determination of arsenic at very low concentrations. Spectroscopic methods are some of the popular techniques applied in qualitative and quantitative analysis of metals and metalloids from their natural sources and contaminated media. These are techniques based on interaction of various types of electromagnetic radiation (EMR) with matter. The techniques include atomic absorption spectrometry (AAS), atomic fluorescence spectrometry (AFS) and inductively coupled plasma-atomic emission spectrometry (ICP-AES). Although it is not a spectroscopic technique, inductively coupled plasma-mass spectrometry (ICP-MS) is also a standard technique for arsenic determination.

AAS, AFS and ICP-AES have been applied vastly for elemental analysis in the past, but each has its own limitations. For example, AAS does not provide simultaneous multi-element determination and for ICP-AES the sensitivity is generally low compared to ICP-MS, the latter of which is more advanced and is applicable to a wider range of samples. The technique is one of the most sensitive analytical techniques being used currently for total elemental analysis and it is much more suitable than the other three techniques mentioned because it is more precise, has low detection limits and has the ability to do multi-element analysis thus reducing the analysis time.

The popularity of the mass spectrometric methods is also associated with the application of inductively coupled plasma (ICP) sources. The ICP source is a very high temperature source that can go as high as 10 000 K. ICP is not the only plasma source used in spectrometric techniques. Direct coupled plasma (DCP) and microwave induced plasma (MIP) have been used in the past but their application is not as common as that for ICP.

The spectroscopic techniques on their own are not applicable for speciation analysis and would require separation of the species beforehand. The use of hyphenated methods for speciation analysis has therefore become more common in recent studies (Ma *et al.,* 2016; Choi *et al.,* 2016). These are a combination of separation techniques with the detectors such as the spectroscopic and spectrometric detectors mentioned. Other techniques like nuclear magnetic resonance (NMR) and electrochemical methods which do not require hyphenation but instead provide direct information about the species of interest without incorporation of any separation method have been used (Michalke, 2003). The problem facing direct speciation with NMR is that with environmental samples, the analyte exists in very low concentration levels that are undetectable by NMR. Also, with electrochemical techniques, the presence of high organic load in samples is said to interfere with complete analysis (Michalke, 2003). Therefore the use of hyphenated or combined methods for speciation analysis has worked as a solution for the problems encountered with direct speciation.

Chromatography, capillary electrophoresis (CE) (Caruso and Montes-Bayon, 2003; Shah *et al*., 2004) and field flow fractionation (FFF) (Rosen and Hieftje, 2004) are some of the separation techniques that have been employed coupled with spectroscopic or spectrometric detectors in hyphenated methods. The methods involving the use of mass spectrometry for detection have proved to be more useful and hence more popular than the initial arrays which employed AAS, AES and AFS as detectors in hyphenated techniques (Rosen and Hieftje, 2004).

Different liquid chromatographic (LC) techniques combined with ICP-MS have been applied for arsenic speciation. For example, Mattusch and Wennrich (1998)

developed and successfully used ion chromatographic methods to separate arsenic species from sewage samples detecting suspended and soluble species as well as neutral and cationic species of arsenic in a single chromatographic run. Londesborough *et al*. (1999) and He *et al*. (2016) also made use of the qualities of high performance liquid chromatography (HPLC) coupled with ICP-MS to study arsenic species from mushroom extracts collected from an arsenic contaminated area as well as for determination of total arsenic and speciation in apple juice.

Detection of arsenic with ICP-MS is also faced with complications. The accuracy of results is often affected by interferences arising from the polyatomic ions that have the same mass number as arsenic. $^{40}Ar^{35}Cl$ is the common interferant as it gives the mass number of 75 which may lead to the measurement of more elevated concentrations than the actual analyte concentrations. Literature suggests that use of a reaction dynamic cell can help overcome this problem (Hsieh *et al*., 2010). The use of this cell allows the analyte to react with a different reaction gas thereby forming ions of the analyte with a different mass number as compared to that of the polyatomic interferences. For example, Hsieh *et al*. (2010) used CH_4 as a reaction gas and determined arsenic as $^{75}As^{12}CH_2^+$ at m/z = 89.

Though advanced, most of the discussed spectroscopic detectors and hyphenated techniques have bulky, highly sophisticated instrumentation which are usually very expensive. Therefore simpler and cheaper techniques for arsenic speciation analysis are worth exploring.

2.6.3 Electrochemical methods, electrodes and interferences

Electrochemical methods study the analyte by measuring an electrical parameter of the solution and relating it to the amount of analyte in an electrochemical cell. They give both qualitative and quantitative information and can be classified into different types. Some of the fundamental classes of electrochemical methods are potentiometry, coulometry and voltammetry. The classification is based on the electrical parameters that are controlled and monitored in the cell during measurement. In potentiometric analysis, a two electrode system is used and the potential difference between the two electrodes is measured. In coulometry a

constant amount of current is applied to convert an analyte from one oxidation state to another and the number of electrons transferred is obtained. In this study, a deeper review of voltammetry was focused on because of its applicability in arsenic speciation analysis.

2.6.3.1 Voltammetry

Techniques based on voltammetry use a three electrode system made up of a working, auxiliary and reference electrode (Figure 2.5). In this technique, information about the analyte is obtained by measuring current as a function of applied potential. The method is applicable to samples containing species that can undergo redox reactions. This electrochemical technique has been widely used for arsenic speciation analysis (Raj *et al.*, 2014; Zhou *et al*., 2017).

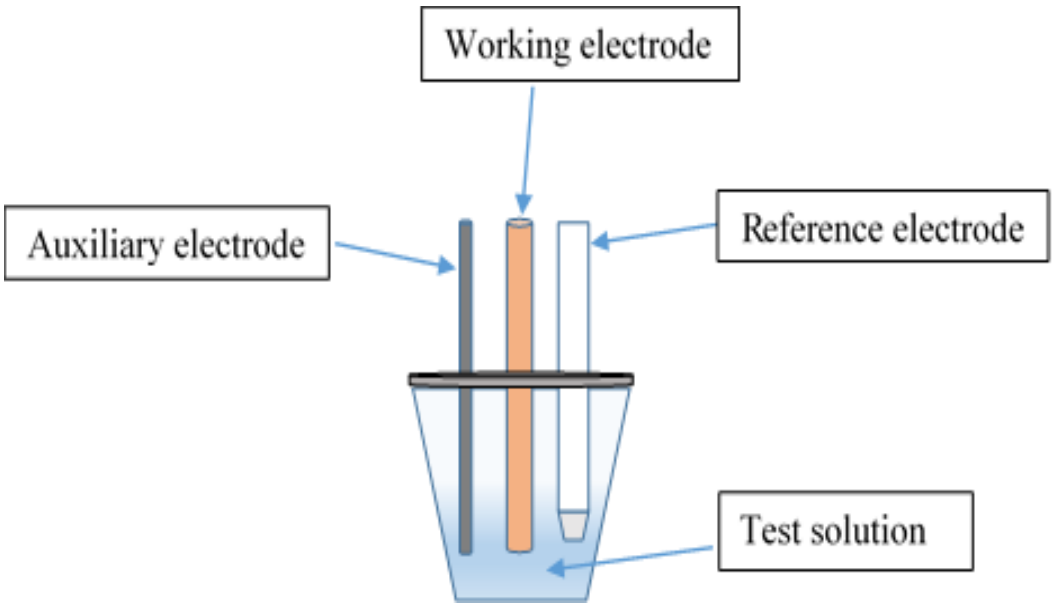

Figure 2.5 Schematic representation of a three electrode system

Cyclic voltammetry (CV) is a powerful technique for the study of electro-active species. The potential is applied to the working electrode (normally in reference with silver/silver chloride or saturated calomel electrodes) and scanned linearly or in a stepwise manner back and forth in a potential range while recording the current produced. For CV investigations, the potential is ramped linearly against time and if the analyte has a reversible property, then it implies that if it gets oxidised during a positive going scan, in the negative going scan it will be reduced back to its initial

state or vice versa giving the anodic peak and the cathodic peak in one CV scan. For any electrochemical analysis, it is important that the analyte studied is redox active in the potential range used.

Stripping voltammetric techniques have been explored for arsenic speciation and have been classified as highly sensitive electrochemical techniques with low detection limits (Paul *et al*., 2007; Raj *et al*., 2014; Salaün *et al*., 2007). According to Mays and Hussam (2009) stripping voltammetry requires minimum sample preparation, exhibits distinctive selectivity for As(III) with exceptionally high sensitivity and very low detection limits close to those of atomic absorption and inductively coupled plasma spectroscopic techniques. In addition to these characteristics, other advantages include portability of the instruments used in electrochemistry hence more applicability for field analysis and low cost (Mays and Hussam, 2009). Though electrochemical techniques seem to have more advantages over other speciation analysis techniques, they are limited by the short stability time of electrodes (Jedryczko *et al*., 2016).

The analyte determination in stripping voltammetry involve two main steps, the pre-concentration step and the determination step. During the pre-concentration, a constant potential is applied to the solution either reducing or oxidising the analyte to the form that will be deposited on the working electrode. This step is followed by the determination step which involves stripping of the deposited analyte from the electrode surface by the process opposite to that applied in the pre-concentration step. This is achieved by varying the potential at the working electrode and monitoring the current produced. Depending on the process happening during the determination step, the technique can either be classified as anodic stripping voltammetry (ASV) when the analyte is determined by oxidation or cathodic stripping voltammetry (CSV) when the analyte is determined by reduction. During the pre-concentration step, the analyte flux to the electrode surface is improved by stirring or making use of a rotating disk electrodes. For arsenic speciation, these electrochemical techniques are applicable to inorganic arsenic species. For example, Antonova and Zakharova (2016), Jedryczko *et al*. (2016) and Salaun *et*

al. (2007) all used electrochemical techniques (though they were different methods) to study inorganic arsenic species.

In stripping techniques during the determination step, the potential applied can be in a normal pulse, differential pulse or square wave form. Paul *et al*. (2007) indicated that the pulse voltammetric methods have high performance and low detection limits that enable quantification at levels as low as 10^{-8} M. Paul *et al*. (2007) further compared differential pulse anodic stripping voltammetry (DPASV), square wave anodic stripping voltammetry (SWASV) and normal pulse anodic stripping voltammetry (NPASV) for arsenic speciation and determined SWASV to be more selective and appropriate among the other methods. Salaün *et al*. (2007) also indicated that for arsenic speciation, most methods recently used were based on ASV, CSV and anodic stripping chronopotentiometry (ASC) and all depend almost entirely on the detection of As (III) using either gold (Au) or mercury (Hg) based electrodes.

2.6.3.2 Electrodes used in voltammetry

Various electrodes have been explored for application the in electrochemical determination of trace pollutants in the environment. Most electrodes are made from inert materils or precious metals such as carbon, platinum and gold. Mercury based electrodes have also been applied vastly if the field of electrochemical analysis however, Greschonig and Irgolic (1992) indicated that the low solubility of As(0) in mercury, makes these electrodes less ideal for anodic stripping determinations. That been said, He *et al*. (2007) determined arsenic species on a hanging drop mercury electrode (HDME) using differential pulse cathodic stripping voltammetry. Although mercury based electrodes provides high sensitivity because of the renewability of the mercury drops, they are disadvantaged by the high toxicity of mercury hence application of other environmentally friendly electrodes is preferred over them.

For electrochemical arsenic determination, various electrodes have been explored as alternatives to mercury electrodes. Carrera *et al*. (2017) indicated that because of the good interaction between gold and arsenic, gold electrodes are the most suitable

working electrodes. Gold electrodes have been applied in their bare and modified forms in the electro analytical field depending on the type of application. For example, Nombona *et al*. (2009) used self-assembled derivatives of Co(II) phthalocyanines to modify a gold disc electrode, gold coated fibre and gold ultra-micro cylinder for comparison in the detection of L-cysteine and obtained better results with a gold disc.

For detection of arsenic, other electrodes, modified with gold or in their pure form have been applied. A platinum working electrode (Wei and Somasundaran, 2004), carbon fibre ultra-microelectrode modified with gold nanoparticles (Carrera *et al*., 2017) and a gold wire microelectrode (Zhou *et al*., 2017) are examples of electrodes that have been used for arsenic studies.

2.6.3.3 Interferences in electrochemical determination of arsenic

Electrochemical determinations are highly sensitive hence have a potential of being affected by small traces of contaminants. The determination of arsenic by ASV on a gold electrode is said to be affected by presence of traces of other metal ions such as those of mercury and copper (Greschonig and Irgolic, 1992). The oxidation of these elements interfere with arsenic determination because of their close anodic potentials which lead to overlapping of peaks. The interference of mercury is associated by the high affinity of mercury to gold which results in Au-Hg amalgam formation at the electrode surface. Giacomino *et al*. (2008) indicated that this affinity is useful when the analyte of interest is mercury since it enhances the pre-concentration effect of Hg, but they further stated that the amalgamation changes the structure of the electrode surface.

2.6.4 Geochemical modelling

Geochemical models are tools that use specific computer softwares to simulate the processes occurring in the environmental systems. Environmental processes are affected by diverse aspects such as the composition of the system, the pH and redox potential of the medium. These aspects are significant as they affect the processes occurring in the environment hence the model output too, therefore they should be defined in the model to get accurate results. The processes occurring in the

environment that can affect the quality of the water systems include dissolution, precipitation and evaporation. Speciation of the elements in the water matrix also has a great impact on the water quality. PHREEQC is a common program used in geochemical modelling to study these processes. It is based on chemical kinetics and equilibrium chemistry.

Application of these models in geologic systems is associated with difficulties in experimental speciation studies of sulfidic matrices (Couture and Cappellen, 2011). Various studies involving applications of geochemical models for different environmental simulations are available in literature (Grover *et al*., 2016; Nekhunguni *et al*., 2017). For example, they can be used to understand the possible reactions occurring in the system and the way they proceed, or to predict the processes that led to a known environmental condition. The latter case is referred to as inverse modelling.

Though PHREEQC modelling has various capabilities, summarised in this research is its use in speciation modelling as found applicable in this study. For elements that exist in different oxidation states like arsenic, geochemical models can be used to predict the dominant species under specified environmental conditions or even study the conditions that influence the dominance of one species over another. For this calculation, it is important to know the total concentration of the analyte and the composition of other elements (both cationic and anionic species) known to affect the precipitation and dissolution of the analyte as they too contribute to the distribution of species. In speciation studies, the geochemical models can therefore complement experimental data gathered from field and laboratory techniques such as ICP-MS and IC to provide relevant speciation results with less effort applied than when using the speciation techniques mentioned earlier in this chapter. Those techniques rely on the basis that the species distribution will be maintained after sampling however, the species distribution can vary greatly once a sample has been removed from the natural system (Reeves, 1997).

While both hyphenated techniques and electrochemical methods have been applied widely for arsenic speciation around the world only few publications are available in literature on applications to AMD, possibly because of the complex matrix.

Geochemical modelling on the other hand offers a simpler analysis for the complex matrices such as AMD compared to these techniques as it only uses the total analyte concentration to predict the distribution of species. In South Africa, there is limited published information on the degree of arsenic pollution from the mining activities and its potential effects on the surrounding environment. Therefore there is a need to identify and quantify arsenic species in areas around the mining sites. This study explored the use of DPASV, spectroscopic and spectrometric techniques in combination with geochemical modelling for the determination of arsenic species present in AMD from the Witwatersrand area.

2.7 Method validation

Before application of any method for analysis, validation to confirm that the method is suitable for that application is necessary. The method validation results help judge the performance of the method and this judgement is based on various parameters called figures of merit. These include accuracy, precision, linearity and range and the limits of detection and quantification.

2.7.1 Accuracy

It is described as the closeness of results to the true value. The certified reference materials or standard solutions with known amount of analyte and are analysed and utilized to check if the amount determined by the method is within the confidence limits.

2.7.2 Precision

This is described as the measure of the closeness of results to each other. It expresses the reproducibility of results. Ideally the precision of results should not be greater than 10%.

2.7.3 Linearity and range

These parameters are determined from the method calibration. The calibration is expected to be linear over a certain range indicating good correlation between the

analytical response and the analyte concentration. The wider the linear range, the better the method as it becomes more applicable for different analyte concentrations. The linearity is evaluated by the coefficient of determination (R^2), which must be close to 1 for a good correlation of the x and y values.

2.7.4 Limits of detection and quantification

Limit of detection (LOD) is the minimum amount of analyte that can be confidently distinguished from the signal of the blank (background signal) while limit of quantitation (LOQ) is the minimum amount of analyte that can be quantified with good precision and accuracy. There are different approaches towards the calculation of these parameters described in literature. Using the regression method, the LOD and LOQ are represented by equations 1 and 2 respectively.

$$\text{LOD} = \frac{3\ \text{SDresponse}}{b} \tag{2.2}$$

$$\text{LOQ} = \frac{10\ \text{SDresponse}}{b} \tag{2.3}$$

Where $SD_{response}$ is the standard deviation of the signal and b is the slope of the regression line.

CHAPTER 3

AIM AND OBJECTIVES

The chapter gives the general aim, objectives and hypothesis of this study.

3.1 Aim

The main aim of this research was to assess the speciation and bioavailability of arsenic in acid mine drainage and natural water from the Witwatersrand mining area.

3.2 Objectives

This was achieved by addressing the following objectives:

- Optimization and validation of differential pulse anodic stripping voltammetry (DPASV) method for determination of inorganic As(III).
- Optimization of the reduction process of As(V) to As(III) prior electrochemical determination of the total arsenic.
- Assessing the applicability of DPASV as a tool for the determination of arsenic species in AMD and natural water.
- Use of geochemical modelling in combination with experimental data to study distribution of arsenic species in AMD.

3.3 Hypothesis

This study was based on the hypothesis that AMD arising from mining activities in the Witwatersrand basin contains high concentrations of toxic and bioavailable arsenic species which can result in contamination of the surrounding water sources. Conditions such as temperature and pH can also affect the stability of the present arsenic species hence influence bioavailability.

CHAPTER 4

METHODOLOGY

The chapter covers the sampling, sample preparation and analytical methods followed for this study.

4.1 Chemicals and reagents

All solutions were prepared using deionized water (18.2 MΩ.cm at 25°C) obtained from a Milli-Q-RO4 water purification system by Millipore (Bedford, USA). The chemicals used in this work were of pure analytical grade. For electrochemical studies, stock solutions of As(III) and As(V) were prepared by dissolving the required quantity of arsenic trioxide (As_2O_3) (May and Baker LTD, Dagenham, England) and sodium hydrogen arsenate ($Na_2HAsO_4 .7H_2O$) (J.T Baker Chemicals, Phillipsburg, USA) respectively, in deionized water. Potassium ferricyanide ($K_4Fe(CN)_6$, hydrochloric acid (HCl) and ICP stock solutions were purchased from Sigma Aldrich (Johannesburg, SA) while Nitric acid (HNO_3) was purchased from Associated Chemical Enterprises (Johannesburg, SA).

4.2 Instrumentation

For field measurements, a portable field probe supplied by Hanna Instruments (Johannesburg, SA) was used for determining the redox potential, conductivity, temperature and pH of samples. The anion concentrations were determined using a Metrohm 761 Compact IC (Herisau, Switzerland) while all electrochemical analyses were obtained using a Metrohm Autolab potentiostat (PGSTAT 10) connected to a VA 663 stand. The electrochemical system used in this study was interfaced to a computer using GPES software. Spectrometric analyses of the samples was achieved by ICP-MS (Agilent 7700 Series) for low concentrations and ICP-OES (Spectro Genesis) for more concentrated metals. For all mass measurements, an analytical balance with up to 4 decimal places and 220 g capacity supplied by OHAUS was used.

4.3 Sampling and sample preparation

Clear polyethylene bottles were used as sample collection. The bottles were cleaned with detergent, rinsed with tap water then again with deionized water before leaving them in 10% nitric acid. The nitric acid bath was used to remove any metals that could be adsorbed onto the containers. On the day of sampling, the containers were

rinsed thoroughly with deionized water and at each sampling site, they were further rinsed with AMD and dam water respectively, before collecting the sample.

Spot sampling was used in this work. The sampling site was decided based on the geological information from literature which indicates that the Witwatersrand gold reef has arsenic bearing minerals within it (Naicker et al., 2003). Therefore an area near in the Central Rand goldfield of the Witwatersrand basin in SA, where toxic metal ions are thought to be at high levels was sampled (Figure 4.1).



Figure 4.1 Photograph of the sampling site showing tailings, AMD run off and small AMD ponds

The samples were collected at different points in Meadowlands, Roodepoort in Johannesburg. The region is an old gold mining area and has several mine dumps. The mine drainage water flows from upstream down to M77 road and goes through to the other side of the road which has human settlements further down. An AMD sample was collected just near to the M77 road (on the left side) (26°11'07.4''S 27°52'51.1''E) and another sample was collected from Fleurhof dam (a mine polluted dam downstream near human settlements) (26°11'53.7''S 27° 54'34.3''E). Redox potential (Eh), conductivity and pH of the samples were recorded at the sampling sites then the samples were put in a cooler bags and transported to the laboratory.

On arrival to the lab, the samples were filtered using a 45 μm syringe filters then the clear polyethylene bottles used for storage were covered with aluminium foil to prevent light from going through and promoting photocatalytic reactions. The AMD sample was not acidified as was done by other authors for water samples (Salaün *et al*., 2007) also because the field measurements already indicated a very low pH (below 3), which was enough to prevent adsorption of the metal/metalloid ions to the container. For Fleurhof dam water, the samples were acidified to pH 2 using either hydrochloric acid or nitric acid (HNO_3) depending on the method to be used for metal analysis. The portions of the samples that were to be analysed for total anion concentrations did not require any pH adjustment. The samples were then stored at 4°C until analysis was done.

For this study, electrochemical methods, spectrometric techniques and geochemical modelling were employed.

4.4 Electrochemical analysis

Cyclic voltammetry (CV) was used as a preliminary method to characterise the electrode, to investigate the behaviour of the electrolyte in the potential range used, to investigate the behaviour of potassium ferricyanide on a gold disk electrode to check if the electrode functions properly and later to study the oxidation/reduction of arsenic and determine the oxidation potential of arsenic. Following this, a more

sensitive technique-DPASV was used for both qualitative and quantitative arsenic studies.

In DPASV, the voltage is applied in pulsed forms and the current is sampled twice just before the pulse application and once again late in the pulse life. The current difference is determined and plotted against the potential to give a voltammogram. The peak height is directly proportional to the analyte concentration.

For both electrochemical methods, a three electrode system with a gold rotating disk working electrode (2 mm diameter), Ag/AgCl (3 M KCl) reference electrode (separated from the test solution by a salt bridge) and a glassy carbon rod counter electrode was used (Metrohm, SA) . All the potentials reported in this work are with respect to the Ag/AgCl (3 M KCl) electrode.

The suppliers of the gold disk electrode used in this work do not recommend polishing of the gold electrode unless sensitivity decreases significantly hence the working electrode was not polished as suggested until it started showing a significant decrease in sensitivity. In that case, the electrode was polished on a polishing mat first using 1 μm alumina, then finally 0.3 μm alumina.

Before any analysis, the working electrode had to undergo a pre-treatment procedure. The solid disk gold electrode was cleaned by immersing it in 0.1 M NaOH for 30 minutes before each experiment. The electrode was then rinsed with deionised water, then ethanol and with deionised water again to ensure thorough cleaning. This was followed by electrochemical activation of the electrode using 50 cyclic voltammetry scans (Raj *et al*., 2014), which were done daily in 0.5 M HCl electrolyte solution before the beginning of the experiment. In general, after 8 scans the voltammograms would start to show consistency and remained unchanged with further scans.

For DPASV studies, the step potential of 0.005 V, modulation time of 0.05 s and interval time of 0.5 s were used. Other parameters including deposition potential (DP), deposition time (DT), rotation speed (RS) and modulation amplitude (MA) were optimized and they are further discussed in chapter 5.

A 20 ml test solution was used for each analysis. The solution was purged for 10 min with ultra-high purity nitrogen gas to remove oxygen followed by application of the appropriate electrochemical method. The oxygen was removed from solution to avoid its interference by reacting with the analyte and also to avoid production of hydrogen peroxide as oxygen is also electro-active. Solution homogeneity and flux of the analyte toward the electrode surface were achieved by using a rotating disc electrode. The concentrations were determined by standard addition and a linear baseline in the GPES software was used to fit the peaks. The peak currents were then plotted against the concentrations of the added arsenic standard and the percentage recovery was calculated using the equation below:

$$\text{Percentage recovery} = \frac{\text{Measured concentration}}{\text{Prepared concentration}} \times 100\% \qquad (4.1)$$

The setup of the system used for this work is illustrated in Figure 4.2.

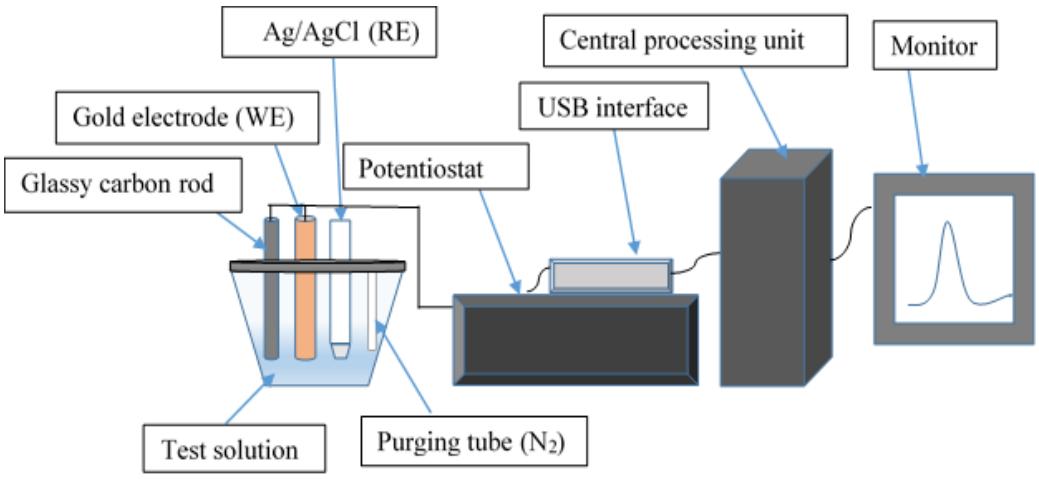

Figure 4.2 Schematic representation for the electrochemical system used for determination of arsenic

As(V) is electrochemically inactive (Greschonig and Irgolic, 1992), therefore it cannot be directly detected. After detection of As(III), As(V) is the reduced to As(III) to obtain the total arsenic, then the As(V) concentration is evaluated by difference. The reduction of As(V) was achieved by using sodium thiosulphate (Raj *et al*., 2014) as a reducing agent in an acidic medium. The overall reduction of the As(V) species (given here as that below pH 2) is thought to be based on reaction 1

below. The thiosulphate (with S having an oxidation number of +2) is oxidised to sulphur dioxide (with S having an oxidation number of +4). The presence of elemental sulphur is due to the reaction of the thiosulphate with the acid as shown in reaction 2.

$$H_3AsO_{4(aq)} + 4H^+_{(aq)} + S_2O_3^{2-}{}_{(aq)} \rightarrow H_3AsO_{3(aq)} + S_{(s)} + SO_{2(g)} + 2H_2O_{(l)} \quad \text{Reaction 1}$$

$$2H^+_{(aq)} + S_2O_3^{2-}{}_{(aq)} \rightarrow S_{(s)} + SO_{2(g)} + H_2O_{(l)} \quad \text{Reaction 2}$$

According to reaction 1, the molar ratio of As(V) to the thiosulphate species is 1:1 and it occurs in the presence of excess acid. A modified reduction procedure from Raj *et al*. (2013) was used and the mass of sodium thiosulphate needed for reduction of As(V) was optimized. To obtain the optimum mass of sodium thiosulphate for reduction of As(V), equal volumes of As(V) (10 ml) and the electrolyte solution (10 ml) were mixed together such that the final solution contained 25 µg L^{-1} As(V) and 0.5 M HCl. To that concentration, different masses of sodium thiosulphate were added to determine the optimum. The solutions were then heated for 30 minutes at 75°C, stirred for 15 minutes while maintaining the temperature at 75°C and lastly purged for 15 minutes with nitrogen to get rid of SO_2 fumes. The samples were cooled to room temperature before they were taken for instrumental analysis. Figure 4.3 summarises the reduction procedure used.

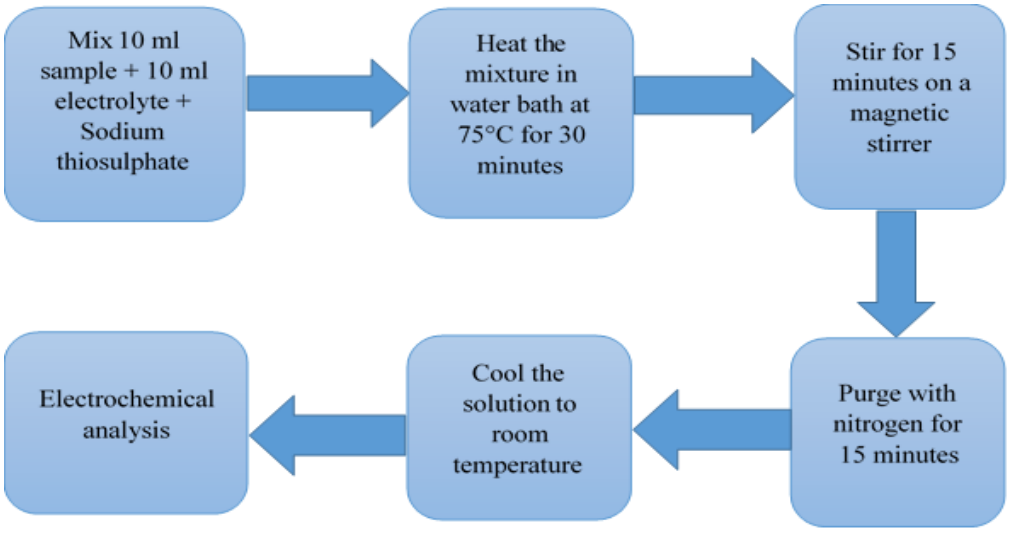

Figure 4.3 Flow chart of the reduction of As(V) for electrochemical analysis.

4.5 Determination of metal concentrations

Total analysis of arsenic (As) and other metals, some of which are known to co-precipitate arsenic including manganese (Mn), iron (Fe), Nickel (Ni), lead (Pb), copper (Cu) and aluminium (Al) was achieved using spectrometric and spectroscopic techniques. For those metals that were in concentrations beyond the ICP-MS calibration, ICP-OES was used instead. The two techniques used for metal content determination both allowed simultaneous determination of elements. All measurements were made against an external calibration curve and the samples were filtered with 45 μg L^{-1} syringe filters before analysis to avoid blocking the instruments tubing and the nebulizers. For samples that required dilution, 1% HNO_3 was used. Calibration standards were prepared daily from a 1000 mg L^{-1} stock solution in 1% HNO_3. The calibration range of 0.5 -1000 μg L^{-1} and 0.1 -10 mg L^{-1} were used for ICP-MS and ICP-OES, respectively. The instruments were set up such that they ran triplicate measurements for each sample to ensure good quality control.

4.6 Determination of anion concentrations

The anion concentrations in the samples were determined using ion chromatography (IC). The technique is a liquid chromatographic technique that uses ion exchange principle to separate the different ionic species based on their affinity to the stationary phase. It can be used for both cations and anions depending on a column used. The column used for this analysis was a Metrosep A supp 5 with 150 mm length and 4.0 mm diameter. The eluent solution was made up of 2.0 mM Na_2CO_3, 50 mM H_2SO_4 and 1.0 mM $NaCO_3$. The samples used for IC analysis did not need to be acidified, they were filtered using a 45 μm syringe filters and because of the high conductivities obtained in the AMD samples, and they were diluted accordingly with deionized water to protect the column. The concentrations obtained were then multiplied by the dilution factor to get the final result.

4.7 Geochemical modelling

The anion and metal/metalloid concentrations obtained from laboratory techniques and data from field analysis including parameters such as pH and pe (calculated from the redox potential) were used in PHREEQC to simulate the distribution of inorganic arsenic species in environment. The temperature effect and that of pH on the distribution of species was also investigated using geochemical modelling. Since the experiments were done at room temperature, 25°C was used for all other simulations except for studies investigating the effect of temperature on the species distribution where temperature was varied. PHREEQC interactive version 3.4.0-12927 and llnl database were used for this study.

Chapter 5

Results and discussion

This chapter presents and discusses the experimental findings of this study. A manuscript titled “Determination of arsenic species in mine polluted water using differential pulse anodic stripping voltammetry” has already been prepared from the findings of this work and submitted for review.

5.1 Preliminary studies

5.1.1 Electrochemical characterization of the gold electrode

Electrochemical parameters adopted from Paul *et al*. (2007) were used as initial conditions for this work. In electrochemical analyses, the electrolyte solution should not undergo redox reactions in the potential window used for analysis as it should only produce limited background current in the range studied. For electrode characterization and to confirm that indeed the electrolyte was fitting for its function, CV and DPASV scans of a bare solid gold disc electrode in 3 M HCl were recorded. Initially on running the CV, it was observed that high currents were produced towards more positive potentials on a CV scan (Figure 5.1) while on a more sensitive technique, DPASV (Figure 5.2), pronounced peaks which were thought to result from contamination were observed around 0 V and 0.3 V.

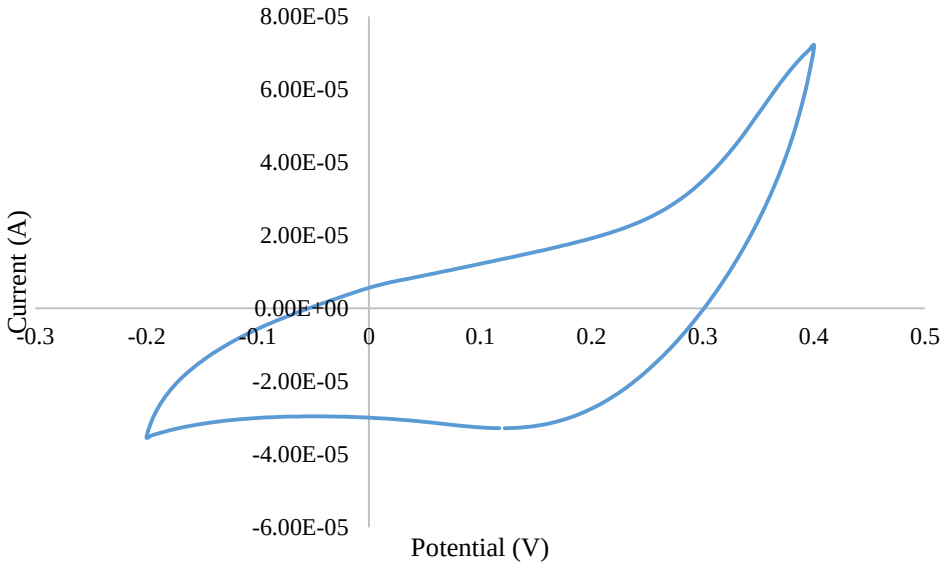

Figure 5.1 CV response of 3 M HCl on a gold disk electrode at 0.2 V s^{-1} scan rate.

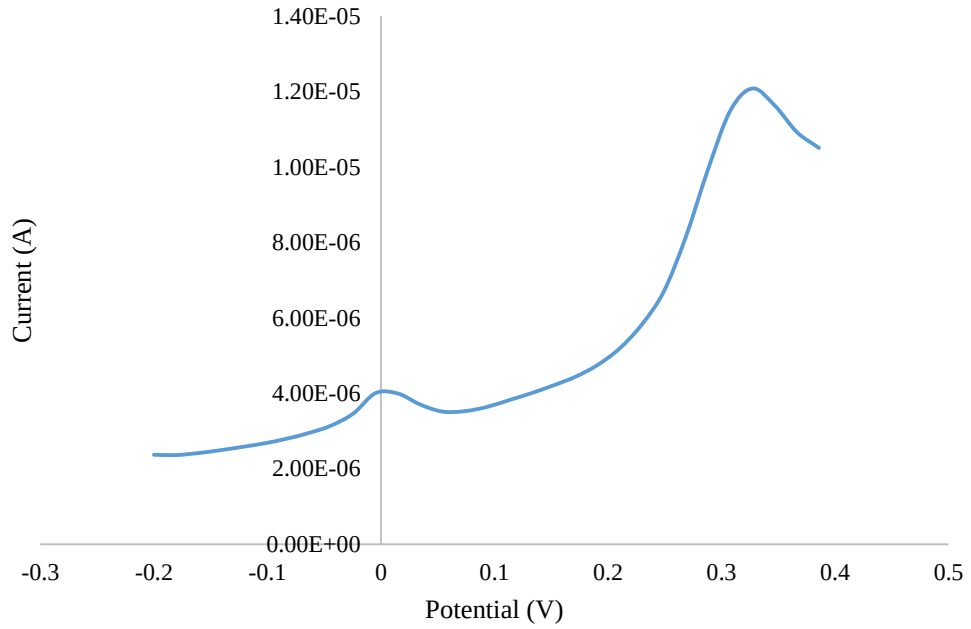

Figure 5.2 DPASV response of 3 M HCl on a gold disk electrode (DP = -0.15 V and DT = 120 s)

As a measure to eliminate the large currents observed in the electrolyte, all solutions were disposed of accordingly, all glassware was washed with detergent, rinsed with deionised water then left in 10% HNO_3 overnight to try to remove any adsorbed metal contaminants. Fresh solutions were prepared and the DPASV analysis repeated. However, pronounced peaks were still observed after the cleaning procedure.

As indicated in literature, mercury and copper interfere with the determination of As(III) by DPASV on a gold electrode (Greschonig and Irgolic, 1992), so the pronounced peak around 0.3 V was thought to result from one of the two elements. In the Metrohm application bulletin for arsenic determination on a gold electrode using DPASV (Application bulletin 226/2 e), the suppliers also indicate that electrodes used for this determination should be reserved for arsenic only and should not be used in combination with mercury electrodes. On investigating the observed contamination, it was discovered that the glass cell used initially for this work had been used extensively with mercury-based electrodes and for analysis of various other metal ions before. Therefore at this point, the peaks observed from

DPASV of the electrolyte solution were associated with trace mercury contamination.

With the peaks from the interfering elements still there, a DPASV scan for the electrolyte containing 0.5 mg L^{-1} As(III), was also recorded to try to understand the effect and intensity of the interfering contamination in the presence of As (III). DPASV analysis of this test solution, produced another peak at approximately 0.17 V corresponding to the analyte but it did not suppress the peaks that were initially observed in the electrolyte solution (Figure 5.3). With that observation, As(III) concentration in solution was increased by doing standard additions, adding 0.5 ml increments of 1 mg L^{-1} As(III) (Figure 5.3). This attempt was aimed at determining if accurate recovery of the concentration in the initial solution could be achieved in the presence of the observed peaks. However, the contamination effect proved to be substantial.

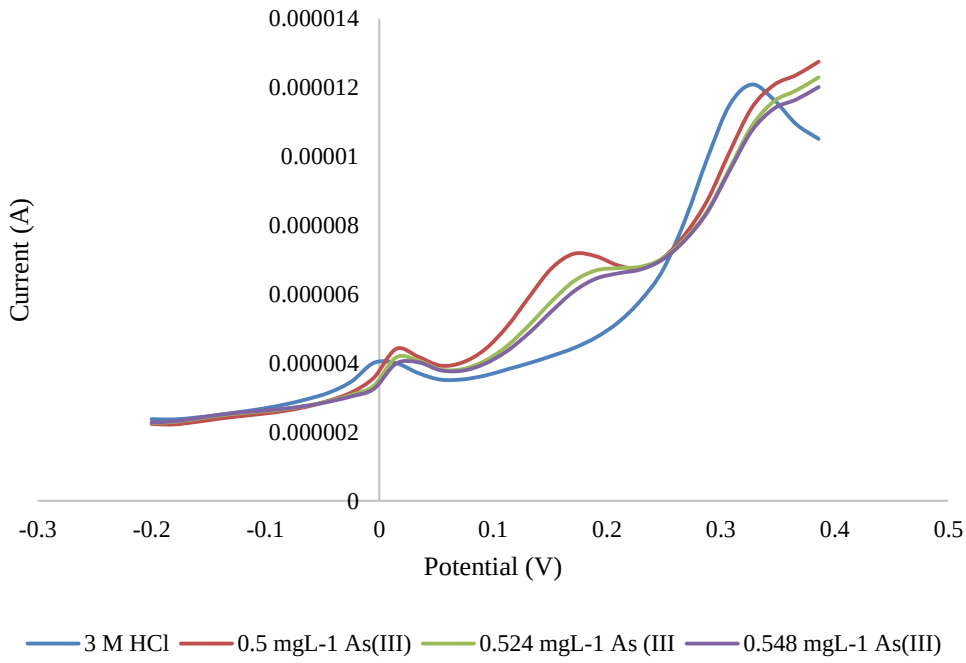

Figure 5.3 DPASV response of 0.5 ml of 1 mg L^{-1} As(III) standard additions (DP = -0.15 V and DT = 120 s)

Even though the standard addition resulted in only a small concentration increase, the current was still expected to increase with concentration, but instead, a signal

decrease was observed with each addition. At this stage, the assumption was that the observed current intensity decrease was due the electrode surface changing with each deposition due to some analyte or impurity remaining on the electrode surface after the stripping step therefore blocking or changing the surface for successive depositions. The presence of foreign species in the test solution indicated in the DPASV scans could also compete with the desired deposition and stripping of the target analyte (As(III)). Further studies were conducted to understand the observed results.

In an attempt to eliminate these problems, a pre-treatment procedure by Raj *et al.* (2014) was adopted combined with a conditioning step at 0.28 V for 60 s to remove any materials left on the electrode surface following each stripping step. Figure 5.4 summarises the results observed after the pre-treatment step and standard additions of 50 mg L^{-1} As(III) (in 0.1 ml increments) to the initial solution of 0.5 mg L^{-1} As(III). The concentration was increased more significantly after each addition to observe a more clear change peak current.

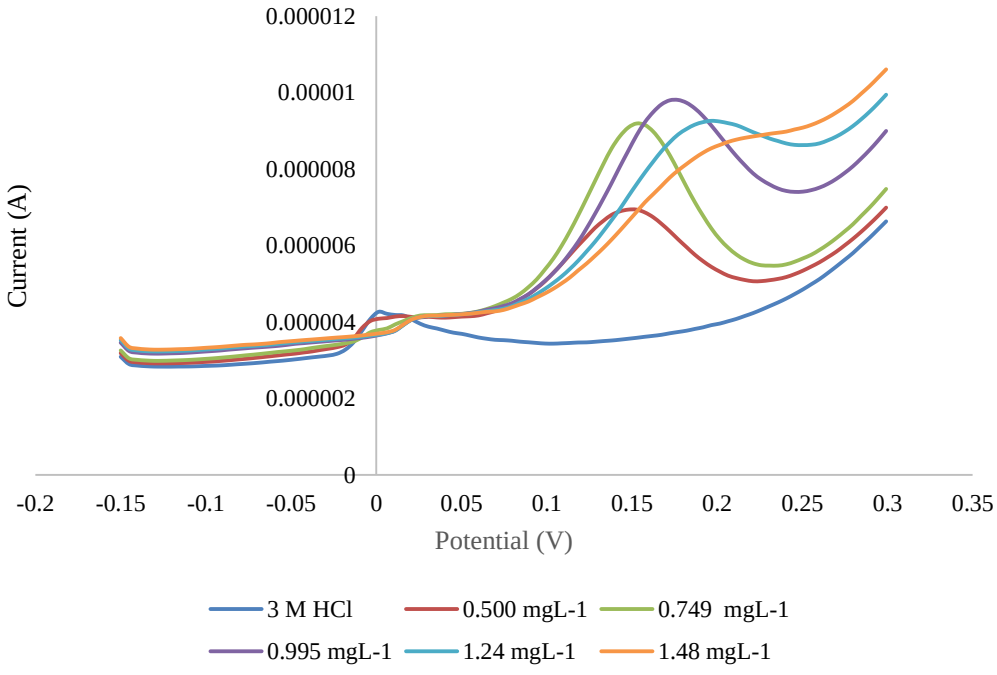

Figure 5.4 DPASV response on addition of 0.1 ml of 50 mg L^{-1} As(III) standard with electrode conditioning at 0.28 V for 60 s (DP = -0.15 V and DT = 120 s)

With the first standard addition, the signal increased and the peak potential was reproduced but for the following additions there was a major shift in peak position and a significant signal decrease. The positive shift of peak position and the change in current response, suggested a change in the electrode surface. On hindsight, a more positive conditioning potential might have produced better results. With the surface reproducibility complications associated with solid electrodes (Uslu and Ozkan, 2007) and the problems persisting in this study, it was rational to consider the possibility of electrode instability. Hence an investigation into the stability of the gold rotating disk electrode was done by running six replicate DPASV scans of As(III). The peak current and the peak position for the 6 replicates were expected to be reproducible for a stable electrode however, neither were reproducible (Figure 5.5). A decrease in peak current and a shift towards the more positive potentials was observed with replicate determinations instead. This again indicated a clear change in electrode surface with successive measurements.

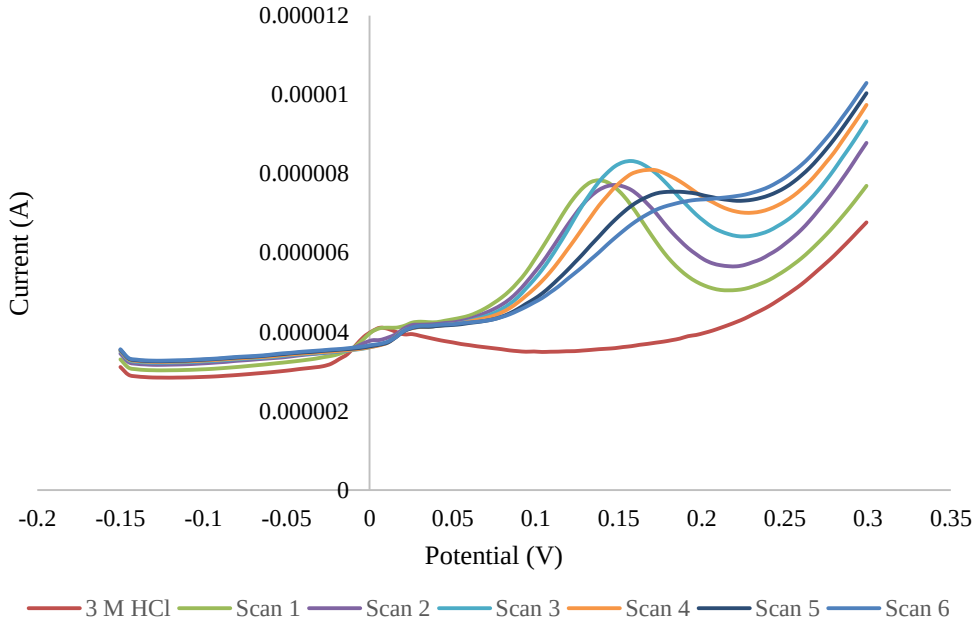

Figure 5.5 Replicate DPASV scans of 0.5 mg L^{-1} As(III) standard in 3 M HCl with electrode conditioning at 0.28 V for 60 s (DP = -0.15 V and DT = 120 s)

After extensive cleaning and investigations, it was clear that the presence of mercury in the cell affected the As(III) determination on a gold electrode when

using DPASV therefore a new set of electrodes and a new electrolyte vessel were used for future work.

Other changes included covering the nitrogen gas tubing with a pipette tip such that a clean tip was in contact with the test solution instead of the original tubing and the background electrolyte concentration was lowered from 3 M to 0.5M. Since the electrochemical cell was not kept in a fume hood during analysis and due to the corrosive nature of HCl and high volatility especially during purging, the electrolyte concentration was kept fairly low at 0.5 M unlike Paul *et al*. (2007) who used 6 M HCl. With these changes and a new set of electrodes, the signal from the interferences was significantly reduced and better pronounced As(III) peaks were observed therefore electrode characterization proceeded as will be indicated in Figure 5.6 and 5.8.

As an aside test on a simple and well known system, cyclic voltammetry was employed to investigate the oxidation and reduction of potassium ferricyanide ($K_3Fe(CN)_6$) on a gold disk electrode and study the effect of the scan rate on the CV scans (Figure 5.6 and Table 5.1). This was also a diagnostic measure to check if the working electrode and the rest of the three-electrode system used in this study were functioning properly. Since a cyclic voltammogram of $K_3Fe(CN)_6$ is distinct and it illustrates both oxidation and reduction in a single CV scan as observed in a study by Liu *et al*. (2007), a voltammogram different from what is typical would imply a problem in a three-electrode system used for this study. For this investigation, 10 mM $K_3Fe(CN)_6$ in 0.5 M HCl as a supporting electrolyte was used as test solution at varying scan rates resulting in CV scans shown in Figure 5.6.

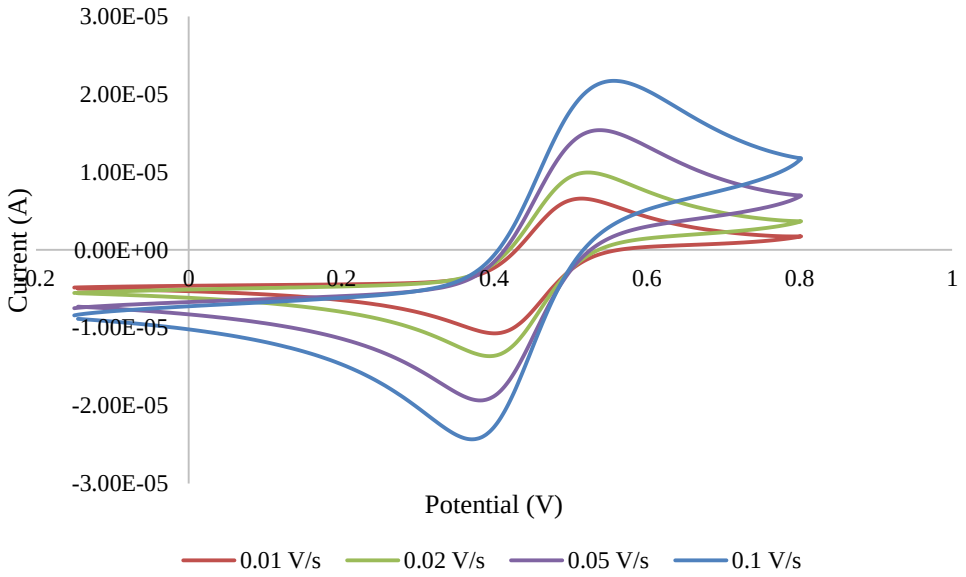

Figure 5.6 Electrochemical response of $K_3Fe(CN)_6$ on a gold disk electrode at various scan rates

Table 5.1 The effect of increasing scan rate on the anodic and cathodic peak properties of a ferricyanide standard solution

Scan rate ($V\ s^{-1}$)	Peak to peak separation (V)	Anodic peak		Cathodic peak	
		Peak potential (V)	Peak current (µA)	Peak potential (V)	Peak current (µA)
0.01	0.107	0.509	8.329	0.402	-9.627
0.02	0.117	0.514	10.75	0.397	-13.12
0.05	0.137	0.524	14.83	0.387	-19.29
0.1	0.161	0.538	18.30	0.377	-25.36

The ferricyanide CV showed chemical reversibility since both the oxidation and reduction were observed to occur in one CV scan. The electrochemical processes were however, quasi-reversible not completely electrochemically reversible. Zanello (2007) described a completely reversible process as that in which the forward peak potential is independent of the scan rate and the peak-to-peak separation between the anodic and cathodic peaks is 59/n mV (where n is the number of electrons transferred) at room temperature. For quasi-reversible

processes the peak-to-peak separations are much greater and exhibit a shift in potential with increasing scan rate (a shift in the positive direction for oxidation and in the negative direction for reduction). In addition to this, it was also mentioned that for quasi-reversible processes, the forward peak height is not directly proportional to the square root of the scan rate ($v^{½}$). In this study, the peak-to-peak separations for the scans were greater than 0.1 V hence greater than that for a completely reversible process. The peak potentials also shifted with the increasing scan rate and the plot of forward peak current against the square root of the scan rate (Figure 5.7) did not show direct proportionality as only 2 points followed a straight line.

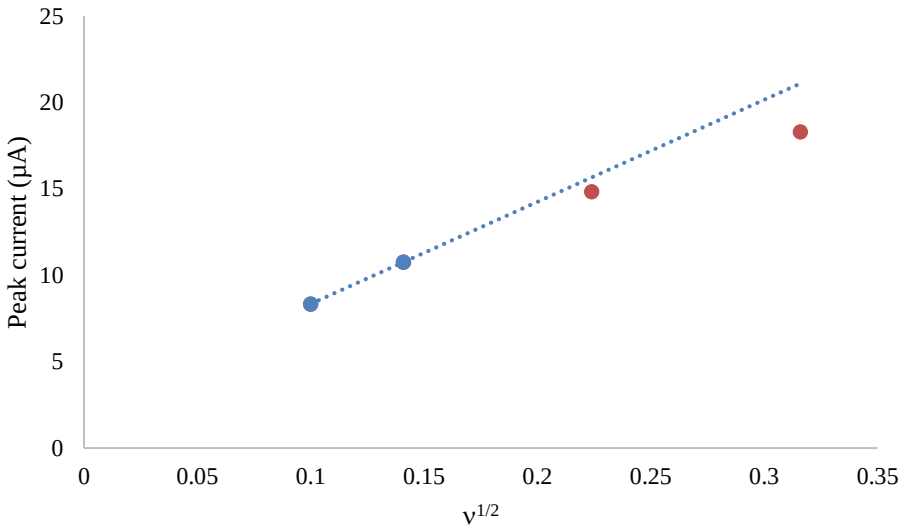

Figure 5.7 The plot of the square root of the scan rate against the forward peak height of a ferricyanide standard solution

The CV procedure was also applied to investigate the As(III) system but first a CV scan of 0.5 M HCl supporting electrolyte on the gold disc electrode was recorded and there were no impurity peaks observed. A CV scan of 0.1 mg L^{-1} As (III) standard solution was also recorded following that of the electrolyte. There was no significant difference between the two scans except a slightly lower capacitance and a small bump around 0.2 V for a CV scan of As(III) which was suspected to result from oxidation of As(0) to As(III). The scans are overlaid in Figure 5.8.

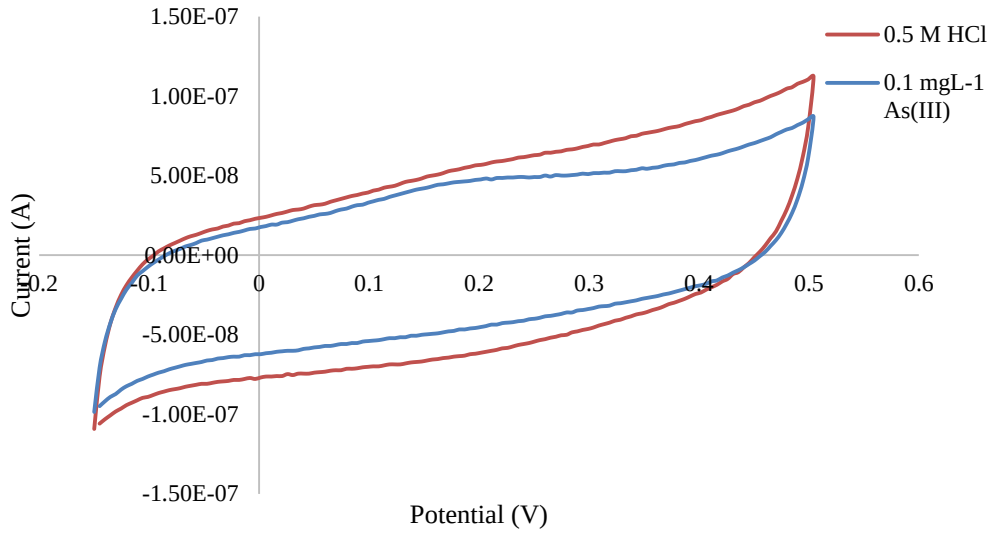

Figure 5.8 Overlay of CV responses for 0.5 M HCl and 0.1 mg L^{-1} As(III) recorded at the scan rate of 0.2 V s^{-1}

A DPASV response of As(III) and the effect of increasing As(III) concentration on the current were also studied (Figure 5.9). A peak was observed at approximately 0.17 V corresponding to the oxidation of As(0) to As(III) and the current increased with increasing concentration.

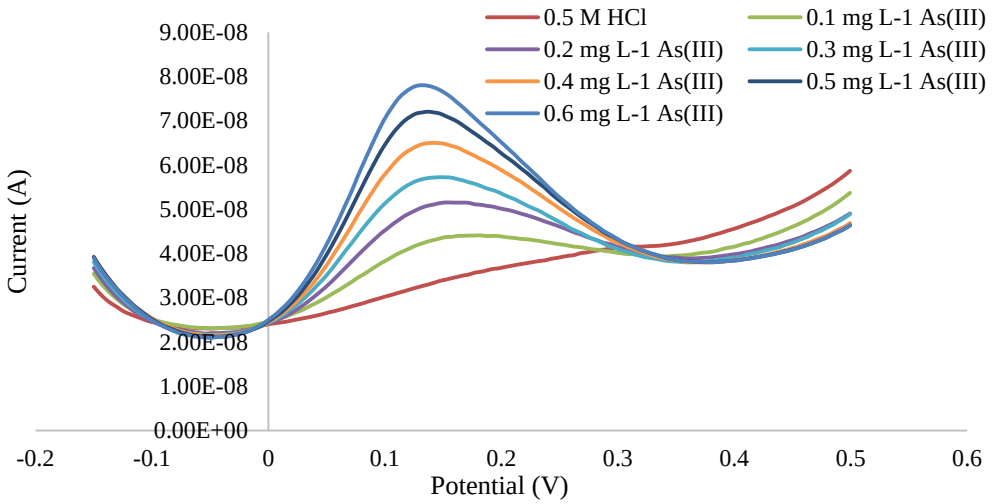

Figure 5.9 DPASV response of As(III) standard addition in 0.5 M HCl on a solid gold electrode (DP= -0.15 V and DT= 120 s)

With the interference effect decreased and showing less effect on As(III) determination, the method still required optimization to improve its efficiency.

5.2 Method optimization

The effectiveness of DPASV is dependent on a number of parameters. These parameters include, deposition potential, deposition time, modulation amplitude and rotation speed of the working electrode or stirring rate of the solution depending on the mode of transport of the analyte to the electrode surface. For determination of As(III), the measurement parameters were first optimized by studying the effect of those mentioned on the peak height and shape. For optimization of parameters used in As(III) detection by DPASV, the solid disk gold electrode was cleaned by immersing it in 0.1 M NaOH for 30 minutes before each experiment followed by thorough rinsing with deionised water, then ethanol and with deionised water again. This was followed by electrochemical activation of the working electrode as described in section 4.4.

From conditions adapted from Paul *et al*. (2007), HCl was retained as the electrolyte solution but the concentration was lowered to 0.5 M as mentioned in section 5.1.1. In other electrochemical arsenic determinations, electrolyte concentrations below and above that used in this work have been emplyed. For example, Raj *et al*. (2014) used 0.1 M HCl while Dai *et al*. (2004) reported 1 M HCl as the best electrolyte concentration. Several other electrolyte solutions such as HCl, HNO_3 and H_2SO_4 have been studied for electrochemical stripping determinations of arsenic and HCl was determined to give the best results (Dai *et al*., 2004). Zlatev *et al*. (2010) also indicated that HCl is the most suitable electrolyte solution. In this work, a solution containing 100 µg L^{-1} As(III) in 0.5 M HCl as a supporting electrolyte was used for the optimization studies. Once again, all potentials reported are with respect to Ag/AgCl (3M KCl) reference electrode. The results for the optimization of each parameter are discussed below.

5.2.1 Deposition potential

The effect of the deposition potential on the current produced was studied in the potential range of 0 V to -0.5 V (Figure 5.10). Here only the deposition potential was varied while other voltammetric parameters were kept constant. The initial deposition time, rotation speed and modulation amplitude were 120 s, 500 rpm and

0.025 V respectively. Other parameters such as step potential, modulation time and interval time were always kept constant for all DPASV measurements at 0.005 V, 0.05 s and 0.5 s respectively.

Deposition potential controls the effectiveness of the pre-concentration (deposition) of arsenic on the electrode surface therefore it is an important parameter in DPASV. In general, the more negative the deposition step, the more energy is supplied for the reduction process to occur resulting in the increase in current since the process is not diffusion limited but the solution is stirred during deposition. This study was aimed at determining the potential at which As(III) is efficiently reduced to As(0), the species deposited on the working electrode surface. The optimum potential for this reduction process was determined to be at -0.4 V. Deposition potentials close to this have been reported before. For example, Sun et al. (1997) reported no significant difference in the peak currents produced by the deposition potential of -0.3 V and -0.4 V though they chose to work with -0.3 V.

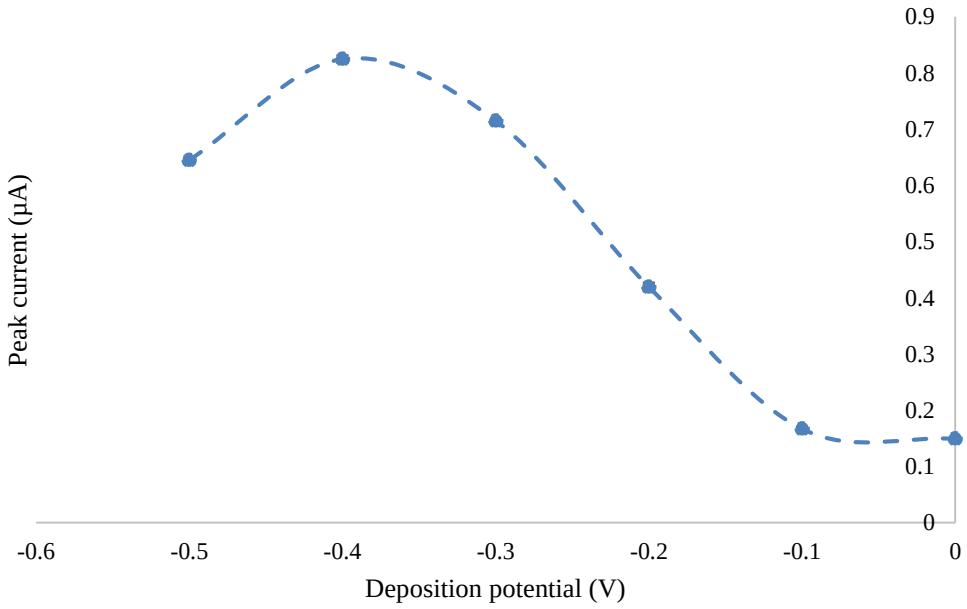

Figure 5.10 The effect of varying deposition potential on the peak current of 100 µg L^{-1} As (III) in 0.5 M HCl supporting electrolyte, (n = 3, SD)

5.2.2 Deposition time and rotation speed

The effectiveness of the deposition step is also dependent on the deposition time and the rate at which the solution is stirred or the rotation speed of the working electrode. The rotation speed does not only keep the bulk solution homogeneous but it also increases the flux of the analyte from the solution to the working electrode surface. The deposition time range studied was 30 to 300 s at 500 rpm and 1000 rpm, respectively. The optimized deposition potential of -0.4 V was used when investigating the effect of these two parameters and all other parameters were kept the same as those in section 5.2.1.

For studies carried out at 500 rpm, the observed peak current increase followed a linear trend initially but declined beyond 180 s deposition time, indicating saturation at the electrode surface (Figure 5.11). Based on this observation, 180 s was the optimum deposition time at 500 rpm suggesting that these conditions can be used for the analysis of As(III) solutions of 100 µg L^{-1} concentrations and lower without saturation at the electrode surface.

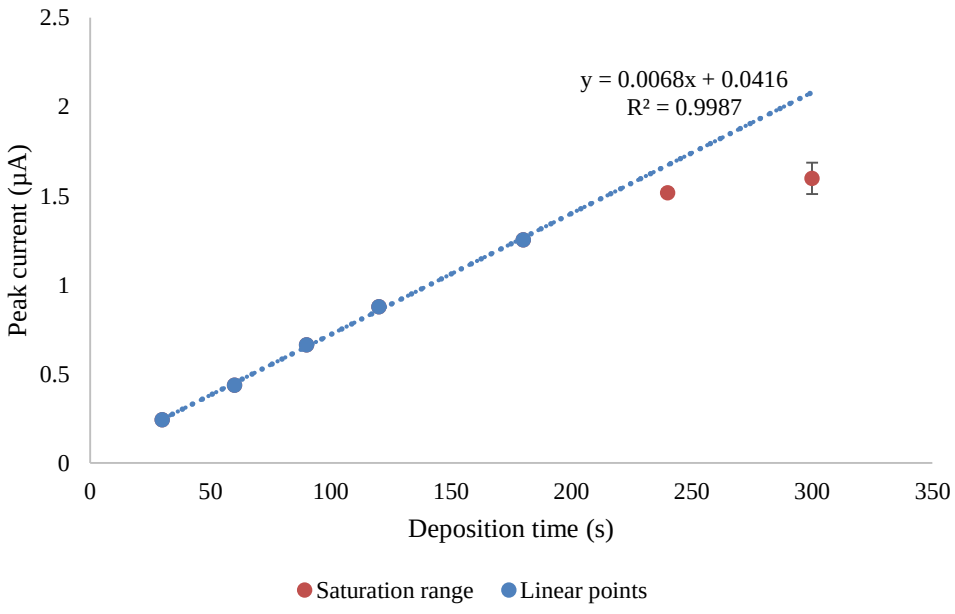

Figure 5.11 Variation of deposition time at 500 rpm for 100 µg L^{-1} As (III) standard solution in 0.5 M HCl supporting electrolyte (DP = -0.4 V)

The same variation of deposition time was repeated at the rotation speed of 1000 rpm to investigate the effect of doubling the rotation speed (Figure 5.12). It was observed that the optimum deposition time was reached sooner (120 s) at this rotation speed and also the current signals were higher but they did not double as compared to those obtained at 500 rpm. From the observations made and the fact that 500 rpm still produced good signals at the As(III) concentration studied, the current increase at 1000 rpm was considered not that significant hence 500 rpm was chosen for further studies.

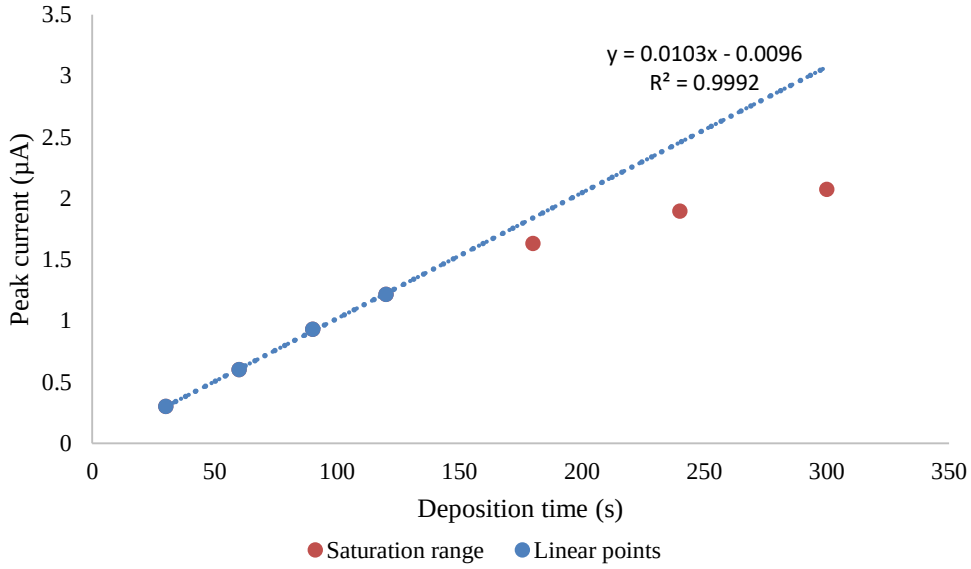

Figure 5.12 Variation of deposition time at 1000 rpm for 100 µg L^{-1} As (III) standard solution in 0.5 M HCl supporting electrolyte (DP = -0.4 V), (n = 3, SD)

Other papers on electrochemical determinations of arsenic have reported deposition times as low as 120 s (Raj *et al*., 2013; Paul *et al*., 2007) but there are some other studies that worked with higher deposition times. For example, Dai *et al*. (2004) compared linear sweep voltammetry and square wave voltammetry for electrochemical As(III) studies using a glassy carbon electrode modified with gold nanoparticles and obtained the deposition time of 180 s as the optimum while Bu *et al*. (2015) used linear sweep anodic stripping voltammetry to study the reduction step of As(III) and As(0) under stirring conditions on a solid gold electrode and determined 400 s as the optimum.

5.2.3 Modulation Amplitude

The effect of varying the modulation amplitude on the peak current and shape was also investigated. The optimized deposition potential, deposition time and rotation speed of -0.4 V, 180 s and 500 rpm were used when investigating this parameter. It was observed the peak current increased with the increase in modulation amplitude (Figure 5.13).

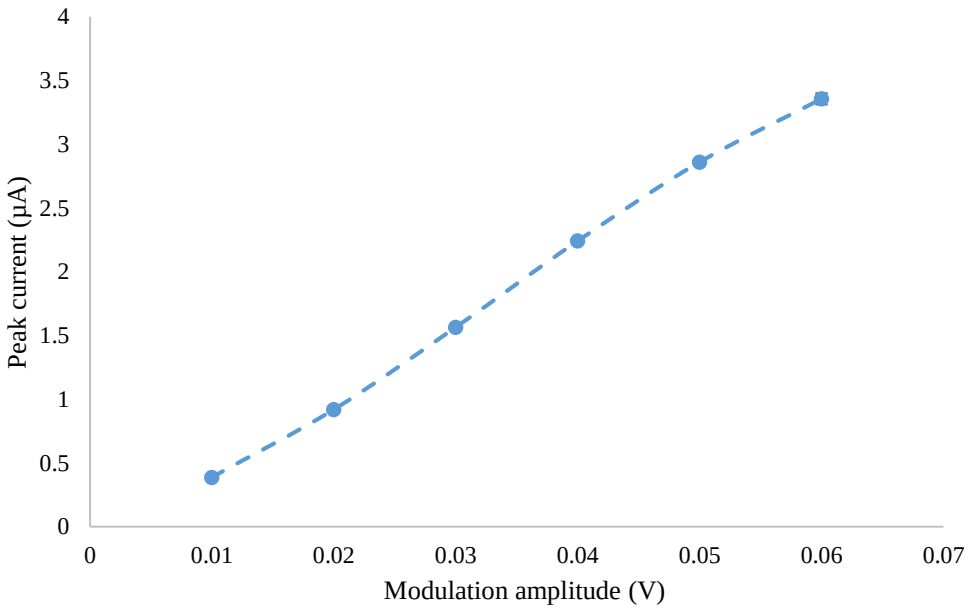

Figure 5.13 The effect of increasing modulation amplitude on 100 µg L^{-1} As(III) peak height, (n = 3, SD)

The observation was in agreement with Wang and Mulligan (2006), who showed that an increase in modulation amplitude results in high peak currents and broad peaks. Wang and Mulligan (2006) further indicated that modulation amplitudes used in most electrochemical studies are in the range of 25-50 mV. In this study, as the modulation amplitude was increased, it was also observed that the peaks shifted towards more negative potentials (Figure 5.14). The observed shift in peak potentials to more negative values at higher modulation amplitudes was associated with the fact that in DPASV, the current is sampled twice, first just before the pulse and again towards the end of the pulse and the difference is recorded. The difference in these currents is plotted against the base potential (the applied potential before

the pulse). At a particular base potential, the current difference will be greater for a larger modulation amplitude if the oxidation process occurs at the potential of the applied pulse. Thus, a current difference is observed earlier (from more negative potentials) for larger modulation amplitudes. The half widths at different amplitudes did not show a large variance (Table 5.2), therefore peak broadening described by Wang and Mulligan (2006) was not observed in this study. However, 0.04 V was chosen as the modulation amplitude for further work since the peaks became more distorted (less symmetrical) at higher modulation amplitudes. This behaviour was also described by Metrohm Autolab B.V. (2018), which indicated that, larger modulation amplitudes result in large currents, broad peaks and peak distortion due to non-linearity effects.

Table 5.2 Effect of modulation amplitude on peak properties of 100 µg L^{-1} As(III) standard solution

Modulation amplitude (V)	Peak potential (V)	Peak current (µA)	Half width (V)
0.01	0.148	0.3904	0.068
0.02	0.143	0.9166	0.073
0.03	0.138	1.555	0.073
0.04	0.133	2.222	0.073
0.05	0.128	2.836	0.068
0.06	0.119	3.311	0.073

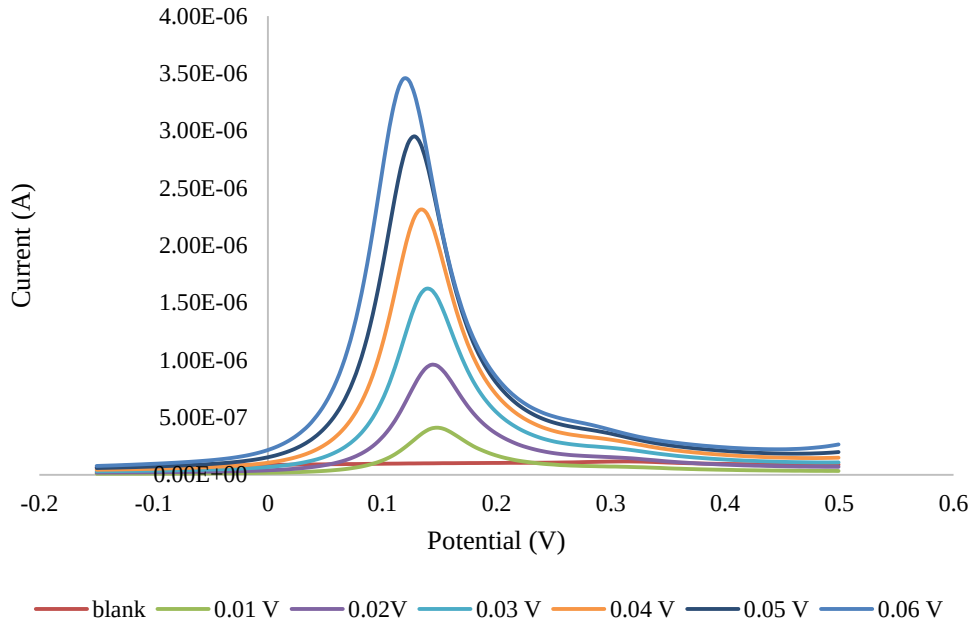

Figure 5.14 Effect of varying modulation amplitude on the voltammograms of a 100 µg L^{-1} As(III) standard solution (DP= -0.4 V, DT= 180 s and RS= 500 rpm)

5.3 Calibration

Calibration experiments were performed using the optimized voltammetric conditions in As(III) concentration range of 12.5 - 100 µg L^{-1}. A calibration curve was then constructed by plotting the current produced by each standard solution versus the concentration (Figure 5.15).

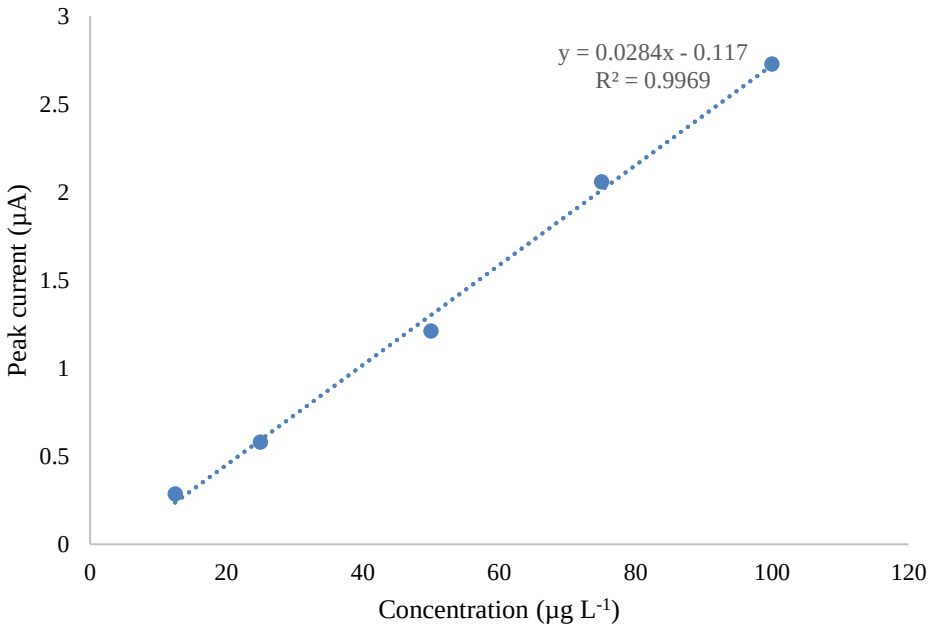

Figure 5.15 Calibration curve for DPASV determination of As(III) in 0.5 M HCl using -0.4V DP, 180 s DT, 500 rpm RS and 0.04 V MA (n = 3, SD)

A linear dependence of the As(III) concentration and the peak current was observed in the range studied giving a calibration graph with a linear equation y = 0.0284x-0.117 and R^2 = 0.9969. The coefficient of determination obtained from the graph approximates 1 hence indicating good linearity. Using the linear regression method, the LOD and LOQ were determined to be 5.95 µg L^{-1} and 19.8 µg L^{-1}, respectively. This indicates that the method with the applied parameters provides a sensitive detection for As(III).

For the other performance characteristics, the measurements were carried out in triplicates but for repeatability studies, 6 replicate measurements on 100 µg L^{-1} As(III) standard were performed and the relative standard deviation (RSD) of 1.1% was obtained. The low deviation value obtained indicates good method precision.

5.4 Optimization of the reduction of As(V)

As discussed in section 4.4, As(V) cannot be directly detected electrochemically, instead, it is evaluated by difference after determination of total arsenic and As(III). Different studies have applied variety of chemicals for reduction of As(V) for purposes of electrochemical determinations. For example, Profumo *et al*. (2005)

used, sodium dithionite as a reducing agent followed by determination of total arsenic on a HMDE while Paul *et al*. (2007) and Raj *et al*. (2014) used sodium sulphite and sodium thiosulphate, respectively, followed by detection on gold electrodes. This study employed sodium thiosulphate as a reducing agent. The optimum amount of $Na_2S_2O_3$ needed for the reduction of As(V) was investigated and initially, 15 mg (9.49×10^{-5} moles), 60 mg (3.79×10^{-4} moles) and 90 mg (5.69×10^{-4} moles) $Na_2S_2O_3$ masses were used. The maximum mass (90 mg $Na_2S_2O_{3)}$ was close to the 100 mg used by Raj *et al*. (2014).

Initially a calibration curve method was used for recovery studies using a solution concentration of 50 µg L^{-1} As(V) (1.3×10^{-8} moles in 20 ml cell volume). It was observed that As(V) reduction using the lowest $Na_2S_2O_3$ mass (15 mg) gave the highest recoveries while 90 mg thiosulfate led to the DPASV signal disappearing completely (Figure 5.16).

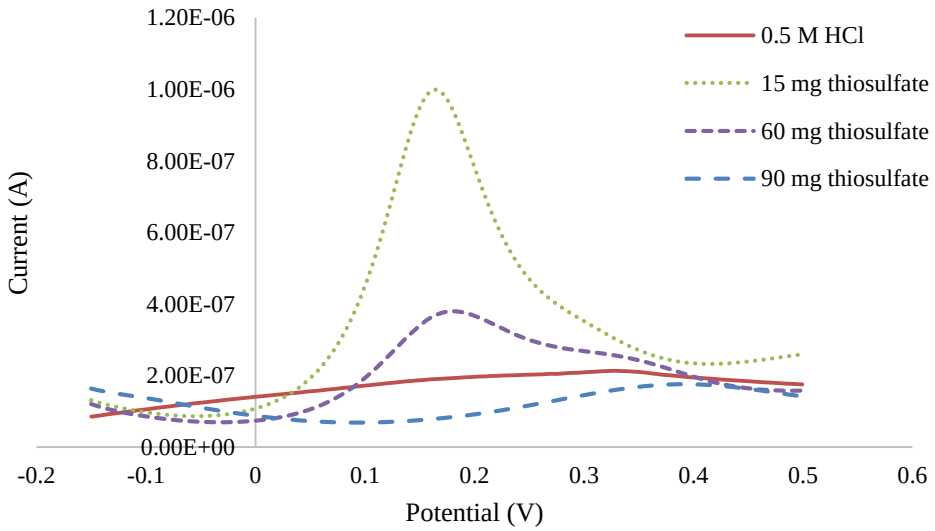

Figure 5.16 DPASV response of 50 µg L^{-1} As(V) after reduction to As(III) with sodium thiosulphate (15-90 mg) using DP = -0.4 V, DT = 180 s and RS = 500 rpm.

Even though a reasonable signal was observed for a test solution containing 15 mg $Na_2S_2O_3$, the recovery was low therefore further investigations were necessary. For studies that followed, the concentration of As(V) in the test solution was reduced to 25 µg L^{-1} and since a clear trend from the initial investigations indicated that a

large access of $Na_2S_2O_3$ significantly reduced the signal, an investigation based on the use of lower $Na_2S_2O_3$ concentrations for reduction of As(V) was done.

For reduction of 25 µg L^{-1} As(V) (6.0×10^{-9} moles in 20 ml cell volume), initial investigations were done using 1 mg (6.32×10^{-6} moles), 5 mg (3.16×10^{-5} moles), 10 mg (6.32×10^{-5} moles) and 15 mg (9.49×10^{-5} moles) $Na_2S_2O_3$. A similar trend as that observed with the 50 µg L^{-1} As(V) solution was observed (Figure 5.17). A test solution with the highest amount of $Na_2S_2O_3$ (15 mg) gave the lowest peak current while that with 1 mg $Na_2S_2O_3$ gave the highest signal for this investigation.

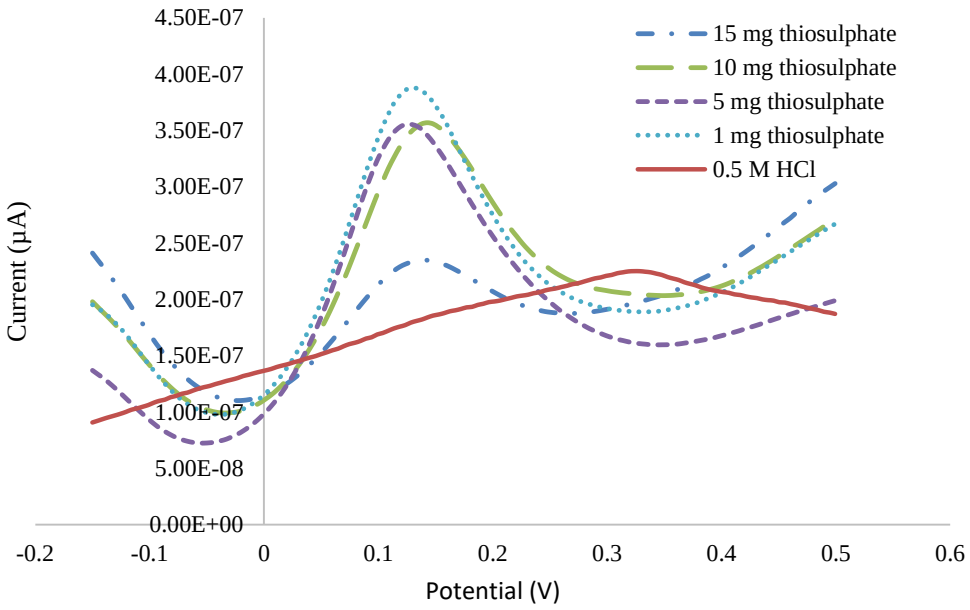

Figure 5.17 DPASV response of 25 µg L^{-1} As(V) after reduction to As(III) with sodium thiosulphate (1-15 mg) using DP= -0.4 V, DT= 180 s and RS= 500 rpm.

With the observed trend (decrease of peak current with increasing amount of the reducing agent) which indicated that the presence of $Na_2S_2O_3$ in the matrix indeed affected the intensity of the peak current (hence also the recovery), the standard addition method was considered for further work. Standard addition is an analytical method essential in quantitative determinations in which the sample matrix affects the analytical signal. This method is used to counteract the matrix effects by adding a known amount of standard to the sample analysed.

Using the standard addition method, 0.1 mg (6.32×10^{-7} moles), 1 mg (6.32×10^{-6} moles), and 10 mg (6.32×10^{-5} moles) $Na_2S_2O_3$ masses were studied for reduction of 25 µg L^{-1} (6.0×10^{-9} moles) As(V). Replicate determinations were done for each $Na_2S_2O_3$ mass studied and the percentage recoveries are given in Table 5.1. As(V) reduction with 1 mg $Na_2S_2O_3$ gave highest recoveries therefore it was determined to be the optimum mass of $Na_2S_2O_3$ to be used for reduction of 25 µg L^{-1} As(V).

Table 5.3 Recoveries after the reduction of 25 µg L^{-1} As(V) to As(III) using various masses of $Na_2S_2O_3$ (n = 3)

$Na_2S_2O_3$ mass (mg)	Concentration recovered (µg L^{-1} ± SD)	Percentage recovery (%)	RSD (%)
0.1	10.42 ± 2.1	41.7	20
1	24.14 ± 3.4	96.6	14
10	12.64 ± 4.4	50.6	35

After introduction of $Na_2S_2O_3$ to the matrix, it was however observed that, electrode sensitivity decreased and lower coefficients of determination were obtained, consequently, overall results showed high relative standard deviations. The presence of sulphur introduced by addition of sodium thiosulphate to the test solution was suspected to poison the gold electrode, this is indicated by the low signals that were obtained with total arsenic analysis (containing sodium thiosulphate) compared to As(III) analysis. Melashvilli *et al*. (2016), who investigated the response of gold electrodes in a thiosulphate electrolyte specified that even though gold thiosulphate leaching is a slow process, it is considered as a simpler alternative to cyanidation. This means that the presence of the thiosuphate reducing agent in the test solution may slowly leach the gold electrode and thus cause of the mentioned problems. Again, arsenic is known to have very good affinity for sulphide ores (Cheng *et al*., 2009), hence the presence of excess sulphur could result in complexed arsenic forms leading to low recoveries.

Figure 5.18 is an example of two standard addition graphs of equal As(III) concentrations. It shows that the signals for an analysis done before total arsenic studies, were higher compared to those that followed after determination of total

arsenic. This was a sign of electrode poisoning by thiosulphate. Therefore, it was after the observed decrease in sensitivity that the electrode required polishing with alumina as described previously in section 4.4. Even though these observations were made in our study, $Na_2S_2O_3$ has been used as a reducing agent for As(V) before with no indication of such problems (Raj et al., 2014).

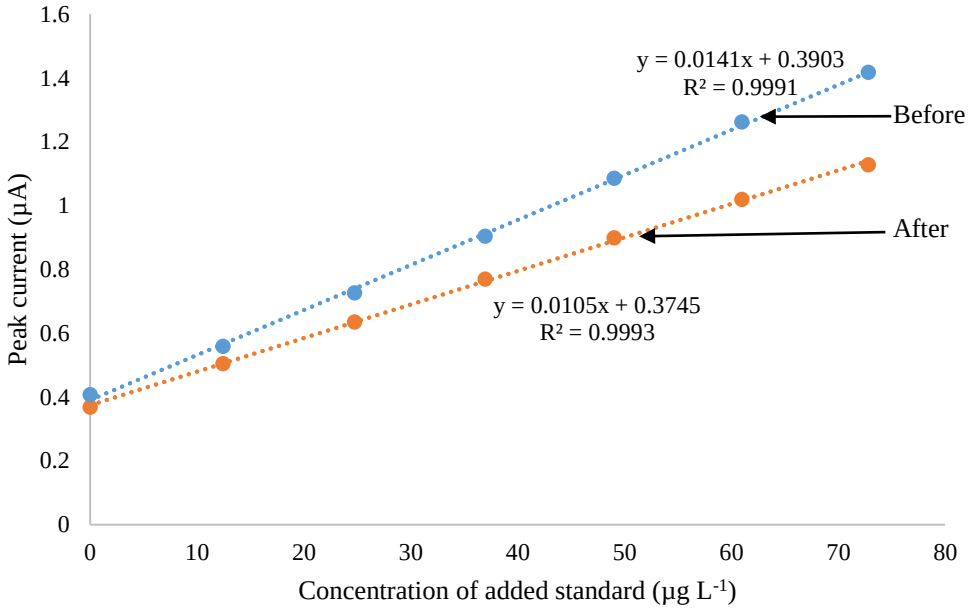

Figure 5.18 Standard addition curves for 25 µg L^{-1} As(III) in a 50 µg L^{-1} arsenic standard (25 µg L^{-1} As(III) + 25 µg L^{-1} As(V)) before and after analysis of total arsenic

Electrochemical reduction of As(V) to As(III) using reduction potential of -1.2 V (Metrohm application bulletin 226/2 e) was also considered as it does not require addition of chemicals, instead a highly negative potential was applied for reduction of As(V). Yamada *et al*. (2008) indicated that As(V) reduction has high activation energy hence the need for highly negative potentials for the process to occur. In this work, this reduction process generated hydrogen at the electrode surface which resulted in a bubble that covered the electrode surface and persisted throughout deposition and the stripping step, hence preventing the determination of the total arsenic. This observation was in agreement with the observations of Yamada *et al*. (2008) on application of low potentials.

Sodium thiosulphate was therefore retained as a reducing agent and 1 mg $Na_2S_2O_3$ (obtained as the optimum mass for reduction of 25 µg L^{-1} As(V)) was further investigated on a mixed standard containing both As(III) and As(V) as the two oxidation states coexist in the environment. A cell containing 0.5 M HCl with 50 µg L^{-1} total arsenic (made up of 25 µg L^{-1} As(III) and 25 µg L^{-1} As(V)) was examined. Quantitative analysis results for As(III) and As(V) in the mixed standard using DPASV are summarised in Table 5.4. Recovered As(V) concentrations were low compared to the prepared concentration while As(III) values were inflated but overall, good recoveries were obtained for total arsenic.

Table 5.4 Recovery of As(III) and total As in 50 µg L^{-1} (25 µg L^{-1} (III) + 25 µg L^{-1} As(V)) As standard (n = 7)

As species	Concentration recovered (µg L^{-1} ± SD)	Percentage recovery (%)	RSD (%)
As(III)	29.88 ± 2.9	120	9.8
Total As	50.35 ± 6.2	101	12
As(V)	20.47 ± 3.8	81.9	18

The effect of electrode poisoning observed earlier in this section was again observed with mixed standard solutions. Figure 5.19 shows an example of standard addition graphs obtained for As(III) and total arsenic analysis. It was observed that currents obtained for As(III) were almost double the currents for the total arsenic. The coefficient of determination was also lower for total arsenic compared to As(III) analysis.

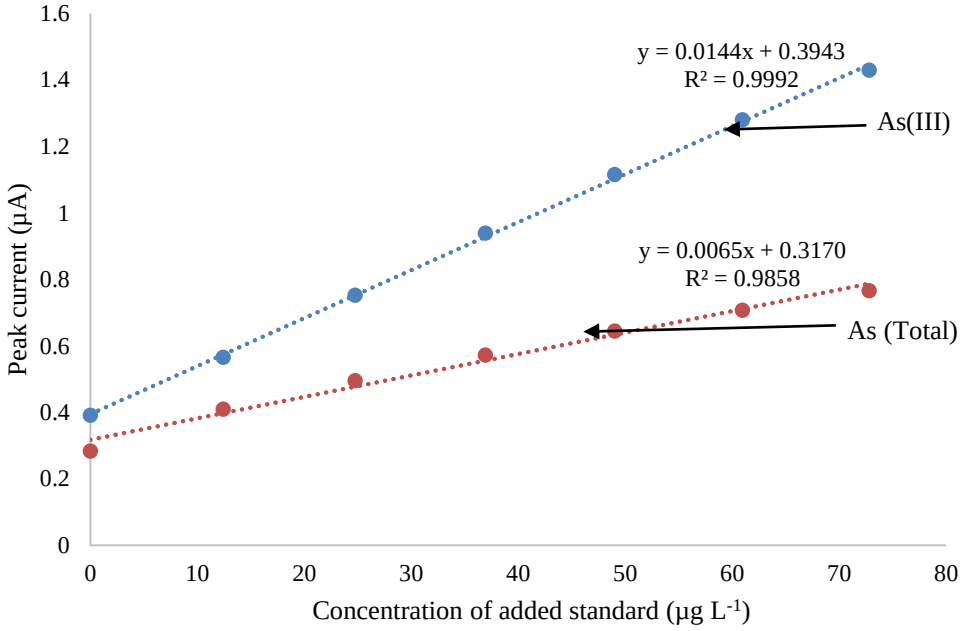

Figure 5.19 Standard addition curves for As(III) and total arsenic in a 50 µg L^{-1} arsenic standard (25 µg L^{-1} As(III) + 25 µg L^{-1} As(V))

To look further into this, a comparison was done between results in Table 5.4 and measurements where recoveries of individual species were done consecutively (Table 5.5). The latter refers to DPASV measurements where As(III) replicate analyses were done following one another and total arsenic measurements which followed one another too instead of cases where no particular pattern was followed. What was different for this measurements was that the electrode was not exposed to poisoning (from thiosulphate) in between As(III) determinations, however, for all total arsenic measurements in this work, the gold working electrode required polishing in between running replicate solutions because of low current intensities. Table 5.5 shows that the RSD values were improved with this but As(V) recoveries were even lower while As(III) values were still inflated. Again inter conversion of species was suspected as constantly inflated As(III) concentrations were obtained.

Table 5.5 Consecutive determinations for As(III) and total arsenic recovery in 50 µg L^{-1} (25 µg L^{-1} (III) + 25 µg L^{-1} As(V)) arsenic standard (n = 4)

As species	Concentration recovered (µg L^{-1} ± SD)	Percentage recovery (%)	RSD (%)
As(III)	28.82 ± 1.6	115	5.7
Total As	46.51 ± 2.4	93.0	5.2
As(V)	17.64 ± 1.14	71.1	6.5

5.5 Analysis of environmental samples

5.5.1 Field analysis

At the sampling sites, pH, Eh and conductivity were recorded for AMD and Fleurhof dam samples. Table 5.6 gives the summary of the field parameters. The pH value for the AMD sample was highly acidic while that for the Fleurhof dam water was only slightly acidic suggesting a low AMD impact on the dam. Further investigation and seasonal measurements may be necessary to support this statement. The redox potentials for the Fleurhof dam sample and AMD were slightly different even though it was lower for Fleurhof dam than for AMD indicating more reducing conditions in the dam water compared to AMD. According to Smedley and Kinniburgh (2002), reducing conditions accompanied by low pH values suggest the dominance of As(III) oxidation state.

Table 5.6 Field measurements for AMD and Fleurhof dam samples

Sample	pH	Eh (V)	Conductivity (mS cm^{-1})
Fleurhof dam water	6.25	0.272	0.39
AMD	2.76	0.346	9.08

5.5.2 Metal/metalloid and anion concentrations in environmental samples

At the laboratory, the environmental samples (Fleurhof dam water and AMD) were analysed for metals/metalloids (As, Cu, Pb, Hg, Mn, Fe, Al and Ni) using ICP-MS and ICP-OES while anions (SO_4^{2-} and Cl^-) were determined by ion chromatography (IC). These techniques were used as reference to DPASV method and as data sources for simulating arsenic speciation in the environmental samples using geochemical modelling.

Concentrations of arsenic were determined to be 0.0120 mg L^{-1} and 0.2781 mg L^{-1} in Fleurhof dam and AMD samples, respectively (Table 5.7). The samples were found to contain high concentrations of other metals too besides arsenic. The presence of high levels of metal concentrations in AMD is indicative of high possibility of contamination in water sources and soil in the surrounding areas. With Fleurhof dam as a water source in the vicinity of the mining dumps, it was an ideal sampling site to assess the contribution of mining to arsenic pollution in the area. Even though arsenic levels in Fleurhof dam seemed low, they are slightly above the WHO (2010) limit for drinking water, which is an indication that the areas around the mining sites are exposed to elevated concentrations of dissolved arsenic. The dam water was also determined to have a high sulphate concentration (above 100 mg L^{-1}) and other metal ion concentrations in the dam were elevated too, with most of them above 1 mg L^{-1}. These elevated concentrations in the Fleurhof dam may be a manifestation of mining related pollution.

Table 5.7 Concentrations of elements in environmental samples

Cation/Anion	Concentration in Fleurhof dam water (mg L^{-1})	Concentration in AMD (mg L^{-1})
Iron (Fe)	6.615	191900
Manganese (Mn)	ND	73.98
Copper (Cu)	1.166	807.5
Lead (Pb)	2.114	651.0
Mercury (Hg)	0.000099	0.00011
Arsenic (As)	0.0120	0.2781
Aluminium	1.896	34300
Nickel	3.076	263.3
Sulphate (SO_4^{2-})	127.7	14253
Chloride (Cl^-)	1.760	39.50

ND: Not detected

5.5.3 Electrochemical analysis of samples

The optimized DPASV method was assessed for determination of arsenic species in environmental samples. The samples were prepared as previously described in section 4.3 and on the day of analysis, they were removed from low storage temperatures and allowed to reach room temperature before instrumental analysis. For the Fleurhof dam sample, As(III) could not be detected even though ICP-MS analysis determined it to be higher than the detection limit of the developed DPASV method. The absence of As(III) in solution was associated with the presence of other elements in higher concentrations (Table 5.7) which could affect the stability of the arsenic forms present resulting in complexed undetectable chemical forms.. On spiking the dam water with As(III), a linear relationship between concentration and current was however observed with the coefficient of determination of 0.994 (Figure 5.20).

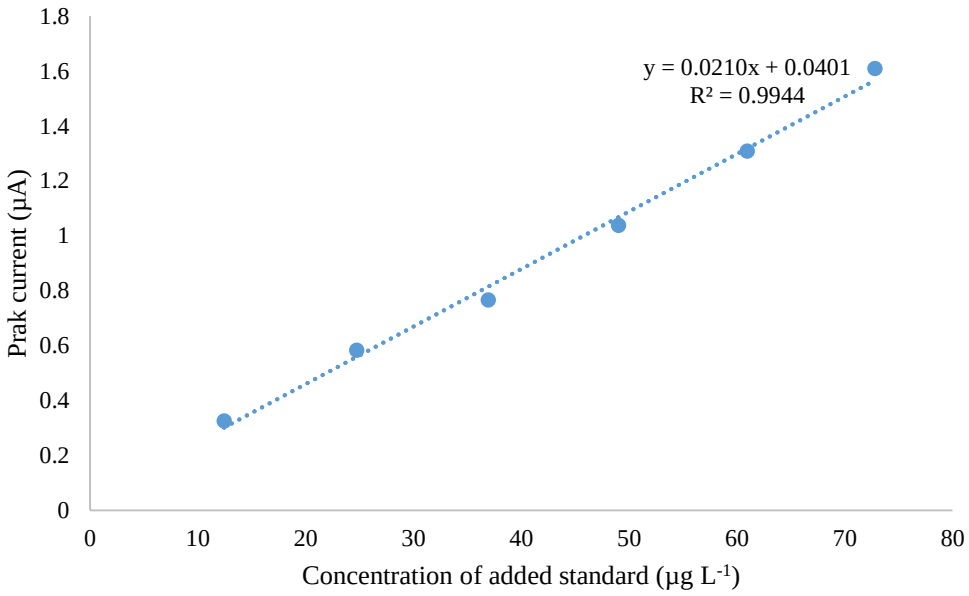

Figure 5.20 As(III) standard addition curve for Fleurhof dam water

Since no As(III) was detected in the sample, 50 µg L^{-1} total arsenic (25 µg L^{-1} As(III) + 25 µg L^{-1} As(V)) was spiked into the water and the viability of the optimized method was tested by doing the recovery studies (Table 5.8). The average recovery of 81.6% was obtained for As(III), 102% for total arsenic and 123% for As(V). For this sample, it was observed that the recovery for As(V) was higher than the prepared concentration and As(III) was lower, while the total arsenic was not far off from the prepared concentration. Except for total arsenic, the observation was the opposite of what was observed with arsenic standard solutions. This was associated with the impact of various other components in the environmental sample compared to clean standard solutions.

Table 5.8 Recovery of As(III) and As(V) in spiked dam water (25 µg L^{-1} (III) + 25 µg L^{-1} As(V)) (n = 3)

As species	Concentration recovered (µg L^{-1} ± SD)	Percentage recovery (%)	RSD (%)
As(III)	20.39 ± 0.59	81.6	2.9
Total As	51.22 ± 3.4	102	6.7

As(V)	30.86 ± 2.8	123	9.2

For AMD, the sample was diluted 10 times on the day of analysis and other preparation steps were as described in section 4.3. There was no As(III) peak on running the DPASV analysis of the AMD sample instead other peaks from interfering elements were observed (Figure 5.21). This was not expected since the ICP/MS analysis used as a reference method had already confirmed the presence of arsenic in the concentration of 278.1 µg L^{-1} which influenced the 10 times dilution of the sample since the DPASV method was only calibrated up to 100 µg L^{-1}. Upon As(III) standard addition, it was confirmed that none of the peaks in the sample were resulting from As(III) as after several standard additions of 2.5 mg L^{-1} As(III) standard in 0.1 ml increments, another peak evolved around 0.2 V (Figure 5.21) correlating to As(III) addition. The peak was only visible after addition of about 50 µg L^{-1} As(III).

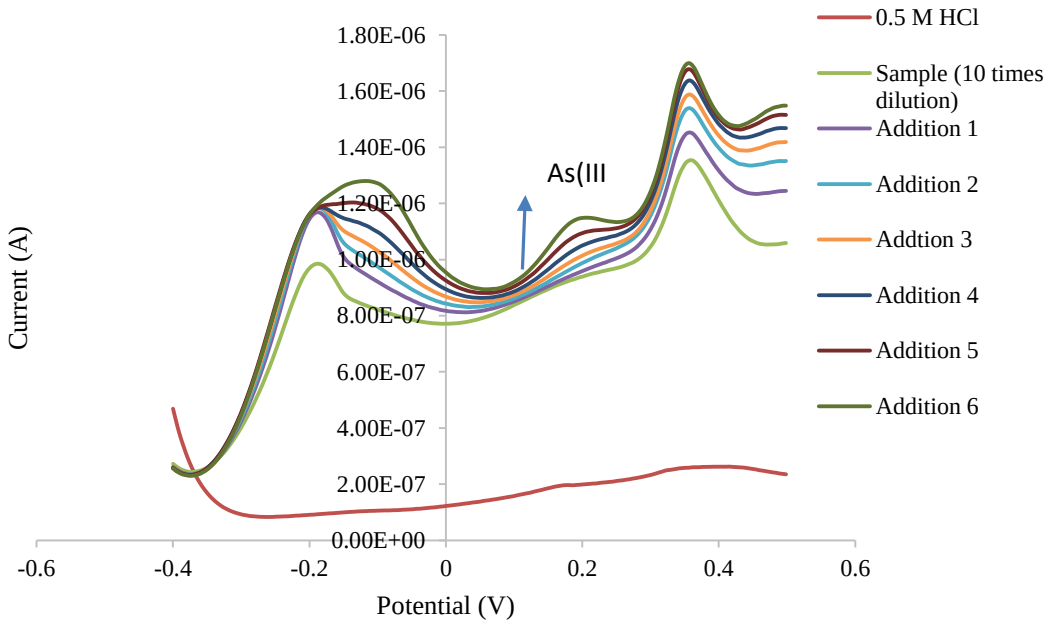

Figure 5.21 DPASV voltammograms of As(III) standard addition on AMD sample (10 times dilution) using -0.4 V DP, 180 s DT, 500 rpm RS and 0.04 V MA

Information from a study by Alves *et al*. (2011) was used to identify the peaks on the left and right side of the arsenic peak (Figure 5.21) as lead (Pb) and copper (Cu) peaks respectively. Nevertheless, to confirm their identity, the background solution was spiked with 25 µg L^{-1} of lead, arsenic and copper and the voltammogram in Figure 5.22 was obtained. This confirmed the identifications made using the findings of Alves *et al*. (2011). At this point, it was realized that the peak observed earlier in Figure 5.2 could have been possibly due to copper as in addition to mercury, the initial cell had previously been used for copper analysis too. It was also observed that the peak currents in Figure 5.22 were comparable to those for AMD sample (Figure 5.21) even though the total concentrations in AMD were much greater. This once again indicated signal depressions (electrode poisoning) in AMD due to high sulphate content (14253 mg L^{-1}) and presence of various other ions in AMD compared to the spiked background solution.

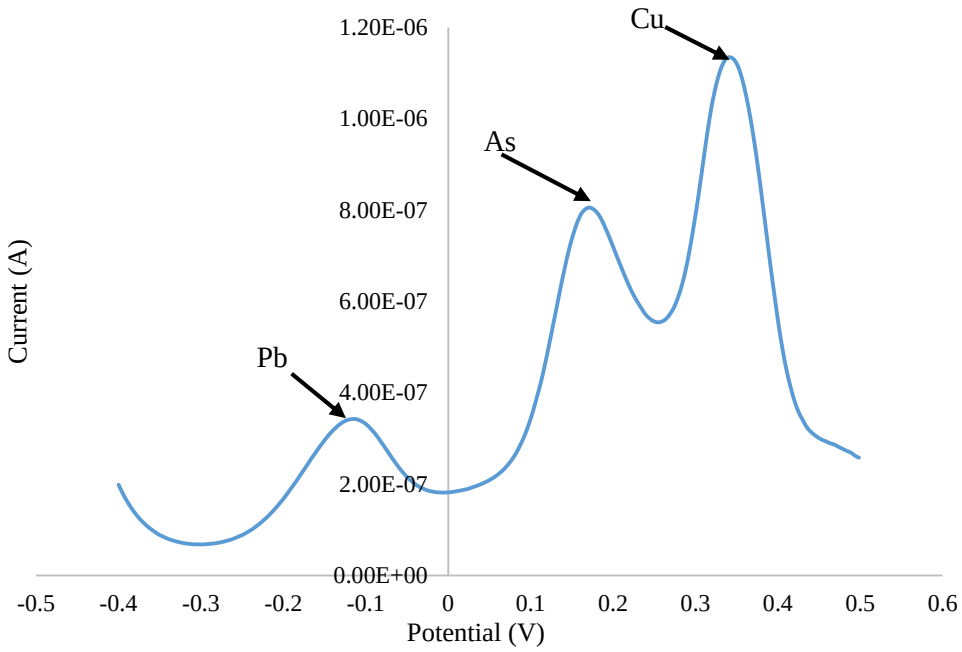

Figure 5.22 DPASV response of 25 µg L^{-1} Pb, As and Cu in 0.5 M HCl on a gold disc electrode using -0.4 V DP, 180 s DT, 500 rpm RS and 0.04 V MA

With no As(III) peak detected in the AMD sample, it was suspected that arsenic was in the arsenate form which is electrochemically inactive, however, in section 5.5.4 it will be shown that As(III) is the dominant species at the low pH values of

AMD. The presence of other dissolved metals with peak potentials close to that of arsenic (Cu and Pb) which may suppress or overlap with the As(III) peak were also thought to contribute to this observation. Since there were more than three orders of magnitude more of both Pb and Cu in solution than total arsenic (as detected by ICP-MS and ICP OES), the high concentrations of these ions collected at the electrode surface during deposition swamped any response from As(III) during the stripping step. The presence of different cations in the matrix solution with similar anodic peak potentials is known to result in overlapping of peaks hence negatively affecting stripping analysis (Alves *et al*., 2011). Li *et al*. (2012) further stated that the As(III) peak can be overlapped completely in the presence of significant amounts of interfering elements.

Zhou *et al*. (2017) investigated the effect of interfering metals on anodic stripping voltammetry determination of arsenic and discovered that in the presence of equal amounts of As(III) and Cu(II) in solution, the anodic peak of arsenic decreased significantly. Therefore considering the large amounts of copper in the AMD sample compared to total arsenic, the absence of As(III) peak is comprehensible. Even though there was no Pb(II) interference observed in the study by Zhou *et al*. (2017) (at equal concentration of As(III) and Pb(II)), in excess amounts observed in AMD, its anodic peak is also suspected to contribute to the absence of As(III) peak.

The As(V) reduction procedure was also undertaken on the AMD sample, however, there was still no As(III) peak observed on running the DPASV analysis after the reduction step (Figure 5.23). It was rather observed that the peak on the positive side of As(III) peak (observed in Figure 5.21) which was identified as Cu(II) anodic peak, disappeared completely while the peak around -0.2 V was not significantly affected by addition of $Na_2S_2O_3$. In their study, Breuer and Jeffrey (2003) indicated that the reaction of copper and thiosulphate reduces Cu(II) and generates trithionate. This leads to the depletion of the thiosulphate needed for reduction of As(V). Therefore the presence of Cu(II) in solution affects the thisulphate reduction of As(V) to As(III).

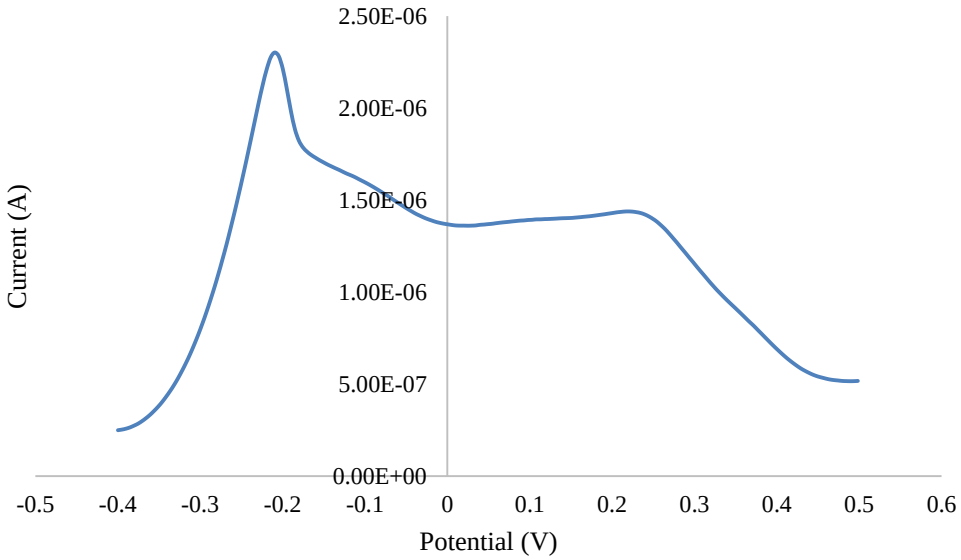

Figure 5.23 DPASV response of AMD sample (10 times dilution) after As(V) reduction to As(III) using -0.4 V DP, 180 s DT, 500 rpm RS and 0.04 V MA

5.5.4 Simulation of the species distribution in environmental samples using PHREEQC interactive code

PHREEQC modelling was used to provide an insight into the speciation and the bioavailability of arsenic in AMD from the Witwatersrand area. To simulate the conditions of the actual environment, the pH and Eh values obtained during field analysis, the total concentrations of the metals/metalloids and the anion concentrations determined from AMD were used as data sources for the model. Table 5.9 shows the distribution of species in the AMD sample at this conditions. A detailed sample PHREEQC script showing all calculated output concentrations at the specified conditions and metal concentrations is included in the appendix section.

The simulation showed that, of the total arsenic obtained by chemical analysis, most of it was in the reduced oxidation state (As(III)) while a smaller portion was associated with the arsenate form (As(V)). The major As(III) species contributing to the overall As(III) concentration at all conditions simulated in this work were $HAsO_2$ and $As(OH)_3$ as determined by the PHREEQC model. The arsenic Eh-pH diagram (Smedley and Kinniburgh, 2002) indicates that in highly acidic conditions

and redox potentials around 400 mV, As(III) is the more dominant oxidation state. This agrees with the geochemical model results obtained. Since As(III) is said to be more soluble and mobile than the oxidised form (As(V)) (Owens *et al*., 2005), the species distribution resulting from this model are a pointer to the presence of highly toxic and bioavailable arsenic species in AMD. The indication of these species in AMD also implies a great danger to the surrounding environment as the species may leach into surface and ground water increasing bioavailability to humans and animals.

Table 5.9 Distribution of species in the AMD sample at room temperature (25°C)

Species	**Moles**	**Precipitating phases**
As(3)	$4.876e^{-6}$	
$HAsO_2$	$2.724e-^{06}$	
$As(OH)_3$	$2.152e-^{06}$	
As(5)	$2.302e^{-8}$	
$H_2AsO_4^-$	$1.398e-^{08}$	
H_3AsO_4	$9.029e-^{09}$	
Al	$1.678e^{+00}$	$AlHO_2$
Fe(2)	$4.535e^{+00}$	
Fe(3)	$2.494e^{-6}$	FeOOH, Fe_2O_3
S(6)	$1.959e^{-1}$	
Cl(-1)	$1.47e^{-3}$	
Cl(1)	$5.910e^{-40}$	
Cu(1)	$3.869e^{-6}$	$CuFeO_2$
Cu(2)	$1.677e^{-2}$	
Mn(2)	1.777^{e-3}	
Mn(3)	$8.905e^{-22}$	
Ni	$5.921e^{-3}$	
Pb(2)	$4.147e^{-3}$	$PbSO_4$
Hg (1)	$6.579e^{-10}$	Hg_2Cl_2, $Hg_{(l)}$
Hg(2)	$5.586e^{-15}$	

Geochemical modelling was also utilized to simulate the variation in the species distribution on changing parameters such as pH (Table 5.10) and temperature (Table 5.11). To study the pH effect, pH 7 was used in the modelling input instead of the acidic pH determined during field analysis while the other parameters were kept constant. This was to study how the speciation of arsenic would be affected at around neutral pH, which is characteristic for most natural waters.

At a neutral pH, the PHREEQC indicated As(V) as the dominant oxidation state while As(III) only existed in lower concentrations. The model also showed that a great proportion of As(V) is constituted by $HAsO_4^{2-}$ and $H_2AsO_4^-$. This again correlates with what is indicated in the Eh-pH diagram for arsenic (Smedley and Kinniburgh, 2002) as it shows these species to be present at near neutral pH. There was also an indication of the formation of lammerite ($Cu_3(AsO_4)_2$) which has As(V) incorporated in its structure thus limiting the dissolved arsenate concentration.

At this pH, the species distribution showed that Fe(III) rather than Fe(II) was the dominant species and there was also an indication of the formation of several precipitated iron species. Even though there is no indication of incorporated arsenic in the iron precipitates formed, the presence of these precipitated phases may limit dissolved arsenic due to sorption interactions. This is supported by Kumar and Riyazuddin (2010) who indicated that for mine waters with high iron concentrations, iron precipitates may provide sorption sites for dissolved arsenic species. O'Day (2004) also indicated that under mild reducing conditions, arsenite may co-exist with oxides of Fe(II) and Fe(III) but further suggested that these adsorptions require further investigation as there are several contributing factors including pH. The precipitation occurring at neutral pH can therefore reduce the bioavailable concentrations in natural waters thus pH can be linked to the low concentrations observed in Fleurhof dam sample.

Besides iron, the simulation shows other metal ions including copper and lead to form precipitates at a neutral pH. This observation again corresponds with the declarations of Smedley and Kinniburgh (2002), who specifies that most trace metals in natural waters are found in insoluble forms as they either exist as

precipitates or they tend to co-precipitate and adsorb to other metal oxide and hydroxide minerals.

Table 5.10 PHREEQC distribution of species in the AMD sample at pH 7 (25°C)

Species	**Moles**	**Precipitating phases**
As(3)	$1.914e^{-17}$	
$HAsO_2$	$1.040e^{-17}$	
$As(OH)_3$	$8.685e^{-18}$	
As(5)	$4.899e^{-6}$	$Cu_3(AsO_4)_2$
$HAsO_4^{2-}$	$4.606e^{-06}$	
$H_2AsO_4^-$	$2.879e^{-07}$	
Al	$1.678e^{+00}$	AlO_2H, Al_2O_3, $AlHO_2$, $Al(OH)_3$,
Fe(2)	$1.177e^{-1}$	
Fe(3)	$4.417e^{+00}$	$Fe(OH)_3$, $CuFe_2O_4$, $Fe(OH)_3$, FeOOH, Fe_2O_3, Fe_3O_4, $FeAl_2O_4$
S(6)	$1.959e^{-1}$	
Cl(-1)	$1.471e^{-3}$	
Cl(1)	$5.910e^{-40}$	
Cu(1)	$1.386e^{-6}$	Cu_2O, $CuFeO_2$
Cu(2)	$1.677e^{-2}$	$Cu_3(SO_4)(OH)_4$, $Cu_4Cl_2(OH)_6$, $Cu_4(SO_4)(OH)_6$, $CuFeO_2$, $CuFe_2O_4$, $Cu_3(AsO_4)_2$, CuO
Mn(2)	1.777^{e-3}	
Mn(3)	$2.197e^{-22}$	
Ni	$5.922e^{-3}$	
Pb(2)	$4.147e^{-3}$	$PbSO_4$, $Pb_2(SO_4)O$, Pb_4SO_7, $Pb_4Cl_2(OH)_6$, Pb_3SO_6, PbClOH
Hg(1)	$6.579e^{-10}$	Hg_2Cl_2, $Hg_{(l)}$
Hg(2)	$5.362e^{-15}$	

To study the effect of temperature, the simulation was based on the South African climate, which has cold winters and warm summers. In Johannesburg, the

maximum winter temperatures are normally below 20°C with an average around 17°C while in summer the average temperatures are around 25°C. Therefore, Table 5.9 is already representative of the species distribution during summer since the model was conducted at room temperature (25°C). Table 5.11 on the other hand shows the possible species distribution and precipitating phases at 17°C. Comparing the species distribution at the two temperatures, they reveal that the distribution of species is almost the same for the winter and summer simulations except that at warm temperatures, $AlHO_2$ had a positive saturation index indicating precipitation, while at low temperatures, it is dissociated in solution. For arsenic and iron species, the dominant species at both temperatures are the soluble forms of these elements, that is As(III) and Fe(II), respectively. The prevalence of the most toxic arsenic species (As(III)) is therefore observed over the normal winter and summer temperatures.

Table 5.11 PHREEQC distribution of species in AMD sample at 17°C (pH 2.76)

Species	**Moles**	**Precipitating phases**
As(3)	$4.889e^{-06}$	
$HAsO_2$	$2.723e^{-06}$	
$As(OH)_3$	$2.167e^{-06}$	
As(5)	$9.418e^{-09}$	
$H_2AsO_4^-$	$5.971e^{-09}$	
H_3AsO_4	$3.442e^{-09}$	
Al	$1.678e^{+00}$	
Cl(-1)	$1.470e^{-03}$	
Cu(1)	$2.947e^{-06}$	
Cu(2)	$1.677e^{-02}$	$CuFeO_2$
Fe(2)	$4.535e^{+00}$	
Fe(3)	$1.907e^{-06}$	Fe_2O_3, FeOOH
H(0)	$2.468e^{-22}$	
Hg(1)	$6.579e^{-10}$	Hg_2Cl_2, $Hg_{(l)}$,
Hg(2)	$2.159e^{-15}$	
Mn(2)	$1.777e^{-03}$	
Mn(3)	$4.729e^{-22}$	
Ni	$5.921e^{-03}$	
Pb(2)	$4.147e^{-03}$	$PbSO_4$,
S(6)	$1.959e^{-01}$	

Chapter 6

General conclusions and recommendations

This chapter discusses the conclusions drawn from the experimental findings of this study. The recommendations for future work are also presented.

6.1 Conclusions

DPASV method for determination of As(III) on a solid gold disc electrode was optimized and validated using standard solutions. Modulation amplitude of 0.04 V was used for this study and other DPASV optimum conditions were obtained as -0.4 V, 180 s and 500 rpm for deposition potential, deposition time and rotation speed, respectively. For As(III), 0.9969 was obtained as the coefficient of determination in the range of 12.5 µg L^{-1} to 100 µg L^{-1} and the method LOD and LOQ were determined to be 5.94 µg L^{-1} and 19.8 µg L^{-1} respectively.

The method viability was tested on real environmental samples, in particular AMD and Fleurhof dam water samples collected in the central rand goldfield of the Witwatersrand basin in SA. The proposed DPASV method was unfortunately challenged by several factors. In an AMD matrix, the co-existence of various components including comparatively high concentrations of dissolved metals and anions interfered with the determination of As(III) thus completely preventing identification and quantification of arsenic species using this electrochemical technique. In dam water, the DPASV method was not sensitive enough to detect and quantify the total arsenic concentration naturally present in the sample. However, for spiked dam water samples, the method was able to recover 81.6% of As(III), 102% of total arsenic and 123% of As(V) respectively.

For determination of As(V) concentration, the use of sodium thiosulphate as a reducing agent was investigated and from the study, 1 mg was determined to be the optimum mass of sodium thiosulphate for reduction of 25 µg L^{-1} As(V) in 0.5 M HCl.

Using ICP-MS, the total arsenic concentration was determined to be 0.2781 mg L^{-1} in the AMD sample while for the Fleurhof dam sample, the concentration was determined to be 0.0120 mg L^{-1}. The Fleurhof dam concentration was more than an order of magnitude lower than in AMD but higher than the WHO (2010) guideline limit for drinking water. With the aid of PHREEQC modelling, which demonstrated capabilities of determining species distribution, the AMD sample was calculated to contain both As(III) and As(V) species in solution. As(III) was determined to be the most dominant species at both summer and winter average temperatures, while

As(V) was determined to be dominant at a neutral pH. The presence of these toxic and bioavailable arsenic species in significant amounts in the AMD sample is an indication of potential harm to the surrounding environment.

6.2 Recommendations

- Future work can focus on ways to lower the interference effects for As(III) determination by DPASV in complex matrices such as AMD by applying ion exchange separations before electrochemical analysis or using modified electrodes to specifically target As(III).
- Other reducing agents need to be explored for application in the reduction procedure of As(V) to As(III) for electrochemical analysis to prevent poisoning of the gold electrode.
- Even though PHREEQC can determine the speciation distribution of elements, further investigation with laboratory analytical techniques such as HPLC-ICP-MS which were not available to us may be used to confirm the findings of the geochemical model.
- The effect of environmental conditions such as temperature and pH need to be further investigated in the lab to support the PHREEQC findings.
- There is a need to sample other media such as soil and plants from the mining areas to gain more insight on the potential risk of arsenic pollution to the surrounding environment.
- Future work should also assess arsenic pollution in other South African mining areas.

References

Alves, G.M., Magalhães, J.M., Salaün, P., Van den Berg, C.M. and Soares, H.M., (2011). Simultaneous electrochemical determination of arsenic, copper, lead and mercury in unpolluted fresh waters using a vibrating gold microwire electrode. *Analytica Chimica Acta*, *703*(1), pp.1-7.

Antonova, S. and Zakharova, E. (2016). Inorganic arsenic speciation by electroanalysis. From laboratory to field conditions: A mini-review. *Electrochemistry Communications*, 70, pp. 33-38.

B'Hymer, C. and Caruso, J. A. (2004). Arsenic and its speciation analysis using high-performance liquid chromatography and inductively coupled plasma mass spectrometry. *Journal of Chromatography A*, 1045(1–2), pp. 1–13.

Bednar, A.J., Garbarino, J.R., Ranville, J.F. and Wildeman, T.R. (2002). Preserving the distribution of inorganic arsenic species in groundwater and acid mine drainage samples. *Environmental Science & Technology*, 36(10), pp. 2213-2218.

Bera, A. K., Rana, T., Das, S., Pan, D., De, S., Samanta, S., Chowdhury, A. N., Mondal, T. K. and Das, S. K. (2010). Ground water arsenic in West Bengal, India-a risk of sub-clinical toxicity in cattle as evident by correlation between arsenic exposure, excretion and deposition. *Toxicology and industrial health*, 26(10), pp. 709-716.

Berg, M., Stengel, C., Trang, P.T.K., Viet, P.H., Sampson, M.L., Leng, M., Samreth, S. and Fredericks, D. (2007). Magnitude of arsenic pollution in the Mekong and Red River Deltas-Cambodia and Vietnam. *Science of the Total Environment*, *372*(2-3), pp. 413-425.

Bowell, R. J., Alpers, C. N., Jamieson, H. E., Nordstrom, D. K., and Majzlan, J. (2014). The environmental geochemistry of arsenic-an overview. *Reviews in Mineralogy and Geochemistry*, 79(1), pp. 1-16.

Breuer, P.L. and Jeffrey, M.I. (2003). The reduction of copper (II) and the oxidation of thiosulfate and oxysulfur anions in gold leaching solutions. *Hydrometallurgy*, *70*(1-3), pp. 163-173.

Bu, L., Gu, T., Ma, Y., Chen, C., Tan, Y., Xie, Q. and Yao, S. (2015). Enhanced cathodic preconcentration of As (0) at Au and Pt electrodes for anodic stripping voltammetry analysis of As (III) and As (V). *The Journal of Physical Chemistry C*, 119(21), pp.11400-11409.

Carrera, P., Espinoza-Montero, P.J., Fernández, L., Romero, H. and Alvarado, J. (2017). Electrochemical determination of arsenic in natural waters using carbon fiber ultra-microelectrodes modified with gold nanoparticles. *Talanta*, 166, pp. 198-206.

Caruso, J. A. and Montes-Bayon, M. (2003). Elemental speciation studies - New directions for trace metal analysis. *Ecotoxicology and environmental safety*, 56(1), pp. 148-163.

Caussy, D. (2003). Case studies of the impact of understanding bioavailability : arsenic. *Ecotoxicology and environmental safety*, 56, pp. 164-173.

Chakraborti, D., Mukherjee, S.C., Pati, S., Sengupta, M.K., Rahman, M.M., Chowdhury, U.K., Lodh, D., Chanda, C.R., Chakraborti, A.K. and Basu, G.K., (2003). Arsenic groundwater contamination in Middle Ganga Plain, Bihar, India: a future danger?. *Environmental Health Perspectives*, *111*(9), p.1194.

Cheng, H., Hu, Y., Luo, J., Xu, B. and Zhao, J., (2009). Geochemical processes controlling fate and transport of arsenic in acid mine drainage (AMD) and natural systems. *Journal of hazardous materials*, 165(1-3), pp.13-26.

Choi, J.Y., Khan, N., Nho, E.Y., Choi, H., Park, K.S., Cho, M.J., Youn, H.J. and Kim, K.S., (2016). Speciation of arsenic in rice by high-performance liquid chromatography–inductively coupled plasma mass spectrometry. *Analytical Letters*, *49*(12), pp.1926-1937.

Chowdhury, U.K., Biswas, B.K., Chowdhury, T.R., Samanta, G., Mandal, B.K., Basu, G.C., Chanda, C.R., Lodh, D., Saha, K.C., Mukherjee, S.K. and Roy, S., (2000). Groundwater arsenic contamination in Bangladesh and West Bengal, India. *Environmental health perspectives*, *108*(5), p.393.

Couture, R. M. and Van Cappellen, P. (2011). Reassessing the role of sulfur geochemistry on arsenic speciation in reducing environments. *Journal of Hazardous Materials*, 189(3), pp. 647–652.

Dai, X., Nekrassova, O., Hyde, M.E. and Compton, R.G., (2004). Anodic stripping voltammetry of arsenic (III) using gold nanoparticle-modified electrodes. *Analytical chemistry*, *76*(19), pp.5924-5929.

Duruibe, J. O. and Egwurugwu, J. (2007). Heavy metal pollution and human biotoxic effects. *International Journal of Physical Sciences*, 2 (5), pp. 112-118.

Esteban, E., Carpena, R.O. and Meharg, A.A. (2003). High-affinity phosphate/arsenate transport in white lupin (Lupinus albus) is relatively insensitive to phosphate status. *New Phytologist*, 158(1), pp. 165-173.

Ferreira, M. A., & Barros, A. A. (2002). Determination of As (III) and arsenic (V) in natural waters by cathodic stripping voltammetry at a hanging mercury drop electrode. *Analytica Chimica Acta*, 459(1), pp. 151-159.

Feris, L. and Kotze, L.J., (2014). The regulation of acid mine drainage in South Africa: law and governance perspectives. *Potchefstroom Electronic Law Journal/Potchefstroomse Elektroniese Regsblad*, *17*(5), pp.2104-2163.

Fukushi, K., Sasaki, M., Sato, T., Yanase, N., Amano, H., and Ikeda, H. (2003). A natural attenuation of arsenic in drainage from an abandoned arsenic mine dump. *Applied Geochemistry*, 18(8), pp. 1267-1278.

Garcia-Manyes, S., Jimenez, G., Padro, A., Rubio, R. and Rauret, G. (2002). Arsenic speciation in contaminated soils. *Talanta*, 58(1), pp. 97-109.

Garelick, H., Jones, H., Dybowska, A. and Valsami-Jones, E., 2008. Arsenic pollution sources. In *Reviews of Environmental Contamination*, 197, pp. 17-60.

Giacomino, A., Abollino, O., Malandrino, M. and Mentasti, E. (2008). Parameters affecting the determination of mercury by anodic stripping voltammetry using a gold electrode. *Talanta*, 75(1), pp. 266-273.

Gillispie, E.C., Sowers, T.D., Duckworth, O.W. and Polizzotto, M.L., (2015). Soil

pollution due to irrigation with arsenic-contaminated groundwater: Current state of science. *Current Pollution Reports, 1*(1), pp.1-12.

Goldberg, S. (2002). Competative adsorption of arsenate and arsenite on oxides and clay. *Soil Science Society of America Journal,* 66, pp. 413-421.

Greschonig, H. and Irgolic, K.J. (1992). Electrochemical methods for the determination of total arsenic and arsenic compounds. *Applied organometallic chemistry*, 6(7), pp. 565-577.

Grover, B.P.C., Johnson, R.H. and Tutu, H. (2016). Leachability of metals from gold tailings by rainwater: an experimental and geochemical modelling approach. *Water SA, 42*(1), pp.38-42.

He, P., Colón, L.A. and Aga, D.S. (2016). Determination of Total Arsenic and Speciation in Apple Juice by Liquid Chromatography–Inductively Coupled Plasma Mass Spectrometry: An Experiment for the Analytical Chemistry Laboratory. *Journal of Chemical Education*, 93(11), pp. 1939-1944.

He, Y., Zheng, Y. and Locke, D.C. (2007). Cathodic stripping voltammetric analysis of arsenic species in environmental water samples. *Microchemical Journal*, 85(2), pp. 265-269.

Hsieh, M.W., Liu, C.L., Chen, J.H. and Jiang, S.J. (2010). Speciation analysis of arsenic and selenium compounds by CE-dynamic reaction cell-ICP-MS. *Electrophoresis*, 31(13), pp. 2272-2278.

Hughes, M. F. (2002) 'Arsenic toxicity and potential mechanisms of action', *Toxicology letters*, 133, pp. 1–16.

Jain, C. K., and Ali, I. (2000). Arsenic: occurrence, toxicity and speciation techniques. *Water research*, 34(17), pp. 4304-4312.

Jedryczko, D., Pohl, P. and Welna, M. (2016). Inorganic arsenic speciation in natural mineral drinking waters by flow-through anodic stripping chronopotentiometry. *Talanta*, 150, pp. 265-271.

Katsoyiannis, I. A., and Zouboulis, A. I. (2004). Application of biological processes

for the removal of arsenic from groundwaters. *Water research*, 38(1), pp. 17-26.

Komorowicz, I. and Barałkiewicz, D. (2016). Determination of total arsenic and arsenic species in drinking water, surface water, wastewater, and snow from Wielkopolska, Kujawy-Pomerania, and Lower Silesia provinces, Poland. *Environmental monitoring and assessment*, 188(9), pp. 504-.

Kumar, A.R. and Riyazuddin, P. (2010). Preservation of inorganic arsenic species in environmental water samples for reliable speciation analysis. *Trends in Analytical Chemistry*, 29(10), pp. 1212-1223.

Li, D., Li, J., Jia, X., Han, Y. and Wang, E. (2012). Electrochemical determination of arsenic (III) on mercaptoethylamine modified Au electrode in neutral media. *Analytica chimica acta*, 733, pp.23-27.

Lin, Y., Wu, B., Ning, P., Qu, G., Li, J., Wang, X. and Xie, R., (2017). Stabilization of arsenic in waste slag using FeCl 2 or FeCl 3 stabilizer. *RSC Advances*, *7*(87), pp.54956-54963.

Liu, G., Böcking, T. and Gooding, J. J. (2007). Diazonium salts: Stable monolayers on gold electrodes for sensing applications. *Journal of Electroanalytical Chemistry*, 600(2), pp. 335–344.

Llorente-Mirandes, T., Calderón, J., Centrich, F., Rubio, R. and López-Sánchez, J.F. (2014). A need for determination of arsenic species at low levels in cereal-based food and infant cereals. Validation of a method by IC–ICPMS. Food chemistry, 147, pp.377-385.

Londesborough, S., Mattusch, J. and Wennrich, R. (1999). Separation of organic and inorganic arsenic species by HPLC-ICP-MS. *Fresenius' Journal of Analytical Chemistry*, 363(5-6), pp. 577-581.

Ma, L. Q., Komar, K. M., Tu, C., Weihua, Z., Yong, C., and Kennelley, E. D. (2001). A fern that hyperaccumulates arsenic. *Nature*, 409, 579.

Ma, L., Wang, L., Jia, Y. and Yang, Z., (2016). Arsenic speciation in locally grown rice grains from Hunan Province, China: Spatial distribution and potential health risk. *Science of the Total Environment*, *557*, pp.438-444.

Maher, W.A., Ellwood, M.J., Krikowa, F., Raber, G. and Foster, S., (2015). Measurement of arsenic species in environmental, biological fluids and food samples by HPLC-ICPMS and HPLC-HG-AFS. *Journal of Analytical Atomic Spectrometry*, *30*(10), pp.2129-2183.

Mahimairaja, S., Bolan, N. S., Adriano, D. C., and Robinson, B. (2005). Arsenic contamination and its risk management in complex environmental setting. *Advances in Agronomy*, 86, pp. 1-82.

Martinez, V. D., Vucic, E. A., Becker-Santos, D. D., Gil, L. and Lam, W. L. (2011). Arsenic exposure and the induction of human cancers. *Journal of Toxicology*, pp. 1-13.

Mattusch, J. and Wennrich, R. (1998). Determination of anionic, neutral, and cationic species of arsenic by ion chromatography with ICPMS detection in environmental samples. *Analytical chemistry*, 70(17), pp. 3649-3655.

Mays, D. E. and Hussam, A. (2009). Voltammetric methods for determination and speciation of inorganic arsenic in the environment-A review. *Analytica Chimica Acta*, 646(1–2), pp. 6–16.

Melashvili, M., Dreisinger, D. and Choi, Y. (2016). Cyclic voltammetry responses of gold electrodes in thiosulphate electrolyte, *Minerals Engineering*. Elsevier Ltd, 92, pp. 134–140.

Metrohm application bulletin 226/2 e. Determination of arsenic by anodic stripping voltammetry at the rotating gold electrode.

Metrohm Autolab B.V. (2018). Nova 2.1 user manual.

Michalke, B. (2003). Element speciation definitions, analytical methodology, and some examples. *Ecotoxicology and Environmental Safety*. 56(1), pp. 122–139.

Mishra, S., Mattusch, J. and Wennrich, R., (2017). Accumulation and transformation of inorganic and organic arsenic in rice and role of thiol-complexation to restrict their translocation to shoot. *Scientific Reports*, *7*, p.40522.

Mkandawire, M. and Dudel E. G. (2005). Accumilation of arsenic in *Lemma gibba*

L. (duckweed) in tailing waters of two abondened uranium mining sites in Saxony, Germany. *Science of the total environment,*336, pp. 81-89.

Molin, M., Ulven, S.M., Meltzer, H.M. and Alexander, J., (2015). Arsenic in the human food chain, biotransformation and toxicology–review focusing on seafood arsenic. *Journal of Trace Elements in Medicine and Biology*, *31*, pp.249-259.

Moriarty, M. M., Lai, V. W. M., Koch, I., Cui, L., Combs, C., Krupp, E. M., Feldmann, J., Cullen, W. R. and Reimer, K. J. (2014). Speciation and toxicity of arsenic in mining affected lake sediments in the Quinsam water shed, British Culumbia. *Science of the total environment,* 466-467. pp 90-99.

Mukherjee, A., Kundu, M., Basu, B., Sinha, B., Chatterjee, M., Bairagya, M.D., Singh, U.K. and Sarkar, S., (2017). Arsenic load in rice ecosystem and its mitigation through deficit irrigation. *Journal of environmental management*, *197*, pp.89-95.

Naicker, K., Cukrowska, E. and McCarthy, T.S. (2003). Acid mine drainage arising from gold mining activity in Johannesburg, South Africa and environs. *Environmental Pollution*, 122(1), pp. 29-40.

Neingo, P.N. and Tholana, T., (2016). Trends in productivity in the South African gold mining industry. *Journal of the Southern African Institute of Mining and Metallurgy*, *116*(3), pp.283-290.

Nekhunguni, P.M., Tavengwa, N.T. and Tutu, H., (2017). Investigation of As (V) removal from acid mine drainage by iron (hydr) oxide modified zeolite. *Journal of environmental management*, *197*, pp.550-558.

Nkosi, N.Z., Manzi, M.S., Drennan, G.R. and Yilmaz, H., (2017). Experimental measurements of seismic velocities on core samples and their dependence on mineralogy and stress; Witwatersrand Basin (South Africa). *Studia Geophysica et Geodaetica*, *61*(1), pp.115-144.

Nombona, N., Geraldo, D.A., Hakuzimana, J., Schwarz, A., Westbroek, P. and Nyokong, T. (2009). Comparative electrocatalytic behavior of self-assembled monolayer of thiol derivatised Co (II) phthalocyanines on gold disk, ultramicro cylinder and fiber electrodes. *Journal of applied electrochemistry*, 39(5), pp. 727-

736.

Nookabkaew, S., Rangkadilok, N., Mahidol, C., Promsuk, G. and Satayavivad, J. (2013). Determination of arsenic species in rice from Thailand and other Asian countries using simple extraction and HPLC-ICP-MS analysis. *Journal of agricultural and food chemistry*, 61(28), pp.6991-6998.

O'Day, P.A., Vlassopoulos, D., Root, R. and Rivera, N. (2004). The influence of sulfur and iron on dissolved arsenic concentrations in the shallow subsurface under changing redox conditions. *Proceedings of the National Academy of Sciences*, 101(38), pp.13703-13708.

O'Day, P. A. (2006). Chemistry and minarology of arsenic. *Elements*, 2, pp. 77-83.

Owens, G., Naidu, R., Akter, K. F., Owens, G., Davey, D. E. and Naidu, R. (2005). Arsenic Speciation and Toxicity in Biological Systems. *Reviews of Environmental contamination toxicoligy*, 184, pp. 97-149.

Pal, P., and Manna, A. K. (2010). Removal of arsenic from contaminated groundwater by solar-driven membrane distillation using three different commercial membranes. *Water research*, 44(19), pp. 5750-5760.

Pal, P., Sen, M., Manna, A., Pal, J., Pal, P., Roy, S., and Roy, P. (2009). Contamination of groundwater by arsenic: a review of occurrence, causes, impacts, remedies and membrane-based purification. *Journal of Integrative Environmental Sciences*, 6(4), pp. 295-316.

Paul, S.C., Rahman, M.A. and Alam, A.S. (2007). Voltammetric study of Arsenic (III) and Arsenic (V) in Ground Water of Hajigonj and Kalkini in Bangladesh. *Pakistan Journal of Analytical & Environmental Chemistry*, 8(1-2), pp. 49-55.

Pillay, L. and Kindness, A., (2016). A preliminary investigation into the stability of inorganic arsenic species in laboratory solutions simulating sediment pore water. *South African Journal of Chemistry, 69*, pp. 9-14.

Profumo, A., Merli, D. and Pesavento, M. (2005). Voltammetric determination of inorganic As(III) and total inorganic As in natural waters, *Analytica Chimica Acta*,

539(1–2), pp. 245–250.

Raj, K.R., Saxena, S., Kardam, A., Satsangi, S.P. and Srivastava, S. (2014). Voltammetric speciation of arsenic species in plant biomaterial: bioremediation. *Clean Technologies and Environmental Policy*, 16(2), pp. 377-384.

Radke, B., Jewell, L. and Namieśnik, J., (2012). Analysis of arsenic species in environmental samples. *Critical Reviews in Analytical Chemistry*, *42*(2), pp.162-183.

Ratnaike, R. N. (2003). Acute and chronic arsenic toxicity. *Postgraduate Medical Journal*, 79(933), pp. 391–6.

Razo, I., Carrizales, L., Castro, J., Díaz-Barringa, F. and Monroy, M. (2004). Arsenic and heavy metal pollution of soil water and sedimentsin semi-arid climate mining area in Mexico. *Water, air and soil pollution*, 152, pp. 129-152.

Reeves, J. A. (1997). Chemical speciation modelling of the cooling water circuit at matla power station. Dissertation. University of Natal.

Rosen, A. L. and Hieftje, G. M. (2004). Inductively coupled plasma mass spectrometry and electrospray mass spectrometry for speciation analysis: Applications and instrumentation. *Spectrochimica Acta - Part B Atomic Spectroscopy*, 59(2), pp. 135–146.

Rukh, S., Akhtar, M.S., Memon, M., Mehmood, A. and Imran, M., (2015). An overview of arsenic extraction and speciation techniques in soil and water. *Amer. Chem. Sci. J*, *6*, pp.1-15.

Salaün, P., Planer-Friedrich, B. and Van den Berg, C.M. (2007). Inorganic arsenic speciation in water and seawater by anodic stripping voltammetry with a gold microelectrode. *Analytica Chimica Acta*, 585(2), pp. 312-322.

Sanz, E., Munoz-Olivas, R., Camara, C., Sengupta, M.K. and Ahamed, S. (2007). Arsenic speciation in rice, straw, soil, hair and nails samples from the arsenic-affected areas of Middle and Lower Ganga plain. *Journal of Environmental Science and Health Part A*, 42(12), pp. 1695-1705.

Shah, M., Kannamkumarath, S.S., Wuilloud, J.C., Wuilloud, R.G. and Caruso, J.A. (2004). Identification and characterization of selenium species in enriched green onion (Allium fistulosum) by HPLC-ICP-MS and ESI-ITMS. *Journal of Analytical Atomic Spectrometry*, 19(3), pp. 381-386.

Smedley, P. L., Edmunds, W. M. and Pelig-Ba, K. B. (1996). Mobility of arsenic in ground water in the Obuasi gold mining area of Ghana: some implications of human health. *Environmental geochemistry and health*, 113, pp. 163-181.

Smedley, P. L. and Kinniburgh, D. G. (2002). A review of the source, behaviour and distribution of arsenic in natural sources. *Applied geochemistry*, 17(5), pp. 517-568.

Singh, R., Singh, S., Parihar, P., Singh, V.P. and Prasad, S.M., (2015). Arsenic contamination, consequences and remediation techniques: a review. *Ecotoxicology and environmental safety*, *112*, pp.247-270.

Sun, Y.-C., Mierzwa, J. and Yang, M.-H. (1997). New method of gold-film electrode preparation for anodic stripping voltammetric determination of arsenic (III and V) in seawater. *Talanta*, 44, pp. 1379–1387.

Tanaka, T. (1988). Distribution of arsenic in the natural environment with emphasis on rocks and soils. *Applied organometallic chemistry*, *2*(4), pp. 283-295.

Tatke, P. and Jaiswal, Y., (2011). An overview of microwave assisted extraction and its applications in herbal drug research. *Research Journal of Medicinal Plant*, *5*(1), pp.21-31.

Tutu, H., Cukrowska, E.M., Dohnal, V. and Havel, J. (2005). Application of artificial neural networks for classification of uranium distribution in the Central Rand goldfield, South Africa. *Environmental Modeling & Assessment*, 10(2), pp. 143-152.

Uslu, B. and Ozkan, S. (2007). Solid Electrodes in Electroanalytical Chemistry: Present Applications and Prospects for High Throughput Screening of Drug Compounds, *Combinatorial Chemistry & High Throughput Screening*, 10(7), pp. 495–513.

Wei, Z. and Somasundaran, P. (2004). Cyclic voltammetric study of arsenic reduction and oxidation in hydrochloric acid using a Pt RDE. *Journal of applied electrochemistry*, 34(2), pp. 241-244.

Wang, J. S. and Wai, C. M. (2004). Arsenic in drinking water-a clobal environmental problem. *Journal of chemical education*,81(1), pp. 207-213.

Wang, S. and Mulligan, C. N. (2006). Occurance of arsenic contamination in Canada: Sources, behavior and distribution. *Science of the total environment*,366, pp. 701-721.

WHO (2010). Exposure to Arsenic: A Major Public Health Concern. *Agriculture*, p. 5.

Xie, Z. M., and Huang, C. Y. (1998). Control of arsenic toxicity in rice plants grown on an arsenic-polluted paddy soil. *Communications in Soil Science and Plant Analysis*, 29(15-16), pp. 2471-2477.

Yamada, D., Ivandini, T.A., Komatsu, M., Fujishima, A. and Einaga, Y. (2008). Anodic stripping voltammetry of inorganic species of As^{3+} and As^{5+} at gold-modified boron doped diamond electrodes. *Journal of Electroanalytical Chemistry*, 615(2), pp.145-153.

Zanello, P. (2007). *Inorganic electrochemistry: theory, practice and application*. Royal Society of Chemistry.

Zhao, F.J., Dunham, S.J. and McGrath, S.P. (2002). Arsenic hyperaccumulation by different fern species. *New Phytologist*, 156(1), pp. 27-31.

Zheng, J., Hintelmann, H., Dimock, B. and Dzurko, M.S. (2003). Speciation of arsenic in water, sediment, and plants of the Moira watershed, Canada, using HPLC coupled to high resolution ICP–MS. *Analytical and Bioanalytical Chemistry*, 377(1), pp.14-24.

Zhou, C., Yang, M., Li, S.S., Jiang, T.J., Liu, J.H., Huang, X.J. and Chen, X. (2017). Electrochemically etched gold wire microelectrode for the determination of inorganic arsenic. *Electrochimica Acta*, 231, pp.238-246.

Zlatev, R., Stoytcheva, M. and Valdez, B. (2010). As(III) determination in the presence of Pb(II) by differential alternative pulses voltammetry, Electroanalysis, 22(15), pp. 1671–1674.

Appendix

Table A1 Sample PHREEQC script for AMD sample at 25°C

```
SOLUTION 1 ADM sample
    temp      25
    pH        2.76
    pe        5.79
    redox     pe
    units     mg/l
    density   1
    Al        34300
    As        0.2781
    Cl        39.5
    Cu        807.5
    Fe        191900
    Hg        0.0001
    Mn        73.98
    Ni        263.3
    Pb        651
    S(6)      14253
    -water    1 # kg
```

Table A2 Sample PHREEQC output for AMD sample at 25°C

```
-----------------------------------------
Beginning of initial solution calculations.
-----------------------------------------

Initial solution 1.     ADM sample

-----------------------------Solution composition----------------
--------------

      Elements           Molality       Moles

      Al                 1.678e+00   1.678e+00
      As                 4.899e-06   4.899e-06
      Cl                 1.470e-03   1.470e-03
      Cu                 1.677e-02   1.677e-02
      Fe                 4.535e+00   4.535e+00
      Hg                 6.579e-10   6.579e-10
      Mn                 1.777e-03   1.777e-03
      Ni                 5.921e-03   5.921e-03
      Pb                 4.147e-03   4.147e-03
      S(6)               1.959e-01   1.959e-01

----------------------------Description of solution--------------
--------------

                                       pH  =   2.760
                                       pe  =   5.790
                          Activity of water  =   0.903
                 Ionic strength (mol/kgw)  =   1.587e+01
                       Mass of water (kg)  =   1.000e+00
                 Total alkalinity (eq/kg)  =   1.133e+00
```

```
                    Total carbon (mol/kg)  =   0.000e+00
                       Total CO2 (mol/kg)  =   0.000e+00
                         Temperature (°C)  =  25.00
                  Electrical balance (eq)  =   1.263e+01
 Percent error, 100*(Cat-|An|)/(Cat+|An|)  =  99.91
                                Iterations  =  14
                                   Total H  = 1.121844e+02
                                   Total O  = 5.744191e+01

----------------------------Distribution of species--------------
--------------

                                                    Log       Log
Log    mole V
   Species          Molality    Activity  Molality  Activity
Gamma   cm³/mol

   H+              5.605e-04   1.738e-03    -3.251    -2.760
0.491      0.00
   OH-             2.593e-12   5.009e-12   -11.586   -11.300
0.286      (0)
   H2O             5.553e+01   9.035e-01     1.744    -0.044
0.000     18.07
Al             1.678e+00
   Al+3            7.194e-01   1.186e-01    -0.143    -0.926    -
0.783      (0)
   Al3(OH)4+5      2.012e-01   1.604e-06    -0.696    -5.795    -
5.098      (0)
   Al2(OH)2+4      1.629e-01   7.755e-05    -0.788    -4.110    -
3.322      (0)
   AlSO4+          2.553e-02   5.385e-02    -1.593    -1.269
0.324      (0)
   AlOH+2          2.347e-03   6.906e-04    -2.629    -3.161    -
0.531      (0)
   Al(SO4)2-       8.795e-04   1.855e-03    -3.056    -2.732
0.324      (0)
   Al(OH)2+        3.952e-07   8.337e-07    -6.403    -6.079
0.324      (0)
   HAlO2           6.981e-10   6.981e-10    -9.156    -9.156
0.000      (0)
   Al13O4(OH)24+7   8.605e-14   2.076e-24   -13.065   -23.683   -
10.618     (0)
   AlO2-           6.523e-14   1.376e-13   -13.186   -12.861
0.324      (0)
As(-3)         0.000e+00
   AsH3            0.000e+00   0.000e+00   -61.724   -61.724
0.000      (0)
As(3)          4.876e-06
   HAsO2           2.724e-06   2.724e-06    -5.565    -5.565
0.000      (0)
   As(OH)3         2.152e-06   2.152e-06    -5.667    -5.667
0.000      (0)
   AsO2-           3.798e-13   8.013e-13   -12.420   -12.096
0.324      (0)
   H2AsO3-         3.589e-13   7.573e-13   -12.445   -12.121
0.324      (0)
   AsO2OH-2        1.925e-20   4.257e-21   -19.716   -20.371    -
0.655      (0)
As(5)          2.302e-08
```

```
   H2AsO4-          1.398e-08   2.950e-08    -7.854    -7.530
0.324     (0)
   H3AsO4           9.029e-09   9.029e-09    -8.044    -8.044
0.000     (0)
   HAsO4-2          1.274e-11   2.818e-12   -10.895   -11.550    -
0.655     (0)
   AsO4-3           8.072e-19   4.159e-21   -18.093   -20.381    -
2.288     (0)
Cl(-1)         1.470e-03
   FeCl+            8.402e-04   1.773e-03    -3.076    -2.751
0.324     (0)
   Cl-              5.991e-04   1.035e-03    -3.222    -2.985
0.237     (0)
   PbCl+            1.721e-05   3.630e-05    -4.764    -4.440
0.324     (0)
   CuCl+            1.147e-05   2.420e-05    -4.940    -4.616
0.324     (0)
   MnCl+            9.429e-07   1.989e-06    -6.026    -5.701
0.324     (0)
   HCl              4.040e-07   4.040e-07    -6.394    -6.394
0.000     (0)
   CuCl2-           2.553e-07   5.387e-07    -6.593    -6.269
0.324     (0)
   NiCl+            1.611e-07   3.399e-07    -6.793    -6.469
0.324     (0)
   PbCl2            1.430e-07   1.430e-07    -6.845    -6.845
0.000     (0)
   CuCl3-2          1.619e-08   3.581e-09    -7.791    -8.446    -
0.655     (0)
   CuCl2            1.319e-08   1.319e-08    -7.880    -7.880
0.000     (0)
   FeCl2            9.845e-09   9.845e-09    -8.007    -8.007
0.000     (0)
   FeCl+2           8.146e-11   2.397e-11   -10.089   -10.620    -
0.531     (0)
   PbCl3-           3.519e-11   7.424e-11   -10.454   -10.129
0.324     (0)
   FeCl2+           9.520e-12   2.008e-11   -11.021   -10.697
0.324     (0)
   PbCl4-2          2.209e-13   4.884e-14   -12.656   -13.311    -
0.655     (0)
   MnCl3-           2.207e-13   4.656e-13   -12.656   -12.332
0.324     (0)
   FeCl4-2          1.378e-13   3.048e-14   -12.861   -13.516    -
0.655     (0)
   CuCl4-2          1.199e-18   2.652e-19   -17.921   -18.576    -
0.655     (0)
   FeCl4-           1.226e-20   2.587e-20   -19.911   -19.587
0.324     (0)
Cl(1)          5.910e-40
   HClO             5.910e-40   5.910e-40   -39.228   -39.228
0.000     (0)
   ClO-             0.000e+00   0.000e+00   -44.362   -44.038
0.324     (0)
Cl(3)          0.000e+00
   HClO2            0.000e+00   0.000e+00   -77.575   -77.575
0.000     (0)
   ClO2-            0.000e+00   0.000e+00   -78.309   -77.985
0.324     (0)
```

```
Cl(5)          0.000e+00
   ClO3-            0.000e+00   0.000e+00   -98.366   -98.080
0.286     (0)
   PbClO3+          0.000e+00   0.000e+00  -101.540  -101.216
0.324     (0)
   Pb(ClO3)2        0.000e+00   0.000e+00  -199.588  -199.588
0.000     (0)
Cl(7)          0.000e+00
   ClO4-            0.000e+00   0.000e+00  -122.762  -122.476
0.286     (0)
Cu(1)          3.869e-06
   Cu+              3.597e-06   7.589e-06    -5.444    -5.120
0.324     (0)
   CuCl2-           2.553e-07   5.387e-07    -6.593    -6.269
0.324     (0)
   CuCl3-2          1.619e-08   3.581e-09    -7.791    -8.446    -
0.655     (0)
Cu(2)          1.677e-02
   Cu+2             1.589e-02   8.548e-03    -1.799    -2.068    -
0.269     (0)
   CuSO4            8.692e-04   8.692e-04    -3.061    -3.061
0.000     (0)
   CuCl+            1.147e-05   2.420e-05    -4.940    -4.616
0.324     (0)
   CuOH+            1.087e-07   2.292e-07    -6.964    -6.640
0.324     (0)
   CuCl2            1.319e-08   1.319e-08    -7.880    -7.880
0.000     (0)
   CuCl4-2          1.199e-18   2.652e-19   -17.921   -18.576    -
0.655     (0)
   CuO2-2           1.228e-30   2.716e-31   -29.911   -30.566    -
0.655     (0)
Fe(2)          4.535e+00
   Fe+2             4.369e+00   2.351e+00     0.640     0.371    -
0.269     (0)
   FeSO4            1.654e-01   1.654e-01    -0.782    -0.782
0.000     (0)
   FeCl+            8.402e-04   1.773e-03    -3.076    -2.751
0.324     (0)
   FeOH+            1.832e-07   3.865e-07    -6.737    -6.413
0.324     (0)
   FeCl2            9.845e-09   9.845e-09    -8.007    -8.007
0.000     (0)
   FeCl4-2          1.378e-13   3.048e-14   -12.861   -13.516    -
0.655     (0)
   Fe(OH)2          1.596e-15   1.596e-15   -14.797   -14.797
0.000     (0)
   Fe(OH)3-         1.566e-23   3.303e-23   -22.805   -22.481
0.324     (0)
   Fe(OH)4-2        7.766e-35   1.717e-35   -34.110   -34.765    -
0.655     (0)
Fe(3)          2.494e-06
   FeOH+2           1.585e-06   4.665e-07    -5.800    -6.331    -
0.531     (0)
   Fe+3             8.432e-07   1.390e-07    -6.074    -6.857    -
0.783     (0)
   Fe(OH)2+         3.807e-08   8.031e-08    -7.419    -7.095
0.324     (0)
```

```
   Fe2(OH)2+4       1.231e-08   5.858e-12    -7.910   -11.232    -
3.322      (0)
   FeSO4+           2.829e-09   5.968e-09    -8.548    -8.224
0.324      (0)
   FeCl+2           8.146e-11   2.397e-11   -10.089   -10.620    -
0.531      (0)
   Fe(SO4)2-        2.123e-11   4.478e-11   -10.673   -10.349
0.324      (0)
   Fe(OH)3          1.953e-11   1.953e-11   -10.709   -10.709
0.000      (0)
   Fe3(OH)4+5       1.233e-11   9.828e-17   -10.909   -16.008    -
5.098      (0)
   FeCl2+           9.520e-12   2.008e-11   -11.021   -10.697
0.324      (0)
   Fe(OH)4-         1.209e-18   2.550e-18   -17.918   -17.593
0.324      (0)
   FeCl4-           1.226e-20   2.587e-20   -19.911   -19.587
0.324      (0)
H(0)            4.432e-22
   H2               2.216e-22   6.303e-21   -21.654   -20.200
1.454      (0)
Hg(1)           6.579e-10
   Hg2+2            3.290e-10   7.275e-11    -9.483   -10.138    -
0.655      (0)
Hg(2)           5.586e-15
   Hg+2             5.586e-15   2.082e-15   -14.253   -14.682    -
0.429      (0)
Mn(2)           1.777e-03
   Mn+2             1.677e-03   9.026e-04    -2.775    -3.044    -
0.269      (0)
   MnSO4            9.885e-05   9.885e-05    -4.005    -4.005
0.000      (0)
   MnCl+            9.429e-07   1.989e-06    -6.026    -5.701
0.324      (0)
   MnOH+            5.717e-12   1.206e-11   -11.243   -10.919
0.324      (0)
   Mn2OH+3          6.998e-13   1.167e-14   -12.155   -13.933    -
1.778      (0)
   MnCl3-           2.207e-13   4.656e-13   -12.656   -12.332
0.324      (0)
   Mn(OH)2          1.539e-20   1.539e-20   -19.813   -19.813
0.000      (0)
   Mn2(OH)3+        6.832e-23   1.441e-22   -22.165   -21.841
0.324      (0)
   Mn(OH)3-         3.558e-30   7.506e-30   -29.449   -29.125
0.324      (0)
   Mn(OH)4-2        1.494e-40   0.000e+00   -39.826   -40.481    -
0.655      (0)
Mn(3)           8.905e-22
   Mn+3             8.905e-22   1.485e-23   -21.050   -22.828    -
1.778      (0)
Mn(6)           0.000e+00
   MnO4-2           0.000e+00   0.000e+00   -75.772   -76.428    -
0.655      (0)
Mn(7)           0.000e+00
   MnO4-            0.000e+00   0.000e+00   -80.280   -79.994
0.286      (0)
Ni              5.921e-03
```

```
   Ni+2             5.733e-03   3.085e-03    -2.242    -2.511    -
0.269      (0)
   NiSO4            1.879e-04   1.879e-04    -3.726    -3.726
0.000      (0)
   NiCl+            1.611e-07   3.399e-07    -6.793    -6.469
0.324      (0)
   Ni2OH+3          5.922e-12   9.871e-14   -11.228   -13.006    -
1.778      (0)
   Ni(OH)2          8.528e-18   8.528e-18   -17.069   -17.069
0.000      (0)
   Ni4(OH)4+4       2.902e-24   1.381e-27   -23.537   -26.860    -
3.322      (0)
   Ni(OH)3-         2.126e-26   4.485e-26   -25.672   -25.348
0.324      (0)
O(0)           0.000e+00
   O2               0.000e+00   0.000e+00   -53.337   -51.883
1.454      (0)
Pb(2)          4.147e-03
   Pb+2             4.129e-03   1.215e-03    -2.384    -2.915    -
0.531      (0)
   PbCl+            1.721e-05   3.630e-05    -4.764    -4.440
0.324      (0)
   PbCl2            1.430e-07   1.430e-07    -6.845    -6.845
0.000      (0)
   Pb2OH+3          1.854e-08   3.090e-10    -7.732    -9.510    -
1.778      (0)
   PbOH+            6.042e-09   1.275e-08    -8.219    -7.895
0.324      (0)
   PbCl3-           3.519e-11   7.424e-11   -10.454   -10.129
0.324      (0)
   PbCl4-2          2.209e-13   4.884e-14   -12.656   -13.311    -
0.655      (0)
   Pb(OH)2          2.668e-15   2.668e-15   -14.574   -14.574
0.000      (0)
   Pb4(OH)4+4       4.407e-19   2.097e-22   -18.356   -21.678    -
3.322      (0)
   Pb3(OH)4+2       5.866e-22   1.726e-22   -21.232   -21.763    -
0.531      (0)
   Pb(OH)3-         6.651e-24   1.403e-23   -23.177   -22.853
0.324      (0)
   Pb6(OH)8+4       9.922e-37   4.722e-40   -36.003   -39.326    -
3.322      (0)
   PbClO3+          0.000e+00   0.000e+00  -101.540  -101.216
0.324      (0)
   Pb(ClO3)2        0.000e+00   0.000e+00  -199.588  -199.588
0.000      (0)
Pb(4)          0.000e+00
   Pb+4             0.000e+00   0.000e+00   -45.191   -48.513    -
3.322      (0)
S(6)           1.959e-01
   FeSO4            1.654e-01   1.654e-01    -0.782    -0.782
0.000      (0)
   AlSO4+           2.553e-02   5.385e-02    -1.593    -1.269
0.324      (0)
   SO4-2            2.007e-03   4.438e-04    -2.697    -3.353    -
0.655      (0)
   Al(SO4)2-        8.795e-04   1.855e-03    -3.056    -2.732
0.324      (0)
```

```
   CuSO4            8.692e-04   8.692e-04    -3.061    -3.061
0.000     (0)
   NiSO4            1.879e-04   1.879e-04    -3.726    -3.726
0.000     (0)
   MnSO4            9.885e-05   9.885e-05    -4.005    -4.005
0.000     (0)
   HSO4-            3.693e-05   7.791e-05    -4.433    -4.108
0.324     (0)
   FeSO4+           2.829e-09   5.968e-09    -8.548    -8.224
0.324     (0)
   H2SO4            1.277e-10   1.277e-10    -9.894    -9.894
0.000     (0)
   Fe(SO4)2-        2.123e-11   4.478e-11   -10.673   -10.349
0.324     (0)

-------------------------------Saturation indices-----------------
--------------

  Phase               SI** log IAP   log K(298 K,   1 atm)

  Al              -103.71     46.20  149.91  Al
  Al(g)           -154.42     46.20  200.62  Al
  Al2(SO4)3        -30.81    -11.91   18.90  Al2(SO4)3
  Al2(SO4)3:6H2O   -13.73    -12.17    1.56  Al2(SO4)3:6H2O
  Anglesite          1.64     -6.27   -7.91  PbSO4
  Antlerite         -7.42      1.31    8.73  Cu3(SO4)(OH)4
  Arsenolite        -9.79    -29.63  -19.84  As2O3
  As               -18.58     24.10   42.68  As
  As2O5            -22.58    -20.45    2.14  As2O5
  As4O6(cubi)      -19.43    -59.26  -39.82  As4O6
  As4O6(mono)      -19.21    -59.26  -40.05  As4O6
  Atacamite        -12.21      2.05   14.26  Cu4Cl2(OH)6
  Birnessite      -148.23   -233.77  -85.55  Mn8O14:5H2O
  Bixbyite         -28.26    -29.23   -0.96  Mn2O3
  Boehmite          -0.28      7.27    7.55  AlO2H
  Brochantite      -10.75      4.67   15.42  Cu4(SO4)(OH)6
  Bunsenite         -9.50      2.97   12.46  NiO
  Calomel            1.72    -16.11  -17.83  Hg2Cl2
  Chalcanthite      -3.01     -5.64   -2.63  CuSO4:5H2O
  Chalcocyanite     -8.33     -5.42    2.91  CuSO4
  Cl2(g)           -40.38    -37.39    2.99  Cl2
  Claudetite        -9.83    -29.63  -19.80  As2O3
  Corundum          -3.72     14.58   18.29  Al2O3
  Cotunnite         -4.03     -8.89   -4.85  PbCl2
  Cu                -2.15     29.35   31.50  Cu
  Cu(g)            -54.31     29.35   83.66  Cu
  CuCl2            -11.76     -8.04    3.72  CuCl2
  Cuprite           -2.86     -4.76   -1.91  Cu2O
  Delafossite        5.41     -1.03   -6.44  CuFeO2
  Diaspore           0.12      7.27    7.15  AlHO2
  Fe               -27.23     31.79   59.02  Fe
  Fe(OH)2           -8.09      5.80   13.89  Fe(OH)2
  Fe(OH)3           -4.35      1.29    5.64  Fe(OH)3
  Fe2(SO4)3        -26.82    -23.77    3.05  Fe2(SO4)3
  FeO               -7.68      5.85   13.52  FeO
  Ferrite-Cu        -4.16      6.12   10.28  CuFe2O4
  FeSO4             -5.59     -2.98    2.61  FeSO4
  Gibbsite          -0.52      7.22    7.74  Al(OH)3
  Goethite           0.80      1.33    0.53  FeOOH
```

```
  H2(g)            -17.10    -20.20   -3.10  H2
  H2O(g)            -1.63     -0.04    1.59  H2O
  Hausmannite      -36.94    -26.80   10.14  Mn3O4
  HCl(g)           -12.05     -5.75    6.30  HCl
  Hematite           2.64      2.71    0.08  Fe2O3
  Hercynite         -8.38     20.42   28.80  FeAl2O4
  Hg(g)             -2.99     16.74   19.73  Hg
  Hg(l)              2.60     16.74   14.14  Hg
  Hg2SO4            -7.36    -13.49   -6.13  Hg2SO4
  Ice               -0.18     -0.04    0.14  H2O
  Lammerite        -11.78    -10.22    1.55  Cu3(AsO4)2
  Lanarkite         -3.22     -3.71   -0.48  Pb2(SO4)O
  Lawrencite       -14.65     -5.60    9.05  FeCl2
  Litharge         -10.08      2.56   12.64  PbO
  Magnetite         -1.86      8.56   10.42  Fe3O4
  Manganite        -14.47    -14.64   -0.16  MnO(OH)
  Manganosite      -15.48      2.43   17.92  MnO
  Massicot         -10.26      2.56   12.82  PbO
  Melanterite       -0.89     -3.29   -2.40  FeSO4:7H2O
  Minium           -48.70    -32.44   16.26  Pb3O4
  Mn               -54.56     28.37   82.93  Mn
  Mn(OH)2(am)      -12.92      2.39   15.31  Mn(OH)2
  Mn(OH)3          -21.02    -14.68    6.34  Mn(OH)3
  MnCl2:2H2O       -13.10     -9.10    4.00  MnCl2:2H2O
  MnCl2:4H2O       -11.94     -9.19    2.75  MnCl2:4H2O
  MnCl2:H2O        -14.60     -9.06    5.54  MnCl2:H2O
  MnO2(gamma)      -23.61    -39.74  -16.13  MnO2
  MnSO4             -9.01     -6.40    2.61  MnSO4
  Molysite         -29.28    -15.81   13.47  FeCl3
  Montroydite      -11.65     -9.21    2.44  HgO
  Morenosite        -4.11     -6.17   -2.06  NiSO4:7H2O
  Nantokite         -1.34     -8.10   -6.77  CuCl
  Ni               -22.07     28.91   50.98  Ni
  Ni(OH)2           -9.82      2.92   12.75  Ni(OH)2
  Nickelbischofite -11.90     -8.75    3.15  NiCl2:6H2O
  NiCl2            -17.08     -8.48    8.60  NiCl2
  NiCl2:2H2O       -12.49     -8.57    3.92  NiCl2:2H2O
  NiCl2:4H2O       -12.51     -8.66    3.85  NiCl2:4H2O
  NiSO4            -11.14     -5.86    5.28  NiSO4
  NiSO4:6H2O(alpha)  -4.11     -6.13   -2.02  NiSO4:6H2O
  O2(g)            -48.99    -51.88   -2.89  O2
  Paralaurionite    -3.38     -3.18    0.20  PbClOH
  Pb               -18.67     28.50   47.17  Pb
  Pb(g)            -47.10     28.50   75.61  Pb
  Pb3SO6           -11.73     -1.15   10.58  Pb3SO6
  Pb4Cl2(OH)6      -18.62     -1.34   17.28  Pb4Cl2(OH)6
  Pb4SO7           -20.30      1.41   21.71  Pb4SO7
  Plattnerite      -29.60    -37.56   -7.97  PbO2
  Pyrolusite       -22.08    -39.74  -17.66  MnO2
  Scacchite        -17.76     -9.01    8.74  MnCl2
  Tenorite          -4.24      3.41    7.65  CuO
  Todorokite      -123.90   -169.72  -45.82  Mn7O12:3H2O
  Trevorite         -4.10      5.68    9.78  NiFe2O4
  Wustite           -7.34      5.06   12.40  Fe.947O

**For a gas, SI = log10(fugacity). Fugacity = pressure * phi / 1
atm.
  For ideal gases, phi = 1.
```

```
------------------
End of simulation.
------------------

-----------------------------------
Reading input data for simulation 2.
-----------------------------------

--------------------------------
End of Run after 1.104 Seconds.
--------------------------------
```